Optimal Control and Function Identification in Biological Processes

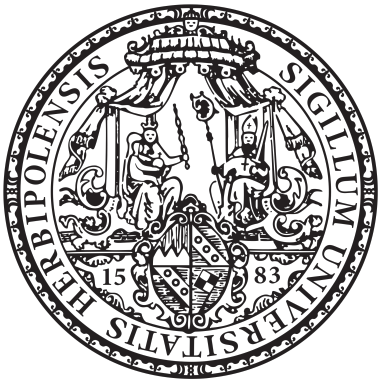

Dissertation zur Erlangung
des naturwissenschaftlichen Doktorgrades
der Julius-Maximilians-Universität Würzburg

vorgelegt von

Juri Merger

Würzburg, 20. Juli 2016

Abstract

Mathematical modelling, simulation, and optimisation are core methodologies for future developments in engineering, natural, and life sciences. This work aims at applying these mathematical techniques in the field of biological processes with a focus on the wine fermentation process that is chosen as a representative model.

In the literature, basic models for the wine fermentation process consist of a system of ordinary differential equations. They model the evolution of the yeast population number as well as the concentrations of assimilable nitrogen, sugar, and ethanol. In this thesis, the concentration of molecular oxygen is also included in order to model the change of the metabolism of the yeast from an aerobic to an anaerobic one. Further, a more sophisticated toxicity function is used. It provides simulation results that match experimental measurements better than a linear toxicity model. Moreover, a further equation for the temperature plays a crucial role in this work as it opens a way to influence the fermentation process in a desired way by changing the temperature of the system via a cooling mechanism. From the view of the wine industry, it is necessary to cope with large scale fermentation vessels, where spatial inhomogeneities of concentrations and temperature are likely to arise. Therefore, a system of reaction-diffusion equations is formulated in this work, which acts as an approximation for a model including computationally very expensive fluid dynamics.

In addition to the modelling issues, an optimal control problem for the proposed reaction-diffusion fermentation model with temperature boundary control is presented and analysed. Variational methods are used to prove the existence of unique weak solutions to this non-linear problem. In this framework, it is possible to exploit the Hilbert space structure of state and control spaces to prove the existence of optimal controls. Additionally, first-order necessary optimality conditions are presented. They characterise controls that minimise an objective functional with the purpose to minimise the final sugar concentration. A numerical experiment shows that the final concentration of sugar can be reduced by a suitably chosen temperature control.

The second part of this thesis deals with the identification of an unknown function that participates in a dynamical model. For models with ordinary differential equations, where parts of the dynamic cannot be deduced due to the complexity of the underlying phenomena, a minimisation problem is formulated. By minimising the deviations of simulation results and measurements the best possible function from a trial function space is found. The analysis of this function identification problem covers the proof of the differentiability of the function–to–state operator, the existence of minimisers, and the sensitivity analysis by means of the data–to–function mapping. Moreover, the presented function identification method is extended to stochastic differential equations. Here, the objective functional consists of the difference of measured values and the statistical expected value of the stochastic process solving the stochastic differential equation. Using a Fokker-Planck equation that governs the probability density function of the process, the probabilistic problem of simulating a stochastic process is cast to a deterministic partial differential equation. Proofs of unique solvability of the forward equation, the existence of minimisers, and first-order necessary optimality conditions are presented. The application of the function identification framework to the wine fermentation model aims at finding the shape of the toxicity function and is carried out for the deterministic as well as the stochastic case.

Zusammenfassung

Mathematische Modellierung, Simulation und Optimierung sind wichtige Methoden für künftige Entwicklungen in Ingenieurs-, Natur- und Biowissenschaften. Ziel der vorliegende Arbeit ist es diese mathematische Methoden im Bereich von biologischen Prozessen anzuwenden. Dabei wurde die Weingärung als repräsentatives Modell ausgewählt.

Erste Modelle der Weingärung, die man in der Literatur findet, bestehen aus gewöhnlichen Differentialgleichungen. Diese modellieren den Verlauf der Populationszahlen der Hefe, sowie die Konzentrationen von verwertbarem Stickstoff, Zucker und Ethanol. In dieser Arbeit wird auch die Konzentration von molekularem Sauerstoff betrachtet um den Wandel des Stoffwechsels der Hefe von aerob zu anaerob zu erfassen. Weiterhin wird eine ausgefeiltere Toxizitätsfunktion benutzt. Diese führt zu Simulationsergebnissen, die im Vergleich zu einem linearen Toxizitätsmodell experimentelle Messungen besser reproduzieren können. Außerdem spielt eine weitere Gleichung für die zeitliche Entwicklung der Temperatur eine wichtige Rolle in dieser Arbeit. Diese eröffnet die Möglichkeit den Gärprozess in einer gewünschten Weise zu beeinflussen, indem man die Temperatur durch einen Kühlmechanismus verändert. Für industrielle Anwendungen muss man sich mit großen Fermentationsgefäßen befassen, in denen räumliche Abweichungen der Konzentrationen und der Temperatur sehr wahrscheinlich sind. Daher ist in dieser Arbeit ein System von Reaktion-Diffusions Gleichungen formuliert, welches eine Approximation an ein Modell mit rechenaufwändiger Strömungsmechanik darstellt.

Neben der Modellierung wird in dieser Arbeit ein Optimalsteuerungsproblem für das vorgestellte Gärmodell mit Reaktions-Diffusions Gleichungen und Randkontrolle der Temperatur gezeigt und analysiert. Variationelle Methoden werden benutzt, um die Existenz von eindeutigen schwachen Lösungen von diesem nicht-linearen Modell zu beweisen. Das Ausnutzen der Hilbertraumstruktur von Zustands- und Kontrolraum macht es möglich die Existenz von Optimalsteuerungen zu beweisen. Zusätzlich werden notwendige Optimalitätsbedingungen erster Ordnung vorgestellt. Diese charakterisieren Kontrollen, die das Zielfunktional minimieren. Ein numerisches Experiment zeigt, dass die finale Konzentration des Zuckers durch eine passend ausgewählte Steuerung reduziert werden kann.

Der zweite Teil dieser Arbeit beschäftigt sich mit der Identifizierung einer unbekannten Funktion eines dynamischen Modells. Es wird ein Minimierungsproblem für Modelle mit gewöhnlichen Differentialgleichungen, bei denen ein Teil der Dynamik aufgrund der Komplexität der zugrundeliegenden Phänomene nicht hergeleitet werden kann, formuliert. Die bestmögliche Funktion aus einem Testfunktionenraum wird dadurch ausgewählt, dass Abweichungen von Simulationsergebnissen und Messungen minimiert werden. Die Analyse dieses Problems der Funktionenidentifikation beinhaltet den Beweis der Differenzierbarkeit des Funktion–zu–Zustand Operators, die Existenz von Minimierern und die Sensitivitätsanalyse mit Hilfe der Messung–zu–Funktion Abbildung. Weiterhin wird diese Funktionenidentifikationsmethode für stochastische Differentialgleichungen erweitert. Dabei besteht das Zielfunktional aus dem Abstand von Messwerten und dem Erwartungswert des stochastischen Prozesses, der die stochastische Differentialgleichung löst. In dem man die Fokker-Planck Gleichung benutzt wird das wahrscheinlichkeitstheoretische Problem einen stochastischen Prozess zu simulieren in eine deterministische partielle Differentialgleichung überführt. Es werden Beweise für die eindeutige Lösbarkeit der Vorwärtsgleichung, die Existenz von Minimierern und die notwendigen Bedingungen erster Ordnung geführt. Die Anwendung der Funktionenidentifikation auf die Weingärung zielt darauf ab die Form der Toxizitätsfunktion herauszufinden und wird sowohl für den deterministischen als auch für den stochastischen Fall durchgeführt.

Acknowledgements

After almost a week since defending my PhD thesis, I have had some time to recover. Now it is time to think about the people who helped and accompanied me during the last three years.

The first person I want to thank is the one who made everything possible: my supervisor Prof. Dr. Alfio Borzi. He gave me his trust although I was new on his research area. At any time his doors were open for discussions on my ideas. Moreover, he was very motivating and encouraging. Hence, he is responsible for the success of my work to an extend I cannot even measure.

My appreciation also goes to my second supervisor and co-author of my first scientific publication Prof. Dr. Roland Herzog. He was not only a very good host at our meetings in Chemnitz, but also helped me a lot to underpin my ideas.

A lot of thanks goes to Petra Markert-Autsch. She does a very great job as the secretary of the WiReMIX-group.

I also want to mention my colleagues during my time at the chair for scientific computing and thank them for different things. Their names are sorted pseudo-randomly (seed 15383 on http://www.randomization.com). I enjoyed many discussions with Stephan on CFD and shape optimization. The introduction into the professional swimming technique of Andrea motivated me to practice further. Souvik was always very kind. The food and stories of Masoumeh's home country opened my mind. My thanks goes also to Mario, who helped me with my master thesis. Gabriele had very encouraging words for me in a time, where the work load was at its height. My long-standing office co-worker Martin helped me several times to clarify results on the theory of parabolic PDEs. The beach volleyball matches with Bea were a lot of fun. I admire the success of Myroslav at learning German. Suttida's idea for the sushi party was great. Duncan presented us delicious food at the Christmas parties. The jokes of Tanvir were always entertaining and brightened the day. Tim challenged me by his questions to rethink the theory for parabolic PDEs and to give precise answers. I will never forget Christian's boeuf bourguignon. Andreas' travel reports were really interesting. Additional thanks goes to Jan, Bea and Andrea for proofreading my work.

I want to thank my parents Alexander and Lilli as well as my brother Dimitri for their support. Last but not least, I thank my love Sali for her never-ending motivation.

Juri 26^{th} of September 2016

Contents

Chapter 1

Introduction

Biological processes play a central role in food, chemical, and pharmaceutical industry. During the improvement of the production of goods in such sectors, appropriate mathematical models can have an accelerating effect, as simulating a process on the computer is often cheaper and faster than performing experimental studies. This thesis deals with the optimal control of the wine fermentation process, which is chosen as a representative biological model, and the identification of the involved toxicity function. The modelling of a general fermentation process is based on ordinary differential equations that describe the kinetics of the bio-chemical reactions. In [LTPM02], tea fermentation kinetics coupled with the flow of air through porous media is discussed. Beer fermentation is considered in [ATGSFB$^+$04, GR88] and also in [RM07], where evolutionary algorithms are used for optimisation. See [Cho] for a review of some fermentation processes.

Regarding models of wine fermentation, we refer to [DDM$^+$10] and [DDM$^+$11], where the evolution of the yeast biomass together with the concentrations of nitrogen, sugar, and ethanol are modelled. In this model, the growth of the yeast population that consumes nitrogen is governed by a Michaelis-Menten term, which is often used for the description of enzymatic biological reactions [MM13]. Another kinetic component of this model governs the conversion of sugar into ethanol, taking into account that high concentrations of ethanol decelerate the fermentation of sugar, which is modelled by an inhibition term. A similar model is also presented in [Vel09, Chapter 3.10.2], whereas an advanced model is proposed in [MFHS04] that also models the necessity of nitrogen for sugar transport in the yeast cells. Furthermore, in [CMS07] thermal phenomena in the fermentation process as the production of heat by the yeast and the heat loss to the environment are considered. In [CDD$^+$10] results of simulations of a fermentation with ordinary differential equations are presented. A first attempt to formulate wine fermentation optimal control problems can be found in [Sab09] with the aim to improve energy saving and aromatic profile.

Our contribution to this research effort is the formulation of a refined fermentation model including space dependent concentrations and variable temperature. Moreover, the toxic influence of ethanol is included in the equation for the yeast population. Further, a control strategy for an ideal fermentation profile is sought. In particular, we augment the diffusion operator with Robin-type boundary conditions for the temperature that accommodates a control mechanism, which is driven by an external temperature of a liquid cooling/heating system.

Additionally, we theoretically and numerically investigate this reaction-diffusion model and discuss a related optimal control problem. The analysis of reaction-diffusion equations is strongly dependent on the characteristics of the reaction term. For some reaction terms there may exist an invariant set of the state space such that if the initial values of the

reaction-diffusion system lie in this region their values will also belong to this set for all future times [Smo94]. Another approach for investigating reaction-diffusion equations can be found in [Pao92, Chapter 8]. In this reference, quasi-monotone type reactions are solved by constructing a sequence of coupled upper and lower solutions that converge from above and below to the unique solution, respectively. In addition, it is possible to use the Leray-Schauder fixed-point theorem as in [BG06], where the optimal control of lambda-omega systems is analysed, and [GV03], where the reaction of two species is considered. In our proofs, we use the Banach fixed-point theorem [Eva10, Part III 9.2.1] and prove that the model equations admit a unique solution. Furthermore, this solution depends continuously on the initial values and the external temperature. These results are obtained by applying established results for parabolic problems, combined with a cut-off technique, which is motivated by the fact that the ordinary differential equations model have the property that the initial values determine a bound for its solutions.

With our fermentation model, we discuss the characteristics of an optimally driven fermentation process and define a corresponding cost functional that has to be minimised. The resulting optimal control problem and the characterisation of its solutions by means of the corresponding optimality system are investigated. In particular, we prove existence of optimal controls. Further, we discuss the numerical solution of the optimally controlled fermentation process. An optimal control is calculated by the Broyden-Fletcher-Goldfarb-Shanno (BFGS) iterative optimisation procedure, which is a gradient-based quasi-Newton method. Using the adjoint framework, the gradient of the reduced cost functional is evaluated by solving the forward and backward reaction-diffusion equations appearing in the optimality system. These equations are discretised by implicit-explicit (IMEX) finite differences, where the diffusion terms are treated implicitly and the reaction terms are treated explicitly. We present numerical results, which show that the amount of sugar at the end of the fermentation process can be considerably reduced by an optimally chosen boundary temperature profile.

The next aspect treated in this thesis is the identification of an unknown function, which is participating in a differential equation. The idea for investigating such problems originates from the situation that the toxic effect of ethanol on the yeast cells cannot be derived by biological arguments, as the phenomena that are involved are too complex. If the toxicity could be at least given by a parametrised function, we would use parameter estimation techniques (see [Bar74, Boc87, BDB86, LOP05]) to find the optimal parameters for the yeast strain used in a special application. As this is not possible, we formulate a minimisation problem, where the sought function is an element of a Sobolev space and no further restrictions on its shape are prescribed. Most problems in optimal control theory of differential equations consider a distributed or boundary control. Hence, the control function is dependent on the space and time variable. In contrast, the minimisation variable in our proposed function identification framework is defined on the range of the state variable and not on the time interval. In particular, the composition of the unknown function and the state appear in the differential equation.

We would like to give a short overview of the available publications on the topic of identifying an unknown function involved in a differential equation from measurement data. In [Lor82] the author investigates an overdetermined parabolic equation with a non-linear reaction term to be identified, where both Neumann and Dirichlet boundary conditions are given. It is proven that from coinciding simulations subject to two instances of the unknown function it follows that the corresponding identified functions must be equal on the domain of the simulation. Moreover, [Lor82] contains a Hölderian-type estimate for the dependence of the identified non-linearity with respect to given

data. Another problem analysed in [EPS14a] is an elliptic equation, where the diffusion coefficient depends on the solution. In this publication, the authors also prove the identifiability of the unknown function, whereas in [EPS14b] an additional space-dependent coefficient is identified simultaneously. Stability of this identification procedure is investigated in [EPS15b]. The identification of non-linearities in a chemotaxis model is carried out in [EPS15a] by defining a perturbed linear operator and using a standard Tikhonov H^1-regularisation, whereas a stationary transport-diffusion model for crowded motion is analysed in [BPW13].

In contrast to the afore-mentioned theoretical results on the well-posedness and stability of identifying a function in a differential equation from some given data, there are also publications that have a constructive focus. In [OIL08] a boundary element method is used to identify the non-linear temperature dependent heat transfer coefficient in a heat equation. The author in [EFP05] regularises the direct calculation of the non-linearity of the same problem by using simulation results obtained with faulty measurement data. Besides the two latter publications, the main idea of the following references is to formulate an optimal control problem where the unknown function acts as a control. The unknown function is identified by minimising an objective functional that measures the discrepancy between a simulation subject to a given function and measurement data, where the differential equation is incorporated as a constraint. The optimal control problem for a temperature dependent heat transfer coefficient is extensively analysed in [RT92, Rös94, Rös96a, Rös96b, Rös98, Rös02], where unique solvability of the differential equation, the existence of a minimiser, and the first-order necessary optimality conditions are shown. Moreover, unique identifiability is also shown for this model and numerical computations are carried out, where the heat transfer coefficient is discretised by linear splines. In [Rös96a] the Fréchet differentiability of the forward problem is proven and in [Rös96b] stability estimates are given. The same results are achieved in [HHTL15] for a more general transfer coefficient mapping that is also dependent on the boundary data in a non-linear way. Here, piecewise constant functions are used to approximate the unknown function. The analysis for a state-dependent non-linear diffusion coefficient in a semi-linear elliptic equation can be found in [KE02, Küg03], where a Tikhonov-regularisation is analysed with respect to its convergence for diminishing measurement errors. In [HLT12, HLSY14] coupled parabolic PDE-ODE systems are the constraints to the minimisation problem and existence of minimisers and Gâteaux derivatives of the objective functional are given.

The purpose of our work is to contribute to the theory and numerical solution of function identification problems as in the latter references. In contrast to the works mentioned above, no a priori known constraints on the function or its derivative are necessary because of the use of functions in a Sobolev space. Furthermore, we introduce the "data–to–function" map to analyse the effect of measurement errors on the identified function. Therefore, it is essential to prove that the regarded minimisation problem admits a unique solution. Regarding the discretisation of our optimisation problem, the novelty of our work is to choose radial basis functions (RBFs). This choice is advantageous with respect to other approaches, e.g., splines, because it allows to consider functions defined on the whole real line and makes possible to generalise the function identification problem to unknown functions that depend on several variables. This can be done straightforwardly for radially symmetric ansatz functions, whereas splines have to be adjusted to the dimension of the problem. In multidimensional approximation theory, many classes of RBFs are available that guarantee the solvability of the approximation of a function on scattered data. Approximation orders have been shown for approximands in the so-called

native space; see [Buh03]. In particular, in [Wen95] it is shown that the native space for Wendland's compactly supported radial basis function of minimal degree matches the Sobolev space we use for the function identification method. Therefore, we use this kind of RBFs.

The last part of this thesis extends the proposed function identification method from the deterministic world of ordinary differential equations to the probabilistic world of stochastic differential equations. This is done to overcome the problem of uncertainties in biological models. In this area, it can happen that the evolution of observed variables is not only governed by a deterministic mechanism but is perturbed randomly due to the inhomogeneity of a population. In order to formulate a minimisation problem for the identification of an unknown function, we use the corresponding Fokker-Planck equation rather than the stochastic differential equation itself. Fokker-Planck equations have been successfully used in many different fields, such as physics, chemistry, or electrical engineering. [Ris89] provides a good survey of this topic. Recent publications for the optimal control of Fokker-Planck equations are given by [AB13a, AB13b, ABMW15], whereas [RAB16] treats a similar problem as ours.

This thesis is organised as follows. In Chapter 2, we discuss the ordinary differential equations that govern the wine fermentation process. These equations are extended to partial differential equations by including a vector Laplace operator that models diffusion of substances. The optimal control of the system of reaction-diffusion equations is analysed in Chapter 3. Hereby, a review on the theory of parabolic equations settles the foundation for the proof of the existence of unique weak solutions of the wine fermentation model. Moreover, the existence of a minimiser is shown and first-order necessary optimality conditions are presented. These conditions are used in a gradient-based optimisation procedure to compute an optimal control numerically. Chapter 4 is organised into two parts. The first one deals with a function identification method for ordinary differential equation. The corresponding minimisation problem is analysed and supplemented with two numerical test cases. The second part extends the function identification methods to stochastic differential equations. Necessary results from the theory of stochastic processes governed by stochastic differential equations and of the corresponding Fokker-Planck equation are presented. Besides the theoretical analysis of this framework, the identification of the toxicity function is carried out numerically. A conclusion in Chapter 5 completes the exposition of our work.

The results presented in this thesis are partly based on the following publications:

- J. Merger and A. Borzì. Dynamics identification in evolution models using radial basis functions. *Journal of Dynamical and Control Systems*, 2016.
- J. Merger, A. Borzì, and R. Herzog. Optimal Control of a System of Reaction-Diffusion Equations Modeling the Wine Fermentation Process. *Optimal Control Applications and Methods*, 2016.
- A. Borzì, J. Merger, J. Müller, A. Rosch, C. Schenk, D. Schmidt, S. Schmidt, V. Schulz, K. Velten, C. von Wallbrunn, and M. Zänglein. Novel model for wine fermentation including the yeast dying phase. *arXiv*:1412.6068, 2014.

Chapter 2

Wine Fermentation as a Representative Biological Process

In any process where living organisms participate, microbiological mechanisms play an important role. Hence, for understanding these processes, it is indispensable to take the biological phenomena into account. Examples of applications for such processes can be found in many daily situations. One large area is medicine, where, on one hand, the human being itself is a very complex system of biological processes and, on the other hand, it is also influenced by bacteria and other unicellular organisms. Moreover, there is pharmacy, where medicinal products are often produced by microbes. In addition to that, the chemical industry manufactures many products by fermentation and other biologically reactive processes. Those examples are just the beginning of a large list of applications. Therefore, it is beneficial to pursue the mathematical modelling of such processes for gaining a deeper understanding and obtaining realistic models that allow for reliable simulations and predictions. The ability to simulate a process numerically enables one to analyse many different situations and to compute optimal conditions and control strategies without costly experiments. This procedure of mathematical modelling, simulation, and optimisation (MMSO) is applied in a growing number of scientific and industrial areas and its features makes it a good methodology for future developments.

Models describing biological reactions have some characteristics in common regardless of the area they arise. Usually a large number of biological species and chemical substrates are involved and the evolution of their concentrations has to be modelled. Moreover, biological systems often admit some kind of conservation of chemical amount such that substances are only transformed into others and do not vanish. Hence, there is also no infinite source of substrates and, consequently, these models should not exhibit some kind of blow up behaviour. Without such characteristics a general biological process is hard to analyse mathematically and its presentation would be unnecessarily complex, thereby obfuscating the main ideas used in the analysis during the course of this work. This thesis considers wine fermentation as a representative biological process, which has a moderate number of participating species and three basic mechanisms that determine their dynamics. These are the growth of the yeast population, the conversion of sugar to ethanol, and the death of yeast cell due to toxic ethanol concentrations. The rest of this chapter is devoted to the description of a wine fermentation model, which will be used throughout this work.

2.1 A Wine Fermentation Model Using Ordinary Differential Equations

Wine has a long tradition for most cultures in the world. For thousands of years people have been producing wine and during the production of wine the fermentation is the last step. Oenologists say that the quality of wine is made in the vineyard by choosing the right type of grape for the given soil and taking care of the plant. Whereas the winemakers can only maintain the given quality of the must during the fermentation step. Nevertheless, one could improve the production of wine in terms of quality and cost efficiency by developing a good model for the wine fermentation process, to calibrate it and optimise the fermentation procedure in a desired way.

In the following, we discuss the wine fermentation model, which is used in the succeeding chapters and is based on the publications [CMS07, Vel09, DDM$^+$10, BMM$^+$14]. In our model the evolution of six relevant quantities is described by the functions X, N, O, S, E, and T, which are time dependent in the case of ordinary differential equation models, see Subsection 2.1.4, and also space dependent in the case of models with partial differential equations; see Section 2.2 and Section 2.3. We discuss them in detail here.

The reason why fruit juice when left alone changes its taste to sour and alcoholic is due to unicellular fungi called yeasts, which produce alcohols and acids within their metabolism. There are many different known yeast strains and the grape skin itself already contains plenty of different types of such micro-organisms. Nevertheless, these naturally arising yeast strains are undesirable in professional wine production. They introduce uncertainties in view of the reactions rapidity and the produced compounds that influence the taste of the product. Hence, winemakers usually choose a certain yeast strain, which is cultured for some special properties and is suitable for a desired taste of the produced wine. In the beginning of the fermentation, this yeast strain is added to the must. Therefore, we can assume that there is just one yeast strain present as other strains are unable to compete with the enormous number of cells of the added strain. The amount of yeast cells that are present at different points in time is important for the fermentation. Therefore, we must model the evolution of the yeast cell number, which we denote throughout this thesis by X, the concentration of the one main yeast strain. For models with partial differential equations X denotes not the total concentration in the fermenter, but the local concentration at a given point inside the tank.

Measurements during a fermentation process show that the initially added number of yeast cells rises significantly in the first few days and stagnates at a saturated level afterwards. This effect can be explained by the limitation of nutrients, which are available in the must. Hence, we must also track the amount of available nutrients in our model. Yeast cells need compounds with nitrogen to produce amino acids and build up their cell structures. Therefore, we collect within the function N the main ingredients for the growth and reproduction of yeast cells, namely the assimilable nitrogen sources.

Moreover, the available oxygen is of great importance as yeasts can metabolise energy aerobically or anaerobically. Elementary oxygen is initially solved in the must and as long as it is available, the yeast metabolism works aerobically, as in this case sugar is completely decomposed in carbon dioxide and water. This provides the yeast cell with a lot of energy, which they use for growth and reproduction. After some days, all of the oxygen is consumed, as the fermenter is usually held closed and no oxygen from the environment solves into the must. Besides the limited nitrogen sources, this is an additional reason why the increase of the yeast population stagnates after some days.

Therefore, we include the concentration of oxygen in our model denoted by the function O.

To motivate the next variable in our model, we mention that sugar is decomposed not only during an aerobic metabolism, but also in the absence of oxygen. In the latter case the yeast is not able to decompose sugar molecules completely into carbon dioxide and water. During the anaerobic metabolism, ethanol is formed and much less energy is produced by this conversion. Although this prohibits the yeast strain to reproduce very fast, it is sufficient for its survival and the population number is maintained. As the wine quality depends very strongly on both the final ethanol concentration and the consumption rate of sugar during the fermentation, it is indispensable to model the evolution of sugar and ethanol concentrations. In the following, the concentration of sugar is denoted by S and that of ethanol by E. Moreover, the role of ethanol is two-fold. It is not only the product of the alcoholic fermentation, but also changes the living conditions of the yeast. As the concentration of ethanol rises, two effects can be observed. On one hand, it inhibits the consumption of sugar and decreases the reaction rate at which sugar is turned into ethanol. On the other hand, very high ethanol concentrations are toxic for yeast cells so that they have to struggle to reproduce, which eventually leads to extinction.

The last relevant factor we consider is the role of the temperature, which is denoted by T. Most microbiological and chemical reactions happen faster in a warmer environment. Hence, the temperature of the must influences not only the reaction rates of the yeast metabolism, which accelerates the growth of its population, but also the sugar consumption rate and production of ethanol. Moreover, the fermentation process is an exothermic reaction and heat is produced, which accelerates the process. Therefore, the temperature of the must tends to rise quickly and thus large fermenter usually have some kind of a cooling system to maintain a temperature that is suitable for the desired aromatic profile of the produced wine.

After defining the relevant variables of wine fermentation, we describe in the following subsections how their interaction is modelled.

2.1.1 Yeast Growth

The yeast biomass concentration is a very important factor. A great increase of yeast cells is observed in the first few days of a wine fermentation. Hence, we give in the following a description of this phenomenon by ordinary differential equations. The simplest population growth model is given by the following linear equation

$$\frac{\mathrm{d}y}{\mathrm{d}t}(t) = \mu y(t), \qquad y(0) = y_0, \tag{2.1}$$

where μ denotes the reproduction rate. The solution to (2.1) is $y(t) = y_0 e^{\mu t}$ and it exhibits an exponential growth. While for small time scales and moderate population numbers exponential growth is indeed observed in nature, this model fails as soon as limited resources such as food or living space occur. Therefore, a reproduction rate that is dependent on such limitations is more appropriate. In the case of yeast growth, we assume that it occurs mainly during the aerobic phase and the nutrients that are necessary for reproduction are the assimilable nitrogen N, oxygen O, and sugar S.

Hence, we define the growth model for the yeast strain used in the fermentation process

as follows

$$\frac{\mathrm{d}X}{\mathrm{d}t} = \quad a_1\mu_1(N,O,S,T)X, \tag{2.2a}$$
$$\frac{\mathrm{d}N}{\mathrm{d}t} = -a_2\mu_1(N,O,S,T)X, \tag{2.2b}$$
$$\frac{\mathrm{d}O}{\mathrm{d}t} = -a_3\mu_1(N,O,S,T)X, \tag{2.2c}$$
$$\frac{\mathrm{d}S}{\mathrm{d}t} = -a_4\mu_1(N,O,S,T)X, \tag{2.2d}$$

where $a_i > 0$ $(i = 1,\dots,4)$ are yield coefficients and μ_1 is the reproduction rate of the yeast, which is dependent on the temperature and the concentrations of nitrogen, oxygen, and sugar. To ease the notation in (2.2) and the succeeding formulas, we omit to explicitly denote the time and possibly space dependency of functions. Here, we have a conservation property as

$$a_1\frac{\mathrm{d}N}{\mathrm{d}t} + a_1\frac{\mathrm{d}O}{\mathrm{d}t} + a_1\frac{\mathrm{d}S}{\mathrm{d}t} + (a_2+a_3+a_4)\frac{\mathrm{d}X}{\mathrm{d}t} = 0$$

holds. Hence, the linear combination $a_1(N+O+S)+(a_2+a_3+a_4)X$ is constant throughout the fermentation and is determined by the initial concentrations. This is due to the choice of the right-hand sides of (2.2) as we assume that the loss of nutrient mass is proportional to the mass of generated yeast cells. Moreover, we assume that the reproduction rate μ_1 is not only dependent on the nutrients N, O, and S but also on the temperature T. We define it as follows

$$\mu_1(N,O,S,T) = (T-b_1)\frac{N}{c_1+N}\frac{O}{c_2+O}\frac{S}{c_3+S}. \tag{2.3}$$

For the nutrients N, O, and S we include the Michaelis-Menten terms $\frac{N}{c_1+N}$, $\frac{O}{c_2+O}$, and $\frac{S}{c_3+S}$, which are used in [MM13, JG11] for the description of an enzymatic reaction and can be found in many models in microbiology. They lead to a saturation of the reaction rate for high concentrations and prohibit a reaction if any nutrient is consumed. The Michaelis constants $c_i > 0$ $(i = 1,\dots,3)$ correspond to the concentrations of the corresponding substance, where the reaction rate equals half the maximal possible reaction rate.

We remark that Michaelis-Menten kinetics usually feature a temperature dependent maximum reaction velocity $V(T)$ as a pre-factor, see [GR88] and [Fog10, Appendix C], which is modelled by the following Arrhenius function $V(T) = V_0\exp\left(\frac{-e}{R(T+273)}\right)$, where V_0 is the Arrhenius frequency factor, e is the Arrhenius activation energy, and R is the gas constant. The pre-factor $(T-b_1)$ in (2.3) can be seen as a linearisation of V, justified by the rather narrow temperature regime in which wine fermentation takes place. Clearly, this limits the applicability of our model. We mention that the inclusion of Arrhenius terms would not impose any significant mathematical difficulty, but for the sake of notational convenience and numerical implementation, we work with the linear temperature dependence of the reaction velocity as given in (2.3).

2.1.2 Sugar Consumption

Next, we focus on the modelling of the conversion of sugar into ethanol by the yeast culture. During the alcoholic fermentation each sugar molecule is decomposed into two ethanol molecules. Hence, we can assume that the change of the corresponding concentrations of sugar and ethanol is proportional. Moreover, it is well known that this reaction is

exothermic and the temperature of the must increases. We consider the following system of ordinary differential equations as a model for the sugar consumption

$$\frac{\mathrm{d}S}{\mathrm{d}t} = -a_5\mu_2(S,E,T)X, \tag{2.4a}$$
$$\frac{\mathrm{d}E}{\mathrm{d}t} = \quad a_6\mu_2(S,E,T)X, \tag{2.4b}$$
$$\frac{\mathrm{d}T}{\mathrm{d}t} = \quad a_7\mu_2(S,E,T)X. \tag{2.4c}$$

As the production of ethanol is done by each yeast cell, the conversion rate μ_2 on the right-hand side of (2.4) is multiplied by the yeast biomass concentration X. Similarly as in the growth model (2.2), we have yield coefficients $a_i > 0$ $(i = 5, \ldots, 7)$. The conversion rate μ_2 is given by

$$\mu_2(S,E,T) = (T - b_2)\frac{S}{c_4 + S}\frac{c_5}{c_5 + E}. \tag{2.5}$$

Similar to the reproduction rate μ_1, we assume a linear temperature dependence and a Michaelis-Menten term $\frac{S}{c_4+S}$ for sugar with an analogue argumentation as in Subsection 2.1.1. Moreover, the inhibition property of ethanol for the sugar consumption is taken into account by the term $\frac{c_5}{c_5+E}$, which yields a lower reaction rate for high ethanol concentrations. The parameter $c_5 > 0$ is equal to the concentration of ethanol, where the sugar consumption rate is half as high compared to the case of absent ethanol.

Finally, note that the energy equation (2.4c) can be derived from $\frac{\mathrm{d}T}{\mathrm{d}t}t = k\frac{\mathrm{d}E}{\mathrm{d}t}t$ and (2.4b). The factor k is dependent on the heat capacity and the density of the must as well as the energy production of the exothermic alcoholic fermentation. See [CMS07] and references therein for more details.

2.1.3 Ethanol Toxicity

As the reproduction rate in (2.2) is non-negative, the yeast biomass concentration in the wine fermentation model so far would increase until one of the nutrients is consumed and remain constant afterwards. But the late stage of a fermentation experiment shows rather a decline in the yeast population. This can be explained by the toxic influence of high ethanol concentrations. Hence, this feature must be included in the fermentation model. Similarly as in the growth equation (2.1), we assume that the yeast concentration declines with the ethanol dependent death rate $\Psi(E)$ according to

$$\frac{\mathrm{d}X}{\mathrm{d}t} = -\Psi(E)X. \tag{2.6}$$

For the analysis of an optimal control problem of the wine fermentation process in Chapter 3, we use the following term for the toxicity

$$\Psi(E) = \left(0.5 + \frac{1}{\pi}\arctan\left(k_1(E - E_{\mathrm{tol}})\right)\right)k_2(E - E_{\mathrm{tol}})^2. \tag{2.7}$$

Expression (2.7) represents a trigger function built from the inverse tangent function arctan, because ethanol acts toxic only above a certain tolerance value E_{tol}. Hence, in simulations, after an initial growth transient, we can observe a constant yeast population before an exponential decay of the number of living yeast cells sets in. This behaviour is in agreement with experimental measurements and is more realistic than a linear model of

toxicity, e.g. in [Vel09], where the yeast population immediately plunges after the growth phase is over.

Although the simulation results with a toxicity function defined by (2.7) seem quite promising, the quadratic behaviour beyond E_{tol} is rather an educated guess and cannot be underpinned by microbiological arguments. In general, the toxicity function Ψ is unknown and we present in Chapter 4 a method for the problem of identifying the shape of an unknown function in differential models.

2.1.4 Combined Model Equations

Having the sub-model equations for yeast growth (2.2), sugar consumption (2.4), and the ethanol induced death of yeast cells (2.6) at hand, we set up the full system of ordinary differential equations to describe the wine fermentation process. It combines the previously discussed features and is given by

$$\frac{\mathrm{d}X}{\mathrm{d}t} = a_1(T-b_1)\frac{N}{c_1+N}\frac{O}{c_2+O}\frac{S}{c_3+S}X - \Psi(E)X, \tag{2.8a}$$

$$\frac{\mathrm{d}N}{\mathrm{d}t} = -a_2(T-b_1)\frac{N}{c_1+N}\frac{O}{c_2+O}\frac{S}{c_3+S}X, \tag{2.8b}$$

$$\frac{\mathrm{d}O}{\mathrm{d}t} = -a_3(T-b_1)\frac{N}{c_1+N}\frac{O}{c_2+O}\frac{S}{c_3+S}X, \tag{2.8c}$$

$$\frac{\mathrm{d}S}{\mathrm{d}t} = -a_4(T-b_1)\frac{N}{c_1+N}\frac{O}{c_2+O}\frac{S}{c_3+S}X - a_5(T-b_2)\frac{S}{c_4+S}\frac{c_5}{c_5+E}X, \tag{2.8d}$$

$$\frac{\mathrm{d}E}{\mathrm{d}t} = a_6(T-b_2)\frac{S}{c_4+S}\frac{c_5}{c_5+E}X, \tag{2.8e}$$

$$\frac{\mathrm{d}T}{\mathrm{d}t} = a_7(T-b_2)\frac{S}{c_4+S}\frac{c_5}{c_5+E}X. \tag{2.8f}$$

In order to simulate a wine fermentation process, we must solve the initial-value problem consisting of equations (2.8) and corresponding initial concentrations and temperature. Moreover, the parameters a_i $(i = 1,\dots,7)$, b_i $(i = 1,2)$, and c_i $(i = 1,\dots,5)$ together with the toxicity function Ψ must be given. This data is different for each yeast strain and a parameter/function identification is necessary to calibrate the model to a specific application.

In Figure 2.1 the results of a simulated fermentation with representative parameters and initial conditions are presented. All previously discussed phenomena can be recognised. The yeast biomass concentration shown in the upper left plot rises in the first few days by a factor of about 100, stays constant for some days and then declines to zero due to the toxic ethanol concentrations. Moreover, the concentrations of the initially available nutrients nitrogen and oxygen rapidly go to zero as the yeast reproduce; see upper plots in the middle and on the right side. The reproduction stops as soon as the nutrients are consumed after approximately three days. The constant conversion of sugar into ethanol can be seen in the left and middle plot on the bottom. This process stops after about 25 days before the sugar in the must is converted completely, as the yeast culture dies out. The increase of the temperature of the must can be seen in the lower right plot.

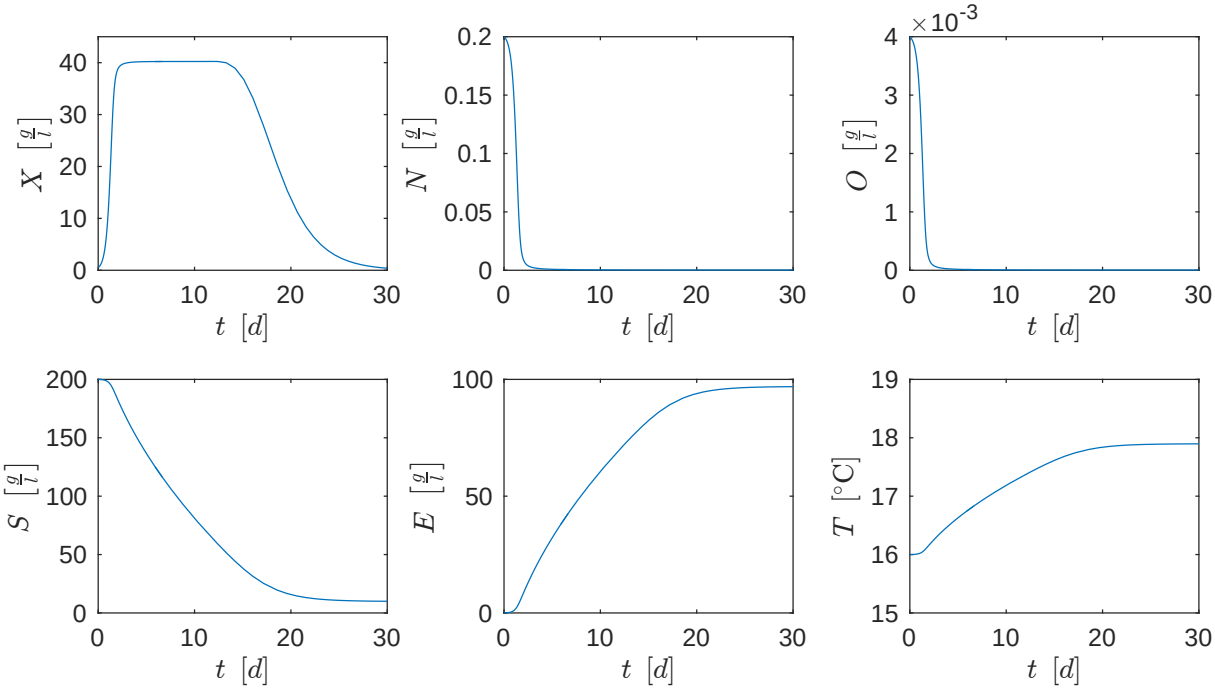

Figure 2.1: Simulation results for the wine fermentation model (2.8).

2.2 Extention by Fluid Dynamics

The wine fermentation model presented so far considers the average concentrations of the relevant variables in the fermenter and describes their evolution. The larger a fermentation vessel is the less we can assume that the must is a homogeneous medium. It is more likely to happen that different local concentrations, e.g., on the bottom and top of the vessel, arise and the spatial inhomogeneity should be incorporated in the model equations. To account for this phenomenon, we assume that the functions X, N, O, S, E, and T are not only dependent on the time variable t, but also on the space variable $x \in \Omega$, where the domain $\Omega \subset \mathbb{R}^3$ represents the interior of the fermenter. Collecting these function in a vector as $y = (X, N, O, S, E, T)^\top$ we model the evolution of the local concentrations with a system of convection-diffusion-reaction equations as follows

$$\frac{\partial y}{\partial t} + \mathbf{u} \cdot \nabla y - D\Delta y = f(y). \tag{2.9}$$

Here, the differential operators $\frac{\partial}{\partial t}$, $\mathbf{u} \cdot \nabla$, and $\Delta = \sum_{i=1}^{3} \frac{\partial^2}{\partial x_i^2}$ are meant to operate component-wise on the vector y, where the dot denotes the euclidean inner product as follows $\mathbf{u} \cdot \nabla = \sum_{i=1}^{3} u_i \frac{\partial}{\partial x_i}$. In (2.9), we assume that the time derivative of the considered variables equals the sum of three terms. The reaction term $f(y)$ on the right-hand side of the equation locally models the fermentation process as in Subsection 2.1.4, where the function $f : \mathbb{R}^6 \to \mathbb{R}^6$ is given by the right-hand side of the ordinary differential equations model (2.8). Moreover, we have the term $\mathbf{u} \cdot \nabla y$ for convection, which models the passive transport of concentrations and the temperature along the velocity field $\mathbf{u}$ of the fluid. Finally, the diffusion, which originates from the Brownian motion for a discrete model with particles, is modelled by the Laplace operator $D\Delta y$ on the continuous level. Here, $D = \mathrm{diag}(\sigma_1, \ldots, \sigma_6)$ is a diagonal matrix with diffusion coefficients σ_i $(i = 1, \ldots, 6)$ corresponding to the six functions X, N, O, S, E, and T, respectively.

The molecular diffusion is a very slow process and the homogenisation of a fluid is

mainly due to convective transport. Therefore, we focus now on determining the fluid velocity field $\mathbf{u}$. A model for fluid flow is given by the incompressible Navier-Stokes equations [LO13], which are as follows

$$\varrho \frac{\partial \mathbf{u}}{\partial t} + \varrho\, \mathbf{u} \cdot \nabla \mathbf{u} - \mu \Delta \mathbf{u} = -\nabla p + \varrho \mathbf{g}, \tag{2.10a}$$

$$\nabla \cdot \mathbf{u} = 0. \tag{2.10b}$$

The momentum equation is given by (2.10a), where ϱ is the density of the fluid, μ is the dynamic viscosity, p denotes the pressure, and $\mathbf{g} = (0, 0, -9.81 \frac{m}{s^2})$ is the gravitational acceleration vector. The incompressibility is encoded in the continuity equation (2.10b), which ensures a conservation of mass.

The density of the fluid, which is the must within the wine fermentation model, is actually not constant. On one hand, high sugar concentrations in the beginning lead to a higher density than water. On the other hand, at the end of the process, there is a lower density than water due to high ethanol concentration. Hence, there is a loss of mass, which is transported to the environment by leaked carbon dioxide. Nevertheless, we use the Boussinesq approximation ([Bou03] and [DR04, Chapter 2.7.2]), which assumes a constant density of the must for the left-hand side of the momentum equation (2.10a) to be $\varrho = \varrho_0$ and takes density changes only for the volume-force on the right-hand side into account. Then, the momentum equation (2.10a) can be written as follows

$$\frac{\partial \mathbf{u}}{\partial t} + \mathbf{u} \cdot \nabla \mathbf{u} - \nu \Delta \mathbf{u} = -\frac{1}{\varrho_0} \nabla p + \frac{\varrho}{\varrho_0} \mathbf{g}, \tag{2.11}$$

where $\nu = \frac{\mu}{\varrho_0}$ is the kinematic viscosity. In a non-reactive fluid, the temperature dependent density ϱ is approximated by the linear relation $\varrho = \varrho_0 \left(1 + \beta(T_0 - T)\right)$, where β is the thermal expansion coefficient of the fluid and T_0 denotes the reference temperature. As we also have dissolved substances in the must that change their concentrations, we must take their impact on the density into account. Therefore, consider a small control volume V of the must, where yeast biomass with concentration X is solved. The total volume splits up in the portion occupied by yeast cells V_X and the volume of pure must V_m, which yields $V = V_X + V_m$. The mass of the yeast contained in the control volume is $m_X = XV$, but can also be calculated as $m_X = \varrho_X V_X$, where ϱ_X is the density of yeast cells. The remaining mass $m_m = \varrho_0 V_m$ is the mass of pure must in the control volume. Hence, we compute

$$\begin{aligned}
\varrho &= \frac{m_X + m_m}{V} = \frac{XV + \varrho_0 V_m}{V} = X + \frac{\varrho_0 (V - V_X)}{V} \\
&= X + \varrho_0 \left(1 - \frac{m_X/\varrho_X}{V}\right) = X + \varrho_0 \left(1 - \frac{XV/\varrho_X}{V}\right) \\
&= \varrho_0 \left(1 + X \left(\frac{1}{\varrho_0} - \frac{1}{\varrho_X}\right)\right).
\end{aligned}$$

The same argument can also be applied to several numbers of dissolved substances with different densities. Hence, taking the temperature dependency as well as the concentrations of sugar S and ethanol E into account, we arrive at

$$\varrho = \varrho_0 \left(1 + \beta(T_0 - T)\right) \left(1 + \gamma_X X\right) \left(1 + \gamma_S S\right) \left(1 + \gamma_E E\right), \tag{2.12}$$

where $\gamma_C = \frac{1}{\varrho_0} - \frac{1}{\varrho_C}$ for $C \in \{X, S, E\}$.

Finally, we arrive at a system of partial differential equations for a model of the wine fermentation process, which also takes spatial inhomogeneities into account. It is given by

$$\frac{\partial y}{\partial t} + \mathbf{u} \cdot \nabla y - D\Delta y = f(y), \tag{2.13a}$$

$$\frac{\partial \mathbf{u}}{\partial t} + \mathbf{u} \cdot \nabla \mathbf{u} - \nu\Delta \mathbf{u} = -\frac{1}{\varrho_0}\nabla p + \tilde{\mathbf{g}}, \tag{2.13b}$$

$$\nabla \cdot \mathbf{u} = 0, \tag{2.13c}$$

where $\tilde{\mathbf{g}} = (1 + \beta(T_0 - T))\,(1 + \gamma_X X)\,(1 + \gamma_S S)\,(1 + \gamma_E E)\,\mathbf{g}$ is the density related gravitational volume-force. These equations are valid in $\Omega \times (0, t_f)$, namely the interior of the fermenter for all times of the time horizon of the simulation, where t_f denotes the final time.

Next, we discuss the boundary conditions. We assume that the fermenter is equipped with a valve. While formed carbon dioxide is transported to the environment due to an overpressure, additional oxygen cannot enter the vessel from the outside. Moreover, we assume that no additional must, nitrogen sources, or yeast strains are added. Therefore, there is no flux of the substances X, N, O, S, and E across the boundary and we apply homogeneous Neumann boundary conditions on $\Gamma := \partial\Omega$ as follows

$$\sigma_1 \frac{\partial X}{\partial n} = \sigma_2 \frac{\partial N}{\partial n} = \sigma_3 \frac{\partial O}{\partial n} = \sigma_4 \frac{\partial S}{\partial n} = \sigma_5 \frac{\partial E}{\partial n} = 0, \tag{2.14}$$

where n denotes the outward unit normal to Γ. For the temperature, we must estimate the heat flux through the fermentation tank wall, which is typically made out of steel for industrial purposes. According to [VDI02, p. A2, eq. (15)], the heat flux density from the interior of the fermentation tank is $\dot{q} = -\lambda \frac{\partial T}{\partial n}$, with the thermal conductivity λ of the fluid, namely must. Moreover the heat flux $\dot{Q} = \dot{q}A$ through the wall of area A of a heat exchanger is given by $\dot{Q} = kA(T_{\text{inner}} - T_{\text{outer}})$, where k is the heat transmittance coefficient; see [VDI02, eq. (1), p. Cb1]. Equating these expressions and dividing the resulting equation by the density ϱ_0 and heat capacity c_p one arrives at

$$\sigma_6 \frac{\partial T}{\partial n} = \frac{\lambda}{\varrho_0 c_p} \frac{\partial T}{\partial n} = \frac{k}{\varrho_0 c_p}(T_{\text{outer}} - T), \tag{2.15}$$

where $\sigma_6 = \frac{\lambda}{\varrho_0 c_p}$ denotes the thermal diffusivity of the fluid. As the fermentation is an exothermic reaction, in vessels of industrial size the must has to be cooled down to prevent too high temperatures. Therefore, cooling mechanisms have to be implemented. We assume that Γ_1 is exposed to the environment, while the other part of the boundary, i.e. $\Gamma_2 := \Gamma \setminus \Gamma_1$, is covered with a cooling cycle. The temperature of the coolant is denoted by u and can be controlled by the winemaker. Therefore, we impose the following boundary conditions for the temperature

$$\sigma_6 \frac{\partial T}{\partial n} = \begin{cases} \tau_{\text{air}}(T_{\text{ext}} - T) & \text{on } \Gamma_1 \times (0, t_f), \\ \tau_{\text{coolant}}(u - T) & \text{on } \Gamma_2 \times (0, t_f), \end{cases} \tag{2.16}$$

where T_{ext} is the external temperature. The positive parameters τ_{air} and τ_{coolant} represent the normalised thermal conductivity according to (2.15) of the fermenter wall exposed to air and coolant, respectively. This possibility to influence the wine fermentation process is

used in Chapter 3 in order to define an optimal control problem and to compute a control, which minimises the sugar concentration at the end of the process while keeping the average temperature as constant as possible. Moreover, we assume that the temperatures u and T_{ext} are homogeneous in space at each time point. Finally, we employ zero slip boundary conditions for the fluid velocity field $\mathbf{u}$, i.e.

$$\mathbf{u} = 0 \qquad \text{on } \Gamma \times (0, t_f). \tag{2.17}$$

For the numerical simulation of the wine fermentation process with spatial inhomogeneity and fluid dynamics we have to solve the convection-diffusion-reaction equations together with the incompressible Navier-Stokes equations (2.13) complemented with initial conditions for $(X, N, O, S, E, T, \mathbf{u})$ and the boundary conditions (2.14), (2.16), and (2.17). In Figure 2.2, we can see the results of one such numerical simulation in a two dimensional domain. The sub-figures show the distribution of the yeast biomass concentration within the fermenter at six different points in time. The initially concentrated yeast culture at the top of the fermentation vessel induces a flow field due to its higher density, which transports the biomass to the bottom of the tank. Note that the time horizon of this simulation is just about seven minutes.

The reason for this short time horizon is that the dimensions of the tank used for the simulation are 2.5 m in height and 1 m in width and the Navier-Stokes equations for this problem are computationally very expensive. The stability of a numerical solution to the Navier-Stokes equations depends on the given mesh, as these equations are highly nonlinear and tend to develop chaotic local behaviour in many situations. A fine resolution of boundary layers and vortices is inevitable for a stable simulation of convective dominant flows. Therefore, numerical errors due to too coarse mesh grids propagate quickly and lead to non-physical blow-ups in the numerical solution. If we pursue a direct numerical simulation, where no further modelling of turbulence like in the Reynolds-averaged Navier-Stokes equations or sub-grid models like in large eddy simulations are necessary, we have to use a very fine mesh. As the distance between neighbouring nodes in a fine mesh is small, the Courant-Friedrichs-Lewy (CFL) condition demands that the time steps, which are used for the time integration of the model equations, have to be small, too. These necessarily small time steps, which are fractions of seconds in the simulation presented in Figure 2.2, are not only needed for a stable numerical solution, but also for accuracy. The velocity field and also the concentrations are changing within seconds, which demands for a high temporal resolution. Consequently, as the time horizon of a fermentation process is about several days or even more than a month, millions of time steps are necessary and it is not possible to obtain a simulation result for the whole fermentation process in a reasonable amount of time.

Besides the fact that the proposed model in this section is computationally very expensive to solve, the question arises if these costs are paid back with a more accurate simulation of the wine fermentation process. It can be seen in both simulations and experiments that the motion of the fluid is very fast compared to the evolution of the reaction of alcoholic fermentation. Hence, two different time scales are involved. On one hand, the reactive part of the model needs several days to first produce a high yeast concentration and afterwards decompose the sugar. On the other hand, the fluid dynamics evolve within seconds or minutes, while the fermentation seems to stand still during this amount of time. Therefore, it is likely that the concentrations are well mixed considering the time scales, on which the fermentation takes place. We conclude that the computation of an accurate velocity field is not only very hard to achieve, but is also not relevant for

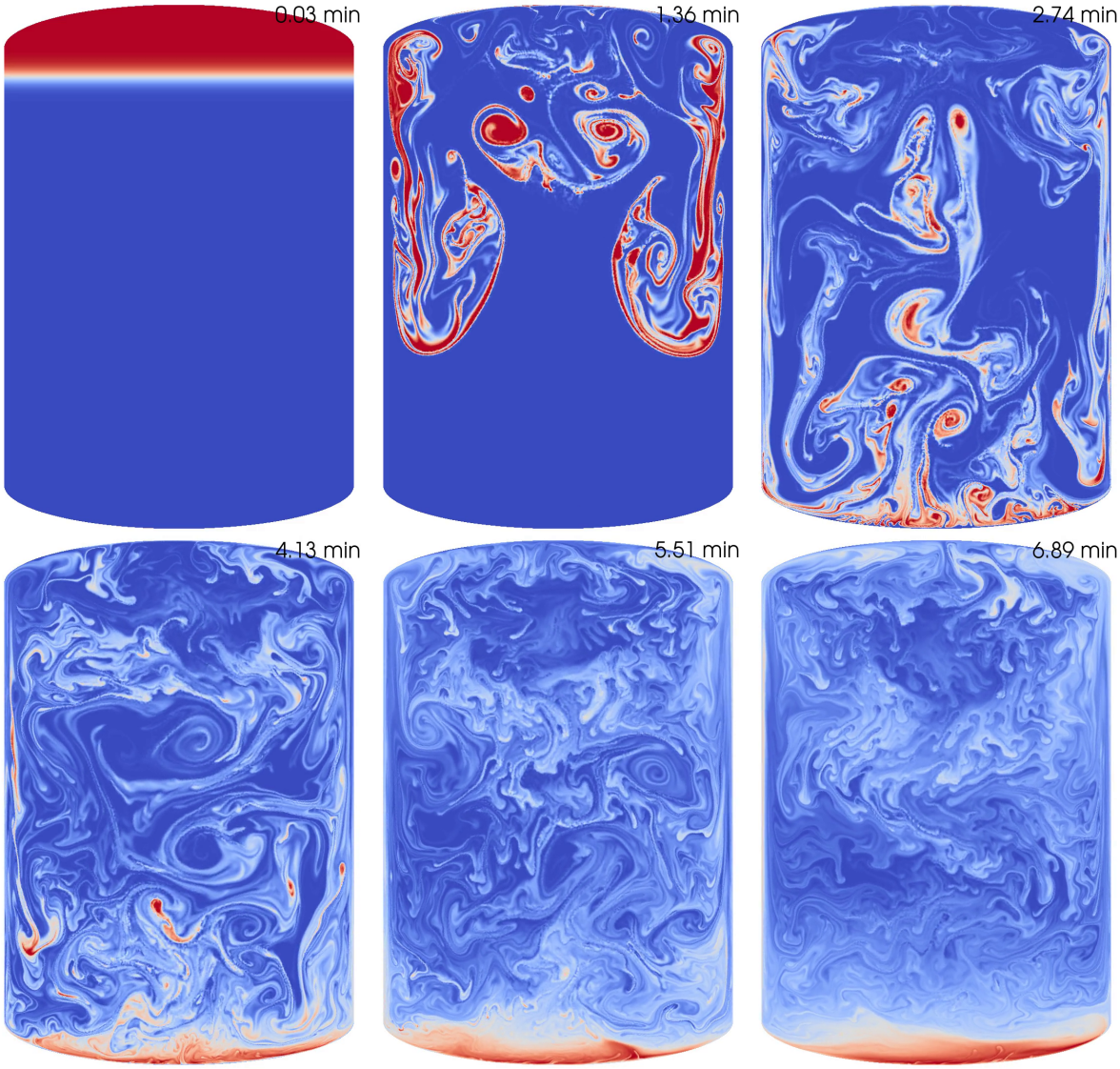

Figure 2.2: Evolution of yeast biomass concentration distributed within a 2D tank. Blue colour corresponds to a zero concentration, whereas high concentration are presented in red colour.

a good simulation of the fermentation. We rather need a more global idea of the distribution of concentrations and the temperature and present, therefore, a simplification of the model in the next section.

2.3 Reduction to Reaction-Diffusion Equations

In the present section, we give reason to the reduction of a wine fermentation model with the Navier-Stokes equations to a model consisting of a system of reaction-diffusion equations.

From the computational point of view it would be advantageous to leave out the convection term $\mathbf{u} \cdot \nabla y$ in (2.13a). On one hand, we would have no CFL-condition, which demands small time steps for stability reasons. On the other hand, the computationally very expensive Navier-Stokes equations could be omitted, as there would be no coupling

to the equations of the fermentation reaction. Nevertheless, by doing so, the spatial component of the model would be worthless. The reason is that the physical diffusion coefficients are too small. Assume that we approximate the physical properties of the must by that of water. In this case, the thermal diffusivity σ_6 is approximately $10^{-7}\,\mathrm{m/s^2}$; see [VDI02, p. Db1]. Moreover, the molecular diffusion coefficients σ_i $(i = 1, \dots, 5)$ have a scale of about $10^{-9}\,\mathrm{m/s^2}$ [NHG10, p. 25]. Without convection, only diffusion is responsible for the exchange of concentrations or temperature across the fermenter. In simulations with such small diffusion coefficients there would be almost no equalisation of spatial inhomogeneities, even during the pretty large time horizon in which the fermentation process takes place. Hence, diffusion is very slow for mixing substances, which is why often mixers are used to induce a fluid flow and to accelerate the homogenisation. To conclude, the convection in the must is an important process, which should not be omitted.

In order to overcome the difficulties that arise when using the Navier-Stokes equations we model the convection by diffusion. By defining a space dependent and possibly time dependent diffusion coefficient $\sigma_i(x,t)$ $(i = 1, \dots, 6)$ we try to mimic the homogenisation of concentration induced by convection. Provided that this approximation is valid on the global scale of the fermenter for large time intervals, the simulation results are only perturbed insignificantly, because the fermentation is a very slow process. Hence, we use the following system of reaction-diffusion equation to model the wine fermentation process for the optimal control problem analysed in Chapter 3:

$$\frac{\partial y}{\partial t} - D\Delta y = f(y) \quad \text{in } \Omega \times (0, t_f), \tag{2.18a}$$

$$D\frac{\partial y}{\partial n} + Zy = g(u) \quad \text{on } \Gamma \times (0, t_f), \tag{2.18b}$$

$$y(0) = y_0 \qquad \text{in } \Omega. \tag{2.18c}$$

The diffusivity coefficients $D = \mathrm{diag}(\sigma_1, \dots, \sigma_6)$ are functions defined in $\Omega \times (0, t_f)$. The fermentation reaction is modelled by the reaction term $f(y)$ that is given by the ordinary differential equations model (2.8). The matrix Z and function g are defined as follows

$$Z = \begin{cases} \mathrm{diag}(0,0,0,0,0,\tau_{\mathrm{air}}) & \text{on } \Gamma_1 \times (0, t_f), \\ \mathrm{diag}(0,0,0,0,0,\tau_{\mathrm{coolant}}) & \text{on } \Gamma_2 \times (0, t_f), \end{cases} \tag{2.19}$$

and

$$g(u) = \begin{cases} (0,0,0,0,0,\tau_{\mathrm{air}} T_{\mathrm{ext}})^\top & \text{on } \Gamma_1 \times (0, t_f), \\ (0,0,0,0,0,\tau_{\mathrm{coolant}}\, u)^\top & \text{on } \Gamma_2 \times (0, t_f). \end{cases} \tag{2.20}$$

in agreement with the boundary conditions (2.14) and (2.16) discussed in Section 2.2. Moreover, the initial conditions y_0 in (2.18c) have to be satisfied.

After having defined the equations modelling the wine fermentation process, we discuss the data that has to be provided for simulating a specific experiment. First, the parameters a_i $(i = 1, \dots, 7)$, b_i $(i = 1, 2)$, c_i $(i = 1, \dots, 5)$, and the toxicity function Ψ that define the reaction function f have to be estimated as they are likely to be different for each yeast strain in use. Moreover, the tank geometry influences the flow behaviour of the contained must. Hence, the space and time dependent diffusion coefficients σ_i $(i = 1, \dots, 6)$ have to be identified for the used fermenter such that they provide a good approximation of the mixing behaviour of concentrations and the transport of heat to the fermenter walls. The exchange of temperature at the tank walls is described by the

normalised thermal conductivity coefficients τ_{air} and τ_{coolant}. These parameters are dependent on the wall material and the cooling mechanism that is provided by the fermenter. The temperatures of the environment T_{ext} and the coolant u are comparatively simple to measure. Finally, the concentrations and the temperature $y_0 = (X_0, N_0, O_0, S_0, E_0, T_0)^\top$ at the beginning of the wine fermentation process have to be known. See Chapter 3 for the analysis and numerical simulation of this model.

To conclude this section, we discuss cases in which the model with reaction-diffusion equations is more favourable compared to a model without spatial resolution. While the zero dimensional model with ordinary differential equations (2.8) is very simple to solve its use is limited to cases with a small fermenter size and little must volume. As for small scale experiments spatial inhomogeneity is unlikely and the temperature is comparable to that of the environment, the extra computational effort of a three dimensional model (2.18) is not rewarded by a more accurate simulation. Nevertheless, for parameter and function identification problems as in Chapter 4, where measured data are obtained by small scale experiments, the use of a simple ordinary differential equations model is justified. In contrast, a more refined model with spatial resolution should be used for the computation of optimal controls of large scale wine production processes as is done in Chapter 3. On one hand, due to the large volume of an industrial fermenter, a homogeneous medium is unlikely and the modelling of the distribution of concentrations within the fermentation vessel is necessary. On the other hand, the temperature is a key factor that influences the reaction rates and a spatial resolution helps to compute its time evolution with greater accuracy. Moreover, the simulation of the vessel domain together with its boundary enables us to describe the cooling control mechanism mathematically in the definition of the boundary conditions, which is not possible for the model with ordinary differential equations.

Chapter 3

Optimal Control Methods for Reaction-Diffusion Equations

In this chapter, we investigate the properties of the wine fermentation model based on the reaction-diffusion equations (2.18). Moreover, we define an optimal control problem governed by these partial differential equation, which is designed to drive the process in a desired way. Therefore, we define in Section 3.1 the necessary function spaces that are used as the solution spaces for partial differential equations. Moreover, we collect results for both linear and non-linear parabolic equations that are used in the succeeding sections. In Section 3.2 some results in functional analysis, which are important to infinite dimensional optimisation, are summarised. In Section 3.3 we apply our results to the wine fermentation model. In particular, the proof for the existence of optimal controls is presented and the first-order necessary optimality conditions that characterise the solutions of the optimal control problem are given. Section 3.4 provides the numerical validation of the proposed framework.

3.1 Analysis of Parabolic Equations

In the following, we present some basic concepts concerning the study of parabolic equations. These are partial differential equations of first order in time with a second-order differential operator in space. The basic example for a parabolic equation is the following heat equation

$$\frac{\partial y}{\partial t} - \sigma \Delta y = 0,$$

which is supposed to model the time evolution of the temperature in a body with a thermal diffusivity constant σ. The Laplace operator Δ is defined by $\Delta y = \sum_{i=1}^{n} \frac{\partial^2 y}{\partial x_i^2}$. A more general second-order differential operator is given by

$$Ay \coloneqq \sum_{i,j=1}^{n} \frac{\partial}{\partial x_i} \left(a_{ij} \frac{\partial y}{\partial x_j} \right),$$

where the positive definite matrix of functions a_{ij} can be space and time dependent. Under reasonable assumptions on the operator A the theory works in the same manner as for a constant diffusion coefficient σ. We present the latter case in the following.

The distribution and diffusion of solved substances in a fluid can also be modelled by the heat equation [Ein05]. Moreover, there are a lot of applications where these substances

participate in a chemical or biological reaction. Combining these two features we call a differential equation of the following type

$$\frac{\partial y}{\partial t} - \sigma \Delta y = f(y)$$

a reaction-diffusion equation, where the possibly non-linear function f models the reaction dynamics.

3.1.1 Function Spaces

We consider real-valued functions defined in a Lipschitz domain, i.e. a bounded open set $\Omega \subset \mathbb{R}^n$ with boundary $\Gamma = \partial\Omega$ that is locally a graph of a Lipschitz continuous function. The results of this section can be found in [AF03, DL92, Trö10].

Lebesgue spaces

We assume that the reader is familiar with the basics of measure theory and the Lebesgue measure. For $1 \leq p < \infty$ the function space $L^p(\Omega)$ consist of equivalent classes of measurable functions u for which the following integral is finite

$$\int_\Omega |y(x)|^p \mathrm{d}x < \infty.$$

Here, functions $y, v \in L^p(\Omega)$ that differ only on a set of measure zero are identified. Moreover, we say that a statement holds almost everywhere (a.e.) in Ω, if it does not hold only in a subset of Ω of measure zeros. We use the notation $y = v$ a.e. in Ω. The space $L^p(\Omega)$ equipped with the norm

$$\|y\|_{L^p(\Omega)} = \left(\int_\Omega |y(x)|^p \mathrm{d}x \right)^{\frac{1}{p}},$$

is a Banach space. For $p = \infty$ the Banach space of measurable functions that are essentially bounded is denoted by $L^\infty(\Omega)$ and the corresponding norm is

$$\|y\|_{L^\infty(\Omega)} = \operatorname*{ess\,sup}_{x \in \Omega} |y(x)|,$$

where the essential supremum is defined as follows

$$\operatorname*{ess\,sup}_{x \in \Omega} |y(x)| = \min \left\{ K \in \mathbb{R}; |y(x)| \leq K \text{ a.e. in } \Omega \right\}.$$

Note that in a bounded domain Ω each function $y \in L^q(\Omega)$ is also in the space $L^p(\Omega)$ for $1 \leq p \leq q \leq \infty$; see [AF03, Theorem 2.14]. This is proven by the following Hölder inequality

$$\int_\Omega |y(x)|^p \, \mathrm{d}x \leq \left(\int_\Omega 1 \, \mathrm{d}x \right)^{1-\frac{p}{q}} \left(\int_\Omega |y(x)|^q \, \mathrm{d}x \right)^{\frac{p}{q}}.$$

In the following, we omit the argument of functions defined in Ω to ease notation.

Sobolev spaces

Sobolev spaces are used in the theory of elliptic equations. They provide us with the possibility to cast an elliptic partial differential equation into an operator equation in the dual space of a Sobolev space. Also in the theory of parabolic differential equations Sobolev spaces play a crucial role. For the necessary definition of weak derivatives we denote by $L^1_{\text{loc}}(\Omega)$ the space of functions that are integrable on every compact set in Ω.

Definition 1 *A function $y \in L^1_{\text{loc}}(\Omega)$ is called **weakly differentiable** with respect to x_i, if the exists a function $w \in L^1_{\text{loc}}(\Omega)$ and*

$$\int_\Omega y \frac{\partial v}{\partial x_i} \,\mathrm{d}x = -\int_\Omega wv \,\mathrm{d}x$$

holds for all functions $v \in C_0^\infty(\Omega)$, which is the space of compactly supported functions that are infinitely many times differentiable. The function w is called weak derivative of y with respect to x_i and is denoted by $\frac{\partial y}{\partial x_i}$.

Definition 2 *For $1 \le p \le \infty$ and the integer $m \ge 0$ the **Sobolev space** $W^{m,p}(\Omega)$ consists of all function u that have weak partial derivatives up to order m, which all belong to the space $L^p(\Omega)$. In particular, for each multi-index $\alpha = (\alpha_1, \dots, \alpha_n) \in \mathbb{N}_0^n$ with $|\alpha| = \sum_{i=1}^n \alpha_i \le m$ we have $\frac{\partial^{|\alpha|} y}{\partial x_1^{\alpha_1} \dots \partial x_n^{\alpha_n}} \in L^p(\Omega)$. Moreover, the space $W^{m,p}(\Omega)$ is a Banach space with respect to the Sobolev norm*

$$\|y\|_{W^{m,p}(\Omega)} = \left(\sum_{|\alpha| \le m} \left\| \frac{\partial^{|\alpha|} y}{\partial x_1^{\alpha_1} \dots \partial x_n^{\alpha_n}} \right\|^p_{L^p(\Omega)} \right)^{\frac{1}{p}}.$$

The case $p = 2$ plays a special role as the corresponding space is also a Hilbert space. We use the notation $H^m(\Omega) = W^{m,2}(\Omega)$.

In order to address boundary conditions, we need to know in which spaces the restrictions to the boundary of a function in a Sobolev space are contained. The following theorem considering traces of Sobolev functions can be found in [Trö10, Theorem 2.1].

Theorem 1 *Let Ω be a bounded Lipschitz domain and let $1 \le p \le \infty$. Then there exists a bounded, linear mapping $\tau : W^{1,p}(\Omega) \to L^p(\Gamma)$ such that for all $y \in W^{1,p}(\Omega) \cap C(\bar{\Omega})$ the values of $\tau(y)$ and y coincide on Γ.*

The following Sobolev embedding theorem examines how the integrability of functions and their weak derivatives can be improved by reducing the maximal order of differentiability; see [AF03, Theorem 4.12]. An embedding $X \hookrightarrow Y$ for two Banach spaces $(X, \|\cdot\|_X)$ and $(Y, \|\cdot\|_Y)$ is present, if every element of X is also contained in Y and there exists a constant C such that

$$\|x\|_X \le C\|x\|_Y,$$

for all $x \in X$.

Theorem 2 *Let $\Omega \subset \mathbb{R}^n$ be a Lipschitz domain. For $1 \le p < \infty$ and the integers $j \ge 0$ and $m \ge 1$ the following embedding holds*

$$W^{j+m,p}(\Omega) \hookrightarrow W^{j,q}(\Omega),$$

where the maximal integrability q can be chosen according to the following three cases:

1. *For $mp > n$ (equality is allowed for $p = 1$) the space dimension n is low compared to the integrability and differentiability properties and the embedding holds for*

$$p \leq q \leq \infty.$$

2. *For the limit case $mp = n$ infinity is excluded for q as the embedding holds only for*

$$p \leq q < \infty.$$

3. *For $mp < n$, we have a comparably high space dimension and get less additional integrability as the embedding holds for*

$$p \leq q \leq \frac{np}{n - mp}.$$

The analogue for compact embeddings is given by the Rellich-Kondrachov theorem [AF03, Theorem 6.3]. An embedding is called compact, if the inclusion operator $i : X \to Y, i(x) = x$ is compact, i.e. bounded sets in X are mapped on pre-compact sets in Y.

Theorem 3 *Let $\Omega \subset \mathbb{R}^n$ be a Lipschitz domain. For $1 \leq p < \infty$ and the integers $j \geq 0$ and $m \geq 1$ the following embedding is compact*

$$W^{j+m,p}(\Omega) \hookrightarrow W^{j,q}(\Omega),$$

where maximal integrability q can be chosen according to the following two cases:

1. *For $mp \geq n$*

$$1 \leq q < \infty.$$

2. *For $mp < n$*

$$1 \leq q < \frac{np}{n - mp}.$$

Notice that it is sufficient to reduce the integrability parameter q of the target space by an arbitrarily small ε to render the embedding in Theorem 2 compact.

The Lebesgue and Sobolev spaces defined above take values in $\mathbb{R}$. As we have a system of equations modelling the wine fermentation process, there are space involved that are vector-valued. For these spaces we use the notation $L^2(\Omega; \mathbb{R}^m)$ and $H^1(\Omega; \mathbb{R}^m)$, etc., and a function $y : \Omega \to \mathbb{R}^m$ is an element of these spaces, if all its components are elements of the corresponding real-valued function spaces.

Abstract functions and spaces involving time

In the definitions of Lebesgue and Sobolev spaces we consider real-valued functions. Similar definitions can be made for functions that take values in some Banach space X. In the following, functions spaces involving time are defined to address time-dependent problems; see [DL92, Trö10].

Definition 3 *Let X be a Banach space and $t_f > 0$. We call $y : [0, t_f] \to X$ an abstract function. The space of continuous abstract functions with values in X is denoted by*

$C([0,t_f];X)$ and its norm is $\|y\|_{C([0,t_f];X)} \coloneqq \max\limits_{0\le t\le t_f} \|y(t)\|_X$. Moreover, by defining measurable abstract functions in an analogous way as in the real-valued case the definition of the Lebesgue spaces for $1 \le p < \infty$ is

$$L^p(0,t_f;X) \coloneqq \left\{ y : (0,t_f) \to X \,\middle|\, \int_0^{t_f} \|y(t)\|_X^p \,\mathrm{d}t < \infty \right\},$$

which is a Banach space with the corresponding norm. The space of essentially bounded abstract functions $L^\infty(0,t_f;X)$ is defined similarly as in the real-valued case.

Parabolic partial differential equations contain the derivative with respect to time. For the following theory is suffices that the time derivative is a mapping with values in the dual space of X and not with values in X. Therefore, we define distributional derivatives [Trö10].

Definition 4 *Let $y \in L^2(0,t_f;X)$. Then we define a **vector-valued distribution** $T : C_0^\infty(0,t_f) \to X$ by*

$$T(v) \coloneqq \int_0^{t_f} y(t)v(t) \,\mathrm{d}t,$$

*where the integral is meant in the Bochner sense [HP57, Yos80]. Its **distributional derivative** $T' : C_0^\infty(0,t_f) \to X$ is defined by*

$$T'(v) \coloneqq -\int_0^{t_f} y(t)v'(t) \,\mathrm{d}t,$$

and is denoted by $\frac{\mathrm{d}y}{\mathrm{d}t}$.

In the following, we describe the idea of a evolution triple that is central for the theory of parabolic partial differential equations. Assume that V and H are two separable Hilbert spaces, where V is densely embedded in H. Note that in this case the embedding $H^* \hookrightarrow V^*$ is also dense. By identifying the space H with its dual H^* by the Riesz representation theorem we get the following chain of embeddings, which is called an evolution triple

$$V \hookrightarrow H \hookrightarrow V^*.$$

Definition 5 *The space $W(0,t_f)$ is defined as the space of all functions $y \in L^2(0,t_f;V)$ with distributional derivative $\frac{\mathrm{d}y}{\mathrm{d}t} \in L^2(0,t_f;V^*)$.*

See [DL92, Chapter XVIII, §1, Proposition 6, Theorem 1, Theorem 2] for a proof of the following theorem.

Theorem 4 *The space $W(0,t_f)$ is a Hilbert space with inner product*

$$(y_1,y_2)_{W(0,t_f)} = \int_0^{t_f} (y_1,y_2)_V \,\mathrm{d}t + \int_0^{t_f} (y_1',y_2')_{V^*} \,\mathrm{d}t$$

and norm

$$\|y\|_{W(0,t_f)} = \left(\int_0^{t_f} \|y\|_V^2 \, \mathrm{d}t + \int_0^{t_f} \|y'\|_{V^*}^2 \, \mathrm{d}t \right)^{\frac{1}{2}}$$

is continuously embedded in $C([0,t_f];H)$ *and the following integration by parts formula is valid for every* $y_1, y_2 \in W(0,t_f)$

$$\int_0^{t_f} \langle y_1', y_2 \rangle_{V^*,V} \, \mathrm{d}t = (y_1(t_f), y_2(t_f))_H - (y_1(0), y_2(0))_H - \int_0^{t_f} \langle y_2', y_1 \rangle_{V^*,V} \, \mathrm{d}t.$$

Moreover, the following holds for all $v \in V$,

$$\frac{\mathrm{d}}{\mathrm{d}t}(y(\cdot), v)_H = \langle y', v \rangle_{V^*,V}.$$

Note that the evaluation of a function in $W(0,t_f)$ at some time point is only possible due to the embedding $W(0,t_f) \hookrightarrow C([0,t_f];H)$. Hence, we are able to prescribe initial conditions for parabolic equations.

Moreover, the following theorem due to Aubin and Lions states a compact embedding result for spaces involving time. It is used to prove the strong convergence of the non-linear term of the system of reaction-diffusion equations in Subsection 3.3.2.

Theorem 5 *Let* V_0, V_1, *and* V_2 *be Banach spaces such that* V_0 *and* V_2 *are reflexive. Moreover, we have that the embedding* $V_0 \hookrightarrow V_1$ *is compact and the embedding* $V_1 \hookrightarrow V_2$ *is continuous. Then for* $1 < p, q < \infty$ *the embedding*

$$W(0,t_f) = \left\{ y \in L^p(0,t_f;V_0); \frac{\mathrm{d}y}{\mathrm{d}t} \in L^q(0,t_f;V_2) \right\} \hookrightarrow L^p(0,t_f;V_1)$$

is compact.

The proof can be found in [Aub63, Theorem 5.1], [Lio69, Theorem 12.1], and [Sho97, Chapter III.1, Proposition 1.3].

3.1.2 Linear Equations

In the following, we give some known results on the theory of linear parabolic equations. There are several ways to tackle the task of proving the existence of solutions to this kind of partial differential equations. We could use the theory of semigroups, as the second-order elliptic operator defines under high regularity assumptions a semigroup, which can be seen as the flow of a differential equation in Banach space subject to its generator. The corresponding theory is developed in , e.g., [DL92, Chapter XVII], but we will not use this theory, as we want to work with time dependent boundary conditions. Hence, we rely on the variational approach that is described in [DL92, Chapter XVIII], in which the space $W(0,t_f)$ is used and weak solutions are considered. First, we cite the following very general theorem and apply it afterwards for our problem.

Theorem 6 *Let* $V \hookrightarrow H \hookrightarrow V^*$ *be an evolution triple. Moreover, let the time-dependent bilinear form* $a : [0,t_f] \times V \times V \to \mathbb{R}$ *satisfy*

$$|a(t,y,v)| \leq M\|y\|_V\|v\|_V,$$
$$a(t,y,y) + m_1\|y\|_H^2 \geq m_2\|y\|_V^2,$$

for constants $M, m_1, m_2 > 0$ and all $y, v \in V$, $t \in [0, t_f]$. Assume that the function $t \mapsto a(t, y, v)$ is measurable for all $y, v \in V$. Further, let $y_0 \in H$ and $F \in L^2(0, t_f, V^*)$ be given. Then there exists exactly one $y \in W(0, t_f)$ that satisfies $y(0) = y_0$ and the variational problem

$$\frac{\mathrm{d}}{\mathrm{d}t}(y(\cdot), v)_H + a(\cdot; y(\cdot), v) = F(\cdot; v)$$

for all $v \in V$ in the sense of distributions. Moreover, the following stability result holds

$$\|y\|_{W(0,t_f)} \leq c \left(\|y_0\|_H + \|F\|_{L^2(0,t_f;V^*)} \right)$$

with a constant $c > 0$ independent of y_0 and F.

This theorem and its proof can be found in [DL92, Chapter XVIII, §3, Theorem 1, Theorem 2, Theorem 3], where the approximation of V by an orthonormal basis is used to construct a sequence of functions that satisfy the variational equality in a finite-dimensional subspace of V. Together with derived energy estimates one proves the convergence of this sequence to the unique solution of the problem. This method is called Galerkin approximation.

For the purpose of proving the solvability of the system of reaction-diffusion equations (2.18) we need results on the following linear second-order differential equation of parabolic type.

$$\frac{\partial y}{\partial t} - \sigma \Delta y + \alpha\, y = f \quad \text{in } Q, \tag{3.1a}$$

$$\sigma \frac{\partial y}{\partial n} + \beta\, y = g \quad \text{on } \Sigma, \tag{3.1b}$$

$$y(0) = y_0 \quad \text{in } \Omega, \tag{3.1c}$$

where the diffusion coefficient σ is a positive real number, the functions α and f are defined in the space-time cylinder $Q \coloneqq \Omega \times (0, t_f)$. Moreover, function β and g are defined in the parabolic boundary $\Sigma \coloneqq \Gamma \times (0, t_f)$ and the initial condition y_0 is defined in Ω. The space and, possibly, time dependency of the afore mentioned function is suppressed in the following to ease the notation.

In the following, we give some ideas that motivate the definition of weak solutions. Assume for the moment that all involved functions are regular enough to justify the computations that follow. Let v be a function defined in Ω. By multiplying the differential equation (3.1a) with v and integrating over Ω we arrive at

$$\int_\Omega \frac{\partial y}{\partial t}\, v - \sigma\, \Delta y\, v + \alpha\, y\, v \,\mathrm{d}x = \int_\Omega f\, v \,\mathrm{d}x.$$

Applying Green's identity for the term $\Delta y\, v$ and changing the order of integration and differentiation with respect to time we get

$$\frac{\partial}{\partial t} \int_\Omega y\, v \,\mathrm{d}x + \int_\Omega \sigma\, \nabla y \cdot \nabla v + \alpha\, y\, v \,\mathrm{d}x = \int_\Omega f\, v \,\mathrm{d}x + \int_\Gamma \sigma \frac{\partial y}{\partial n}\, v \,\mathrm{d}s.$$

We substitute the boundary conditions (3.1b) as follows

$$\frac{\partial}{\partial t} \int_\Omega y\, v \,\mathrm{d}x + \int_\Omega \sigma\, \nabla y \cdot \nabla v + \alpha\, y\, v \,\mathrm{d}x + \int_\Gamma \beta\, y\, v \,\mathrm{d}s = \int_\Omega f\, v \,\mathrm{d}x + \int_\Gamma g\, v \,\mathrm{d}s.$$

By defining the following time dependent bilinear form

$$a(t; y, v) = \int_\Omega \sigma \nabla y \cdot \nabla v + \alpha(t)\, y\, v \,\mathrm{d}x + \int_\Gamma \beta(t)\, y\, v \,\mathrm{d}s \tag{3.2}$$

and the following linear functional

$$F(t; v) = \int_\Omega f(t)\, v \,\mathrm{d}x + \int_\Gamma g(t)\, v \,\mathrm{d}s, \tag{3.3}$$

we conclude that the solution y of the linear parabolic partial differential equation (3.1) satisfies

$$\frac{\mathrm{d}}{\mathrm{d}t}(y(t), v)_{L^2(\Omega)} + a(t; y(t), v) = F(t; v),$$

for all v. This set-up fits in the context of Theorem 6 and we present the necessary details in the following. Note that we explicitly denote the time dependence of relevant functions, but suppresse the dependence on the space variable x. Moreover, we conclude that the following setting is sufficient to have all terms of the variational problem well defined. We choose for the space $W(0, t_f)$ the evolution triple $V \hookrightarrow H \hookrightarrow V^*$, where we define $V = H^1(\Omega)$, as the gradient of y and v is involved in (3.2) and has to be square integrable. Further, the time derivative of the $L^2(\Omega)$ inner product is considered, which is why we define $H = L^2(\Omega)$. Note that $L^2(\Omega)$ is densely embedded in $H^1(\Omega)$ and we, indeed, have the evolution triple $H^1(\Omega) \hookrightarrow L^2(\Omega) \hookrightarrow H^1(\Omega)^*$. For the boundary integrals we need the domain to have a Lipschitz continuous boundary in order to use Theorem 1 and guarantee their existence. Finally, we define the notion of weak solutions of linear parabolic equations as follows.

Definition 6 *We call $y \in W(0, t_f)$ a weak solution of the problem (3.1) if $y(0) = y_0$ holds in $L^2(\Omega)$ and*

$$\frac{\mathrm{d}}{\mathrm{d}t}\int_\Omega y\, v \,\mathrm{d}x + \int_\Omega \sigma \nabla y \cdot \nabla v + \alpha\, y\, v \,\mathrm{d}x + \int_\Gamma \beta\, y\, v \,\mathrm{d}s = \int_\Omega f\, v \,\mathrm{d}x + \int_\Gamma g\, v \,\mathrm{d}s$$

is valid for all $v \in H^1(\Omega)$ in the sense of distributions.

Now, we can state and prove the following theorem that is used multiple times in Subsection 3.3.1 to prove existence and uniqueness of solutions of the wine fermentation model.

Theorem 7 *If $\sigma > 0$, $\alpha \in L^\infty(Q)$, $\beta \in L^\infty(\Sigma)$, $\beta \geq 0$ a.e. in Q, $f \in L^2(Q)$, $g \in L^2(\Sigma)$ and $y_0 \in L^2(\Omega)$, then there exists a unique weak solution $y \in W(0, t_f)$ for the following linear parabolic equation*

$$\frac{\partial y}{\partial t} - \sigma \Delta y + \alpha\, y = f \quad \text{in } Q, \tag{3.4a}$$

$$\sigma \frac{\partial y}{\partial n} + \beta\, y = g \quad \text{on } \Sigma, \tag{3.4b}$$

$$y(0) = y_0 \quad \text{in } \Omega. \tag{3.4c}$$

and there is a constant c independent of f, g, and y_0 such that

$$\|y\|_{W(0,t_f)} \leq c \left(\|y_0\|_{L^2(\Omega)} + \|g\|_{L^2(\Sigma)} + \|f\|_{L^2(Q)} \right).$$

Furthermore,

(i) if $f \geq 0$, $g \geq 0$, and $y_0 \geq 0$ holds, then $y \geq 0$ a.e. in Q.

(ii) if $\alpha \geq 0$, $f = \beta = g = 0$, $y_0 \in L^\infty(\Omega)$ and $y_0 \geq 0$ holds, then

$$0 \leq y \leq \|y_0\|_{L^\infty(\Omega)}.$$

Proof. In order to prove this theorem, we show that for the bilinear form a defined in (3.2) and the right-hand side F defined in (3.3) all assumption of Theorem 6 are satisfied. First, we note that the initial conditions y_0 is in $H = L^2(\Omega)$.

Then, we focus on the time dependent bilinear form $a : [0, t_f] \times H^1(\Omega) \times H^1(\Omega) \to \mathbb{R}$ defined in (3.2). This mapping is well defined as α is essentially bounded and the functions y and v as well as their gradients ∇y and ∇v are in $L^2(\Omega)$, which has the existence of the first integral in (3.2) as a consequence. The second boundary integral is also well defined as the trace of $H^1(\Omega)$ functions is in $L^2(\Gamma)$ by Theorem 1 and β is essentially bounded. Moreover, the linearity of a in y and v is clear and the measurability of $t \to a(t, y, v)$ follows from the fact that α and β are measurable functions.

For the necessary estimates in Theorem 6, let $y, v \in H^1(\Omega)$. Then, for almost all $t \in [0, t_f]$, we compute with the aid of the Cauchy-Schwarz inequality the following estimate

$$\begin{aligned}
|a(t, y, v)| \leq& \int_\Omega |\sigma \nabla y \cdot \nabla v + \alpha(t)\, y\, v| \,\mathrm{d}x + \int_\Gamma |\beta(t)\, y\, v| \,\mathrm{d}s \\
\leq& |\sigma| \|\nabla y\|_{L^2(\Omega)} \|\nabla v\|_{L^2(\Omega)} + \|\alpha\|_{L^\infty(Q)} \|y\|_{L^2(\Omega)} \|v\|_{L^2(\Omega)} \\
&+ \|\beta\|_{L^\infty(\Sigma)} \|y\|_{L^2(\Gamma)} \|v\|_{L^2(\Gamma)},
\end{aligned}$$

which leads to

$$|a(t, y, v)| \leq \left(|\sigma| + \|\alpha\|_{L^\infty(Q)} + c_\tau^2 \|\beta\|_{L^\infty(\Sigma)}\right) \|y\|_{H^1(\Omega)} \|v\|_{H^1(\Omega)},$$

where c_τ is the norm of the trace operator in Theorem 1. This shows that the bilinear form $a(t, \cdot, \cdot)$ is continuous for almost all $t \in [0, t_f]$.

For the coercivity estimate, we have

$$\begin{aligned}
a(t, y, y) =& \int_\Omega \sigma \nabla y \cdot \nabla y + \alpha(t)\, y^2 \,\mathrm{d}x + \int_\Gamma \beta(t)\, y^2 \,\mathrm{d}s \\
\geq& \sigma \|\nabla y\|^2_{L^2(\Omega)} - \|\alpha\|_{L^\infty(Q)} \|y\|^2_{L^2(\Omega)} \\
=& \sigma \|y\|^2_{H^1(\Omega)} - \left(\|\alpha\|_{L^\infty(Q)} + \sigma\right) \|y\|^2_{L^2(\Omega)},
\end{aligned}$$

where the boundary integral disappears because of $\beta \geq 0$ a.e. in Σ.

Finally, we show that $F \in L^2(0, t_f; H^1(\Omega)^*)$, which is defined in (3.3). For a fixed $t \in [0, t_f]$ we estimate

$$\begin{aligned}
|F(t, v)| \leq& \int_\Omega |f(t)\, v| \,\mathrm{d}x + \int_\Gamma |g(t)\, v| \,\mathrm{d}s \\
\leq& \|f(t)\|_{L^2(\Omega)} \|v\|_{L^2(\Omega)} + \|g(t)\|_{L^2(\Gamma)} \|v\|_{L^2(\Gamma)} \\
\leq& \left(\|f(t)\|_{L^2(\Omega)} + c_\tau \|g(t)\|_{L^2(\Gamma)}\right) \|v\|_{H^1(\Omega)}
\end{aligned}$$

and conclude that the linear, continuous operator $v \mapsto F(t, v)$ is an element of $H^1(\Omega)^*$ with norm $\|F(t, \cdot)\|_{H^1(\Omega)^*} \leq \|f(t)\|_{L^2(\Omega)} + c_\tau \|g(t)\|_{L^2(\Gamma)}$. Hence, we prove $F \in L^2(0, t_f; H^1(\Omega)^*)$,

as

$$\int_0^{t_f} \|F(t,\cdot)\|^2_{H^1(\Omega)^*}\,\mathrm{d}t \le \int_0^{t_f} 2\|f(t)\|^2_{L^2(\Omega)} + 2c_\tau^2\|g(t)\|^2_{L^2(\Gamma)}\,\mathrm{d}t = 2\|f\|^2_{L^2(Q)} + 2c_\tau^2\|g\|^2_{L^2(\Sigma)} < \infty$$

holds. Due to Theorem 6, we know that there exists a unique weak solution $y \in W(0,t_f)$ of (3.4) and a constant c such that

$$\begin{aligned}\|y\|_{W(0,t_f)} \le& c\left(\|y_0\|_H + \|F\|_{L^2(0,t_f;V^*)}\right)\\ \le& c\left(\|y_0\|_H + \sqrt{2}\|f\|_{L^2(Q)} + \sqrt{2}c_\tau\|g\|_{L^2(\Sigma)}\right).\end{aligned}$$

Hence, the claimed stability result holds.

In order to prove (i) and (ii) we use the same ideas as in [DL92, Chapter XVIII, §4.5]. The space $H^1(\Omega)$ is stable under the mappings $v \mapsto v^+ := \max(0,v)$ and $v \mapsto v^- := \min(0,v)$, i.e., $v^+, v^- \in H^1(\Omega)$ for all $v \in H^1(\Omega)$; see [DL88, Chapter IV, §7, Proposition 6]. Note that $v(x)v^-(x) = (v^-(x))^2$ hold a.e. in Ω. For (i) assume that $f, g, y_0 \ge 0$ a.e. in the corresponding domains. We estimate the time derivative of the negative part of y as follows

$$\begin{aligned}\frac{1}{2}\frac{\mathrm{d}}{\mathrm{d}t}\|y^-(t)\|^2_{L^2(\Omega)} =& \frac{\mathrm{d}}{\mathrm{d}t}\int_\Omega y^-(t)\,y^-(\tau)\,\mathrm{d}x\Big|_{\tau=t} = \frac{\mathrm{d}}{\mathrm{d}t}\int_\Omega y(t)\,y^-(\tau)\,\mathrm{d}x\Big|_{\tau=t}\\ =& \int_\Omega -\sigma\,\nabla y(t)\cdot\nabla y^-(\tau) - \alpha\,y(t)\,y^-(\tau) + f(t)\,y^-(\tau)\,\mathrm{d}x\Big|_{\tau=t}\\ &+ \int_\Gamma -\beta\,y(t)\,y^-(\tau) + g(t)\,y^-(\tau)\,\mathrm{d}s\Big|_{\tau=t}\\ =& \int_\Omega -\sigma\,\|\nabla y^-\|^2 - \alpha\,(y^-)^2 + f\,y^-\,\mathrm{d}x + \int_\Gamma -\beta\,(y^-)^2 + g\,y^-\,\mathrm{d}s\\ \le& \|\alpha\|_{L^\infty(Q)}\|y^-(t)\|^2_{L^2(\Omega)},\end{aligned}$$

where we used that the products $f\,y^-$ and $g\,y^-$ are non-positive. Note that we have no assumptions on the sign of α and, therefore, we use the upper bound $\|\alpha\|_{L^\infty(Q)}$ for the pre-factor $-\alpha$. Due to $\|y^-(0)\|^2_{L^2(\Omega)} = \|y_0^-\|^2_{L^2(\Omega)} = 0$ we conclude by the Grönwall lemma, see Lemma 1 in Subsection 4.1.2, that $\|y^-(t)\|^2_{L^2(\Omega)} = 0$ for all $t \in [0,t_f]$ and, therefore, $y \ge 0$ a.e. in Q.

We prove claim (ii) by an application of (i) with the function $\widetilde{y} = \|y_0\|_{L^\infty(\Omega)} - y$. In this case we have the system

$$\begin{aligned}\frac{\partial\widetilde{y}}{\partial t} - \sigma\Delta\widetilde{y} + \alpha\,\widetilde{y} &= \alpha\|y_0\|_{L^\infty(\Omega)} && \text{in } Q,\\ \sigma\frac{\partial\widetilde{y}}{\partial n} &= 0 && \text{on } \Sigma,\\ \widetilde{y}(0) &= \|y_0\|_{L^\infty(\Omega)} - y_0 && \text{in } \Omega,\end{aligned}$$

and we observe that the right-hand sides are non-negative, as we assumed $\alpha \ge 0$. Hence, the application of (i) yields $\|y_0\|_{L^\infty(\Omega)} - y \ge 0$, which proves the upper bound for y. The lower bound for y falls under the assumptions of (i) and is already proven. □

3.1.3 Semi-linear Equations

The theory of linear parabolic equations presented in the preceding section is not directly applicable to the wine fermentation model. This results from the non-linearity that the reaction part introduces. However, the differential operators are still linear and these kind of equations are often called semi-linear. In this section, we state and prove a theorem for a class of reaction functions that is used in Subsection 3.3.1 to prove the existence of unique solutions for the wine fermentation model.

The analysis of reaction-diffusion equations is strongly dependent on the characteristics of the reaction term. For some reaction terms there may exist an invariant set of the state space such that if the initial values of the reaction-diffusion system lie in this region the state values will also belong to this set for all future times [Smo94]. Finding such an invariant set and proving thereby the existence of solutions is a non-trivial task.

Another approach for investigating reaction-diffusion equations can be found in [Pao92, Chapter 8]. In this reference, quasi-monotone type reactions are addressed by constructing a sequence of coupled upper and lower solutions that converge from above and below to the unique solution, respectively. For this technique one has to find a set of coupled upper and lower solutions such that the sequence can be initialised and that it converges to the solution of the reaction-diffusion system. This is dependent on the non-linearity and can be cumbersome.

Moreover, it is possible to use the Leray-Schauder fixed-point theorem as in, e.g., [BG06] and the Banach fixed-point theorem as in, e.g., [Eva10, Part III 9.2.1]. The latter is used in Subsection 3.3.1 and is presented along with its proof in the following.

Theorem 8 *Let $f_k : \mathbb{R}^m \to \mathbb{R}$ be Lipschitz continuous, $\sigma_k > 0$, $\beta_k \geq 0$, $g_k \in L^2(\Sigma)$ and $y_{k0} \in L^2(\Omega)$ for all $1 \leq k \leq m$ with m being a positive integer. Then the coupled system*

$$\begin{aligned} \frac{\partial y_k}{\partial t} - \sigma_k \Delta y_k &= f_k(y) && \text{in } Q, \\ \sigma_k \frac{\partial y_k}{\partial n} + \beta_k y_k &= g_k && \text{on } \Sigma, \\ y_k(0) &= y_{k0} && \text{in } \Omega \end{aligned}$$

has a unique solution $y \coloneqq (y_1, \ldots, y_m) \in W(0, t_f)$.

Proof. A similar theorem is stated in [Pao92, Theorem 9.2] and [Eva10, Part III 9.2.1, Theorem 2]. In the following, we show the necessary extensions. The basic idea is to use the Banach fixed-point theorem in the space $X = C([0, t_f]; L^2(\Omega; \mathbb{R}^m))$ with the following norm

$$\|v\| \coloneqq \max_{0 \leq t \leq t_f} \|v(t)\|_{L^2(\Omega;\mathbb{R}^m)}.$$

Therefore, take a fixed $y \in X$ and denote by $S(y) = w$ the solution of the following m uncoupled linear parabolic equations

$$\begin{aligned} \frac{\partial w_k}{\partial t} - \sigma_k \Delta w_k &= f_k(y) && \text{in } Q, \\ \sigma_k \frac{\partial w_k}{\partial n} + \beta_k w_k &= g_k && \text{on } \Sigma, \\ w_k(0) &= y_{k0} && \text{in } \Omega. \end{aligned}$$

Notice that, if $y \in X$ we know that $f(y) \in L^2(Q;\mathbb{R}^m)$, as f is Lipschitz continuous with constant $L > 0$. By Theorem 7, we know that these equations admit a unique solution $w_k \in W(0,t_f)$ $(k = 1,\dots,m)$ and consequently $w = (w_1,\dots,w_m) \in X$, due to the embedding $W(0,t_f) \hookrightarrow C([0,t_f];L^2(\Omega))$. Hence, the operator $S : X \to X$ is well-defined. In order to show that S is a contraction, provided the time window $[0,t_f]$ is small enough, let $y, \widetilde{y} \in X$ be arbitrarily chosen. Then the difference of their images w and $\widetilde{w}$ satisfies the following partial differential equations

$$\begin{aligned}
\frac{\partial(w_k-\widetilde{w}_k)}{\partial t} - \sigma_k\Delta(w_k-\widetilde{w}_k) &= f_k(y) - f_k(\widetilde{y}) && \text{in } Q,\\
\sigma_k\frac{\partial(w_k-\widetilde{w}_k)}{\partial n} + \beta_k(w_k-\widetilde{w}_k) &= 0 && \text{on } \Sigma,\\
(w_k-\widetilde{w}_k)(0) &= 0 && \text{in } \Omega.
\end{aligned}$$

For a fixed k, we know by Theorem 4 and the zero initial conditions that

$$\begin{aligned}
\frac{1}{2}\|(w_k-\widetilde{w}_k)(\tau)\|^2_{L^2(\Omega)} =& \frac{1}{2}\int_0^\tau \frac{\mathrm{d}}{\mathrm{d}t}\|(w_k-\widetilde{w}_k)(t)\|^2_{L^2(\Omega)}\mathrm{d}t\\
=& -\int_0^\tau \left(\int_\Omega \sigma_k\|\nabla(w_k-\widetilde{w}_k)\|^2\,\mathrm{d}x + \int_\Gamma \beta_k(w_k-\widetilde{w}_k)^2\,\mathrm{d}s\right)\mathrm{d}t\\
&+\int_0^\tau\int_\Omega (f_k(y)-f_k(\widetilde{y}))(w_k-\widetilde{w}_k)\,\mathrm{d}x\,\mathrm{d}t.\\
\le& \int_0^\tau \left(\frac{1}{2}\|f_k(y)-f_k(\widetilde{y})\|^2_{L^2(\Omega;\mathbb{R}^m)} + \frac{1}{2}\|w_k-\widetilde{w}_k\|^2_{L^2(\Omega)}\right)\mathrm{d}t\\
\le& \int_0^\tau \left(\frac{L^2}{2}\|y-\widetilde{y}\|^2_{L^2(\Omega;\mathbb{R}^m)} + \frac{1}{2}\|w_k-\widetilde{w}_k\|^2_{L^2(\Omega)}\right)\mathrm{d}t\\
\le& \frac{t_fL^2}{2}\max_{0\le t\le t_f}\|(y-\widetilde{y})(t)\|^2_{L^2(\Omega;\mathbb{R}^m)} + \frac{t_f}{2}\max_{0\le t\le t_f}\|(w_k-\widetilde{w}_k)(t)\|^2_{L^2(\Omega)}.
\end{aligned}$$

As this is valid for all $\tau \in [0,t_f]$, we can deduce

$$\max_{0\le t\le t_f}\|(w_k-\widetilde{w}_k)(t)\|^2_{L^2(\Omega)} \le t_fL^2\|(y-\widetilde{y})(t)\|^2_X + t_f\max_{0\le t\le t_f}\|(w_k-\widetilde{w}_k)(t)\|^2_{L^2(\Omega)}.$$

Hence, for $t_f < 1$ it holds that

$$\max_{0\le t\le t_f}\|(w_k-\widetilde{w}_k)(t)\|^2_{L^2(\Omega)} \le \frac{t_fL^2}{1-t_f}\|(y-\widetilde{y})(t)\|^2_X$$

and moreover the following is true

$$\|w-\widetilde{w}\|^2_X \le \frac{m\,t_fL^2}{1-t_f}\|y-\widetilde{y}\|^2_X.$$

Assume that t_f is small enough such that $\frac{m\,t_fL^2}{1-t_f} < 1$, which corresponds to $t_f \le \frac{1}{1+mL^2}$. Then, S is a contraction and we can apply the Banach fixed-point theorem, which states

that a contraction defined in a metric space has a unique fixed-point. This yields a unique $y \in X$ with $S(y) = y$, which is equivalent to

$$\begin{aligned} \frac{\partial y_k}{\partial t} - \sigma_k \Delta y_k &= f_k(y) && \text{in } Q, \\ \sigma_k \frac{\partial y_k}{\partial n} + \beta_k y_k &= g_k && \text{on } \Sigma, \\ y_k(0) &= y_{k0} && \text{in } \Omega. \end{aligned}$$

Hence, y is a solution of the system of reaction-diffusion equations. If the converse is true and the final time t_f is not small enough. Then, S is not necessarily a contraction and the Banach fixed-point theorem cannot be applied directly. In this case, we divide the interval $[0, t_f]$ into small parts and use the argument described above for each subinterval. We use the final state of the solution in the previous subinterval for the initial condition in subsequent subintervals. This is possible as the functions in the space $W(0, t_f)$ are continuous with respect to time in the $L^2(\Omega; \mathbb{R}^m)$ topology. After a finite number of iterations a unique solution for the whole time interval $[0, t_f]$ is found, which completes the proof. □

3.2 Selected Results in Functional Analysis for Infinite Dimensional Optimisation

In this section, we collect some results of functional analysis, which are important in the theory of infinite dimensional optimisation.

Assume that we want to minimise a real-valued function J defined on a normed linear space X. The Weierstraß theorem states that, if J is continuous in a compact set $C \subset X$, the minimisation problem

$$\min_{x \in C} J(x)$$

has a solution. Though this also holds for X having infinite dimensions its use is very limited in this case. In finite dimensional vector spaces bounded and closed sets are compact due to the Bolzano-Weierstraß theorem. For infinite dimensions this is not the case anymore as, for example, the unit ball is not compact. Heuristically, one can say that very often there exist not enough compact sets in the norm induced topology of an infinite dimensional vector space in order to prove the existence of minimisers by the Weierstraß theorem. Therefore, the notion of the weak topology was introduced, where more compact set are available. Nevertheless, the weak topology has less open sets and this means that there exist less continuous functions. This restriction has been overcome with the notion of lower semicontinuous functions. This property is enough to show the existence of solutions of minimisation problems.

Recall that the dual space X^* of a normed space X contains all linear and continuous functionals $f : X \to \mathbb{R}$. Together with the norm

$$\|f\|_{X^*} := \sup_{0 \neq x \in X} \frac{|f(x)|}{\|x\|_X},$$

the space X^* is a Banach space.

Definition 7 *Let x_n be a sequence in normed vector space X. We say that x_n* ***converges weakly*** *to $x \in X$, if*

$$f(x_n) \to f(x), \text{ as } n \to \infty$$

holds for all $f \in X^*$. In this case we use the notation $x_n \rightharpoonup x$.

We give some results on weak convergence and its connection to the convergence with respect to the norm of the vector space, which we call strong convergence.

Theorem 9 *Let X be a normed vector space. Then the following holds*

- *Every strongly convergent sequence is also weakly convergent to the same limit.*
- *The limit of a weakly convergent sequence is unique.*
- *A weakly convergent sequence is bounded.*

These results are proven in [Cia13, Theorem 5.12-1, 5.12-2] and utilise the Hahn-Banach theorem and the Banach-Steinhaus theorem.

The following theorem is applied in later sections to the solution operator of a linear parabolic equation. Hence, we can deduce from the weak convergence of the problem data also the weak convergence of the solution.

Theorem 10 *Let X and Y be normed vector spaces and $S : X \to Y$ be linear and continuous. Then S is sequentially weakly continuous, that is, $S(x_n)$ converges weakly to $S(\overline{x})$ in Y for a weakly convergent sequence $(x_n) \subset X$ with limit $\overline{x} \in X$.*

Proof. Let $g \in Y^*$ be arbitrary. As S is linear and continuous, we conclude that $f := g \circ S$ defined by $x \mapsto g(S(x))$ is an element of X^*. The sequence x_n is weakly convergent in X. Therefore, $f(x_n) \to f(\overline{x})$ as n tends to infinity. As g was chosen arbitrarily we have proven that $g(S(x_n)) \to g(S(\overline{x}))$ for all $g \in Y^*$, that is the weak convergence of $S(x_n)$ to the limit $S(\overline{x})$. □

The following theorem is used both for the space of controls and also for the solution space of the differential equations modelling the wine fermentation.

Theorem 11 *Let U be a Hilbert space and $(u_n) \subset U$ a bounded sequence. Then there exists a weakly converging subsequence $(u_{n_k}) \subset (u_n)$.*

Proof. Since U is a Hilbert space, it is a reflexive Banach space due to the Riesz representation theorem. We conclude by the Banach-Eberlein-Šmulian theorem, see [Cia13, Theorem 5.14-4], that bounded sequences in U contain weakly convergent sequences. □

In the case of control constraints, one has to prove that the optimal control, which is the limit of an objective minimising sequence, is admissible. Therefore, constraints are often formulated such that the admissible set of controls is closed and convex in order to use the following theorem.

Theorem 12 *Let $C \subset U$ be a convex and closed subset of the Hilbert space U. Then the subset C is sequentially weakly closed, that is, the limit of a weakly convergent sequence in C is an element of C.*

Proof. This theorem is valid for an arbitrary normed linear space, as the Banach-Saks-Mazur theorem shows that for a weakly convergent sequence convex combinations of its members converge strongly to the weak limit. As C is convex, these convex combinations are elements of C and its strong limit is an element of C, since C is closed in the strong topology. See [Cia13, Theorem 5.13-1] for more details.

In this work, we use this theorem only in Hilbert spaces and can prove it in an easier way. Let P denote the projection of a point $u \in U$ on the set C, that is the point $P(u)$ is the element of C with the minimal distance to u. In this case $P(u)$ satisfies $(P(u) - u, v - P(u))_U \geq 0$ for all $v \in C$; see [Cia13, Theorem 4.3-1]. Let $(u_n) \subset C$ be a weakly convergent sequence. Then $(P(u) - u, u_n - P(u))_U \to (P(u) - u, u - P(u))_U$ as n goes to infinity. Hence, we have

$$-\|P(u) - u\|_U^2 = (P(u) - u, u - P(u))_U = \lim_{n\to\infty} (P(u) - u, u_n - P(u))_U \geq 0$$

and conclude $u = P(u) \in C$. □

Moreover, we define sequential weak lower semicontinuity. This concept is necessary as the norm is not continuous in the topology induced by weak convergence and it is not possible to show that the weak limit of a minimising sequence is the minimum of a function. In functional analysis also lower semicontinuity and sequential lower semicontinuity for the strong topology is regarded, but we omit these concepts as they are not necessary for our purpose.

Definition 8 *Let U be a topological space. A function $J : U \to \mathbb{R}$ is called* ***sequentially weakly lower semicontinuous****, if for each weakly convergent sequence $u_n \rightharpoonup u$ in U the inequality*

$$J(u) \leq \liminf_{n\to\infty} J(u_n)$$

holds.

Most applications in optimal control theory define the objective functional by the square of a norm. Therefore, we prove the following theorem that is later applied for the functional, which is minimised to steer the wine fermentation process in a desired way.

Theorem 13 *Let U be a Hilbert space. Then the function $J : U \to \mathbb{R}$ defined by $J(u) = \|u\|_U^2$ is sequentially weakly lower semicontinuous, that is, weak convergence $u_n \rightharpoonup u$ in U implies the inequality*

$$\|u\|_U^2 \leq \liminf_{n\to\infty} \|u_n\|_U^2.$$

Proof. This theorem is proven in [Cia13, Theorem 9.2-3] for an arbitrary convex and lower semicontinuous function defined in a normed space. For its proof the theorems of Hahn-Banach, Banach-Steinhaus, and Banach-Saks-Mazur are essential. In the case of U being a Hilbert space and J defined by $J(u) = \|u\|_U^2$ the proof is simpler, as we compute

$$J(u) = \|u\|_U^2 \leq \|u_n - u\|_U^2 + \|u\|_U^2 = \|u_n\|_U^2 - 2(u_n, u)_U + 2\|u\|_U^2 = J(u_n) - 2(u_n - u, u)_U.$$

As (u_n) converges weakly, we know that $(u_n - u, u)_U$ tends to zero as n tends to infinity. Hence, we conclude $J(u) \leq \liminf_{n\to\infty} J(u_n)$. □

For completeness, we present the notion of Gâteaux and Fréchet differentiability; see [Trö10, Section 2.6].

Definition 9 *Let U and V be Banach spaces. The function $F : O \to V$ defined in the open set $O \subset U$ is called* ***Gâteaux differentiable*** *at $x \in O$, if the mapping A defined by*

$$A_x(h) = \lim_{t \searrow 0} \frac{F(x + t\,h) - F(x)}{t},$$

for $h \in U$ is well-defined and linear.

Moreover, the function F is called ***Fréchet differentiable*** *at $x \in O$, if there exists a linear and continuous operator $A_x : U \to V$ such that*

$$\frac{\|F(x+h) - F(x) - A_x(h)\|_V}{\|h\|_U} \to 0, \qquad \text{for } \|h\|_U \to 0$$

holds.

We present the well-known implicit function theorem, which is used to prove the differentiability property of the solution operator of the wine fermentation model. See [Zei95, Chapter 4.8] or [Cia13, Chapter 7.13] for a proof.

Theorem 14 *Let U, Y, and V be a normed linear spaces such that Y and V are Banach spaces. Suppose a point (u^*, y^*) is given in an open subset $O \subset U \times Y$. Let the function $F : O \to V$ be continuous in O and have the following properties:*

- *The point (u^*, y^*) is a zero of F, that is $F(u^*, y^*) = 0$ holds.*
- *F is continuously Fréchet differentiable with respect to the second variable for all $(u, y) \in O$.*
- *The partial derivative of F with respect to y at the point (u^*, y^*) is continuously invertible.*

Then there exist a continuous function S defined in an open neighbourhoods A of u^* that takes values in an open neighbourhood B of y^* such that $A \times B \subset O$ and

$$\{(u, y) \in A \times B; F(u, y) = 0\} = \{(x, y) \in A \times B; y = S(u)\}$$

holds. In addition, if F is Fréchet differentiable at (u^*, y^*), then S is Fréchet differentiable and

$$S'(u^*) = -\left(F_y(u^*, y^*)\right)^{-1} F_u(u^*, y^*) \tag{3.5}$$

holds.

The characterisation of optimal controls can be done by means of the first-order necessary optimality conditions. They rely on the following theorem for a general minimisation problem; see [Trö10, Lemma 2.21].

Theorem 15 *Let C be a convex subset of a Banach space U. Further, let f be a real-valued mapping that is Gâteaux differentiable in an open subset containing the set C. A solution $\overline{u}$ of the minimisation problem*

$$\min_{u \in C} f(u)$$

satisfies the following variational inequality

$$f'(\overline{u})(u - \overline{u}) \geq 0,$$

for all $u \in C$.

Proof. Since C is convex, the linear convex combination $\overline{u} + s(u - \overline{u})$ is in C for all $s \in [0,1]$ and $u \in C$. Moreover, $\overline{u}$ is a solution of the minimisation problem and we conclude that

$$f(\overline{u} + s(u - \overline{u})) \geq f(\overline{u})$$

holds. Therefore, we have

$$\frac{1}{s}\left(f(\overline{u} + s(u - \overline{u})) - f(\overline{u})\right) \geq 0,$$

for all $s \in [0,1]$. Taking the limit $s \to 0$ we arrive at $f'(\overline{u})(u - \overline{u}) \geq 0$ for all $u \in C$. □

3.3 Optimal Control of the Wine Fermentation Process

This section is devoted to the application of the general results on the optimal control of partial differential equations that are given in the preceding section to the wine fermentation model with reaction-diffusion equations (2.18).

We begin with the analysis of the model equations by proving the unique existence of solutions and their continuous dependence on the temperature control function. Further, we define an objective functional in order to steer the fermentation process in a desired way and prove the existence of minimisers of the corresponding optimal control problem. The computation of locally optimal controls can be achieved by considering the first-order necessary optimality conditions that we present. These conditions are in close relation to the evaluation of the gradient of the reduced functional, which is utilised in the numerical implementation. Finally, we present numerical results at the end of this section that validate our theoretical analysis.

3.3.1 Analysis of the Model Equations

For convenience, we state again the fermentation model equations for the vector of concentrations and the temperature $y = (X, N, O, S, E, T)^\top$ described in Section 2.3, which is as follows

$$\frac{\partial y}{\partial t} - D\Delta y = f(y) \quad \text{in } \Omega \times (0, t_f) =: Q, \tag{3.6a}$$

$$D\frac{\partial y}{\partial n} + Zy = g(u) \quad \text{on } \Gamma \times (0, t_f) =: \Sigma, \tag{3.6b}$$

$$y(0) = y_0 \quad \text{in } \Omega, \tag{3.6c}$$

where the reaction function is given by

$$f(y) = \begin{pmatrix} a_1(T-b_1)\frac{N}{c_1+N}\frac{O}{c_2+O}\frac{S}{c_3+S}X - \Psi(E)X \\ -a_2(T-b_1)\frac{N}{c_1+N}\frac{O}{c_2+O}\frac{S}{c_3+S}X \\ -a_3(T-b_1)\frac{N}{c_1+N}\frac{O}{c_2+O}\frac{S}{c_3+S}X \\ -a_4(T-b_1)\frac{N}{c_1+N}\frac{O}{c_2+O}\frac{S}{c_3+S}X - a_5(T-b_2)\frac{S}{c_4+S}\frac{c_5}{c_5+E}X \\ a_6(T-b_2)\frac{S}{c_4+S}\frac{c_5}{c_5+E}X \\ a_7(T-b_2)\frac{S}{c_4+S}\frac{c_5}{c_5+E}X \end{pmatrix}. \tag{3.7}$$

Moreover, we have the diffusivity matrix $D = \operatorname{diag}(\sigma_1, \ldots, \sigma_6)$ and the boundary condition mappings

$$Z = \begin{cases} \operatorname{diag}(0,0,0,0,0,\tau_{\text{air}}) & \text{on } \Gamma_1 \times (0,t_f) =: \Sigma_1, \\ \operatorname{diag}(0,0,0,0,0,\tau_{\text{coolant}}) & \text{on } \Gamma_2 \times (0,t_f) =: \Sigma_2, \end{cases} \tag{3.8}$$

and

$$g(u) = \begin{cases} (0,0,0,0,0,\tau_{\text{air}} T_{\text{ext}})^\top & \text{on } \Sigma_1, \\ (0,0,0,0,0,\tau_{\text{coolant}}\, u)^\top & \text{on } \Sigma_2. \end{cases} \tag{3.9}$$

In order to guarantee solutions of the fermentation model, we work through the remainder of this chapter under the following assumptions:

1. Ω is a bounded domain with Lipschitz boundary Γ. The control boundary $\Gamma_2 \subset \Gamma$ is of non-zero measure.

2. The yield coefficients a_i $(i = 1, \ldots, 7)$, stagnation temperatures b_i $(i = 1, 2)$, and Michaelis constants c_i $(i = 1, \ldots, 5)$ in (3.7) are positive numbers. Moreover, the toxicity function Ψ is positive and continuously differentiable.

3. The diffusivity parameters σ_i $(i = 1, \ldots, 6)$ are positive reals.

4. The normalised thermal conductivities τ_{air} and τ_{coolant} in (3.8) and (3.9) are positive numbers. The external temperature T_{ext} in (3.9) belongs to $L^\infty(\Sigma)$ and satisfies $T_{\text{ext}} \geq \max(b_1, b_2)$ a.e. in Σ.

5. The initial conditions $y_0 = (X_0, N_0, O_0, S_0, E_0, T_0)^\top$ in (3.6c) belong to $L^\infty(\Omega; \mathbb{R}^6)$. They are non-negative a.e. in Ω and in addition $T_0 \geq \max(b_1, b_2)$ holds.

Note that we assume constant diffusion parameters σ_i in Assumption 3 to simplify the notation. The inclusion of essentially bounded space and time dependent diffusion coefficients $\sigma_i(x,t) \geq \underline{\sigma} > 0$ introduce no mathematical difficulties. Assumptions 4 and 5 ensure that the factors $(T - b_1)$ and $(T - b_2)$ of the reaction rates μ_1 in (2.3) and μ_2 in (2.5) remain positive and the reactions are not reversed.

Before we prove the existence of solutions for the fermentation model, we point out some properties of the reaction function f. In the following theorem, we show that the state y is component-wise non-negative, which is important, as the right-hand side f in (3.6) can formally have several singularities, e.g. for $N = -c_1$. Moreover, the derivative of f is unbounded when its arguments tend to $+\infty$. This is due, on one hand, to the product TX and, on the other hand, to the general continuously differentiable toxicity function Ψ. Nevertheless, the entries of the Jacobian $f'(y)$ are bounded for arguments y with values in the interval $[0, M]$. Hence, the function f is locally Lipschitz continuous for non-negative arguments, i.e., there exists a constant $L(M) > 0$ dependent of M such that

$$\|f(y_1) - f(y_2)\| \leq L(M)\|y_1 - y_2\|, \tag{3.10}$$

for all $y_1, y_2 \in \{x \in \mathbb{R}^6 : 0 \leq x_i \leq M,\ i = 1, \ldots, 6\}$. In fact, the result remains true if we allow $-\varepsilon$ (for some $\varepsilon > 0$) in place of zero as a lower bound, as long as we stay clear of the singularities $N = -c_1$ etc.; see (3.7). This will be utilised in the proof of Theorem 18.

The assumptions given above together with the results from the previous section on parabolic partial differential equations enable us to state the existence and uniqueness of solutions to (3.6).

Theorem 16 *Suppose that u belongs to $L^\infty(0,t_f)$ and satisfies $u \geq \max(b_1,b_2)$. Then there exists a unique solution to* (3.6) *and this solution satisfies the following estimate*

$$\|y\|_{W(0,t_f)} + \|y\|_{L^\infty(Q;\mathbb{R}^6)} \leq q\left(\|y_0\|_{L^\infty(\Omega;\mathbb{R}^6)}, \|u\|_{L^\infty(0,t_f)}, \|T_{\text{ext}}\|_{L^\infty(0,t_f)}\right), \tag{3.11}$$

where the function q depends on the problem data.

Proof. Theorem 8 states the unique solvability of a reaction-diffusion system for reaction functions that are globally Lipschitz continuous. However, the reaction function f of our fermentation model (3.6) is only locally Lipschitz continuous for arguments that are component-wise positive. Nevertheless, we can use this result to prove our theorem by truncating the state vector such that we have a globally Lipschitz continuous reaction. Therefore, we define for some $M > 0$ a truncated reaction term given by

$$f^M(y) \coloneqq f(\max(\ell, \min(y, M))),$$

where the maximum and minimum is understood component-wise with the constant lower bound $\ell = (0,0,0,0,0,\max(b_1,b_2))$ and variable upper bound M in all components. The truncation renders the function f^M *globally* Lipschitz continuous. Hence, by Theorem 8 there exists, for each $M > 0$, a unique solution $y^M \in W(0,t_f)$ of $y_t - D\Delta y = f^M(y)$ subject to the same boundary and initial conditions of (3.6).

In the following, we show that this solution satisfies $\ell \leq y^M \leq K$, where K is a constant independent of M. We denote by $[X^M]$, $[N^M]$, $[O^M]$, $[S^M]$, $[E^M]$ and $[T^M]$ the components of $\max(\ell, \min(y, M))$ and use Theorem 7 to prove the bounds for y^M in the following eight steps.

1. Since y^M satisfies the equation $y_t - D\Delta y = f^M(y)$, we conclude that the yeast concentration X^M satisfies the following linear equation,

   $$\frac{\partial X^M}{\partial t} - \sigma_1 \Delta X^M - \alpha X^M = 0 \qquad \text{in } Q,$$

   subject to the same boundary and initial conditions as in (3.6), where

   $$\alpha \coloneqq a_1([T^M] - b_1)\frac{[N^M]}{c_1 + [N^M]}\frac{[O^M]}{c_2 + [O^M]}\frac{[S^M]}{c_3 + [S^M]}\frac{[X^M]}{X^M} - \Psi([E^M])\frac{[X^M]}{X^M}$$

   belongs to $L^\infty(Q)$. This can be derived by noting that the fraction $\frac{[X^M]}{X^M}$ is zero for non-positive X^M, equals one for $0 < X^M < M$, and is bounded from above by one for $X^M \geq M$, as its value is $\frac{M}{X^M}$ in this case. Hence, the essential maximum of the absolute value of the function α can be bounded by the maximum of this function in the hypercube defined by $\ell \leq y \leq M$. As $X_0 \geq 0$ holds, Theorem 7 (i) gives $X^M \geq 0$.

2. The nitrogen concentration N^M satisfies the following linear equation,

   $$\frac{\partial N^M}{\partial t} - \sigma_2 \Delta N^M + \alpha N^M = 0 \qquad \text{in } Q,$$

   subject to the same boundary and initial conditions as in (3.6), where

   $$\alpha \coloneqq a_2([T^M] - b_1)\frac{[N^M]}{N^M(c_1 + [N^M])}\frac{[O^M]}{c_2 + [O^M]}\frac{[S^M]}{c_3 + [S^M]}[X^M] \geq 0,$$

and α belongs to $L^\infty(Q)$. For the non-negativity of α it is essential that we make the exceptional definition of the lower bound for the temperature in ℓ. As the truncated temperature is greater than the constant b_1, the non-negativity of the factor $([T^M] - b_1)$ is guaranteed. Since $N_0 \geq 0$ holds, Theorem 7 (ii) yields $0 \leq N^M \leq \|N_0\|_{L^\infty(\Omega)}$.

3. By the same argument, we get

$$0 \leq O^M \leq \|O_0\|_{L^\infty(\Omega)} \qquad \text{and} \qquad 0 \leq S^M \leq \|S_0\|_{L^\infty(\Omega)},$$

for the oxygen and sugar concentrations.

4. The ethanol concentration E^M satisfies the linear equation

$$\frac{\partial E^M}{\partial t} - \sigma_5 \Delta E^M = F \qquad \text{in } Q, \tag{3.12}$$

subject to the same boundary and initial conditions as in (3.6), where

$$F \coloneqq a_6([T^M] - b_2)\frac{[S^M]}{c_4 + [S^M]}\frac{c_5}{c_5 + [E^M]}[X^M] \geq 0, \tag{3.13}$$

and F belongs to $L^\infty(Q)$. Since $E_0 \geq 0$ holds, Theorem 7 (i) yields $E^M \geq 0$.

5. In order to prove an upper bound of X^M we consider the system

$$\begin{aligned} \frac{\partial \widetilde{X}}{\partial t} - \sigma_1 \Delta \widetilde{X} &= H \qquad \text{in } Q, \\ \frac{\partial N^M}{\partial t} - \sigma_2 \Delta N^M &= -H \qquad \text{in } Q, \end{aligned}$$

subject to the same boundary and initial conditions as in (3.6), where $\widetilde{X}$ is an auxiliary variable and the right-hand side is defined as follows

$$H \coloneqq a_2([T^M] - b_1)\frac{[N^M]}{c_1 + [N^M]}\frac{[O^M]}{c_2 + [O^M]}\frac{[S^M]}{c_3 + [S^M]}[X^M].$$

Lets assume for the moment that the diffusivity parameters σ_1 and σ_2 are equal. Then, for the sum $\widetilde{X} + N^M$ the following differential equation

$$\frac{\partial \left(\widetilde{X} + N^M\right)}{\partial t} - \sigma_1 \Delta \left(\widetilde{X} + N^M\right) = 0 \qquad \text{in } Q$$

holds. An application of Theorem 7 (ii) yields the upper bound $\widetilde{X} + N^M \leq \|X_0 + N_0\|_{L^\infty(\Omega)}$. As we already know that $N^M \geq 0$, we conclude $\widetilde{X} \leq \|X_0 + N_0\|_{L^\infty(\Omega)}$. The case of non-equal diffusion coefficients σ_i $(i = 1, 2)$ is far more complicated, but it is still possible to derive an upper bound $\widetilde{X} \leq C$, where C is only dependent on the data of the problem. We refer to [Mas83], where such problems with non-linearities on the right-hand side that cancel out for a summation of equations are investigated. Further, we find that the difference $\widetilde{X} - X^M$ satisfies the following parabolic problem

$$\frac{\partial \widetilde{X} - X^M}{\partial t} - \sigma_1 \Delta \left(\widetilde{X} - X^M\right) = \Psi([E^M])[X^M] \geq 0 \qquad \text{in } Q,$$

with a non-negative right-hand side. As the boundary and initial conditions are zeros, the application of Theorem 7 (i) yields $\widetilde{X} - X^M \geq 0$. Together with the upper bound of $\widetilde{X}$ we conclude $X^M \leq C$.

6. The shifted temperature function $T^* = T^M - \max(b_1, b_2)$ satisfies the following heat equation

$$\begin{aligned} \frac{\partial T^*}{\partial t} - \sigma_6 \Delta T^* &= \alpha && \text{in } Q, \\ \sigma_6 \frac{\partial T^*}{\partial n} + \beta T^* &= G && \text{on } \Sigma, \\ T^*(0) &= T_0 - \max(b_1, b_2) && \text{in } \Omega, \end{aligned}$$

where

$$\alpha := a_6 \left([T^M] - b_2 \right) \frac{[S^M]}{c_4 + [S^M]} \frac{c_5}{c_5 + [E^M]} [X^M] \geq 0$$

belongs to $L^\infty(Q)$. Moreover, $G \geq 0$ holds, as $G = \tau_{\text{air}}(T_{\text{ext}} - \max(b_1, b_2))$ holds on Σ_1 and $G = \tau_{\text{coolant}}(u - \max(b_1, b_2))$ on Σ_2, compare (3.8). Since $T_0, T_{\text{ext}}, u \geq \max(b_1, b_2)$ holds, Theorem 7 (i) yields $T^M - \max(b_1, b_2) \geq 0$ and $T^M \geq \max(b_1, b_2)$ follows.

7. To derive the upper bound of the temperature T^M we obtain by three variable transformations a heat equation with non-negative right-hand sides as follows. The first transfomation

$$T^* = T^M - b_2, \tag{3.14}$$

simplifies the term $(T - b_2)$. Moreover, we must take care of two separate sources that can contribute to an increase of the temperature T^M. We use the following transformation

$$T^{**} = e^{-a_7 C t} T^*, \tag{3.15}$$

to account for the heat generation of the yeast. Moreover, the following mapping

$$T^{***} = \gamma - T^{**}, \tag{3.16}$$

takes care of the boundary and initial conditions with the constant γ, which is defined later. Note that for the temperature T^M, the following parabolic equation is valid

$$\begin{aligned} \frac{\partial T^M}{\partial t} - \sigma_6 \Delta T^M &= a_7([T^M] - b_2) \frac{[S^M]}{c_4 + [S^M]} \frac{c_5}{c_5 + [E^M]} [X^M] && \text{in } Q, \\ \sigma_6 \frac{\partial T^M}{\partial n} + \tau T^M &= g_6(u) && \text{on } \Sigma, \\ T^M(0) &= T_0 && \text{in } \Omega, \end{aligned}$$

where τ equals τ_{air} on Σ_1 and τ_{coolant} on Σ_2. The last component of the function g in (3.9) is denoted by g_6. The constant b_2 vanished when applying differential operators. Hence, for the shifted temperature T^* we arrive at the system

$$\begin{aligned} \frac{\partial T^*}{\partial t} - \sigma_6 \Delta T^* &= a_7 T^* \frac{[S^M]}{c_4 + [S^M]} \frac{c_5}{c_5 + [E^M]} [X^M] && \text{in } Q, \\ \sigma_6 \frac{\partial T^*}{\partial n} + \tau T^* &= g_6(u) - \tau b_2 && \text{on } \Sigma, \\ T^*(0) &= T_0 - b_2 && \text{in } \Omega. \end{aligned}$$

During the second transformation the derivative with respect to t gives the extra term $-a_7\,C\,T^{**}$ on the right-hand side and yields the system

$$\begin{aligned}
\frac{\partial T^{**}}{\partial t} - \sigma_6 \Delta T^{**} &= a_7 T^{**} \left(\frac{[S^M]}{c_4 + [S^M]} \frac{c_5}{c_5 + [E^M]} [X^M] - C \right) && \text{in } Q, \\
\sigma_6 \frac{\partial T^{**}}{\partial n} + \tau T^{**} &= e^{-a_7\,C\,t} \left(g_6(u) - \tau b_2 \right) && \text{on } \Sigma, \\
T^{**}(0) &= e^{-a_7\,C\,t} \left(T_0 - b_2 \right) && \text{in } \Omega.
\end{aligned}$$

The last transformation renders the system into

$$\begin{aligned}
\frac{\partial T^{***}}{\partial t} - \sigma_6 \Delta T^{***} + \alpha T^{***} &= a_7 \gamma \left(C - \frac{[S^M]}{c_4 + [S^M]} \frac{c_5}{c_5 + [E^M]} [X^M] \right) && \text{in } Q, \\
\sigma_6 \frac{\partial T^{***}}{\partial n} + \tau T^{***} &= \gamma - e^{-a_7\,C\,t} \left(g_6(u) - \tau b_2 \right) && \text{on } \Sigma, \\
T^{***}(0) &= \gamma - e^{-a_7\,C\,t} \left(T_0 - b_2 \right) && \text{in } \Omega,
\end{aligned}$$

where $\alpha \coloneqq a_7 \left(C - \frac{[S^M]}{c_4 + [S^M]} \frac{c_5}{c_5 + [E^M]} [X^M] \right)$. Now, we observe that the right-hand sides of the parabolic differential equation for T^{***} are non-negative provided that we define γ as follows

$$\gamma \coloneqq \|T_0\|_{L^\infty(\Omega)} + \tau(\|T_{\text{ext}}\|_{L^\infty(\Omega)} + \|u\|_{L^\infty(\Omega)}).$$

Note that we already have proven $X^M \leq C$ and the fractions $\frac{[S^M]}{c_4 + [S^M]}$ and $\frac{c_5}{c_5 + [E^M]}$ are bounded from above by one. Finally, the application of Theorem 7 (i) proves $T^{***} \geq 0$, which subsequently yields $T^{**} \leq \gamma$, $T^{*} \leq e^{a_7\,C\,t_f} \gamma$, and $T^M \leq e^{a_7\,C\,t_f} \gamma + b_2$ after reversing the transformations (3.14)–(3.16).

8. Finally, we find that the right-hand side F in the equation for the ethanol concentration E^M, see (3.12) and (3.13), is bounded from above by $a_6\,\gamma\,e^{a_7\,C\,t_f}\,C$. Using the transformation $E^* \coloneqq \|E_0\|_{L^\infty(\Omega)} + t\,a_6\,\gamma\,e^{a_7\,C\,t_f}\,C - E^M$, we get the system

$$\begin{aligned}
\frac{\partial E^*}{\partial t} - \sigma_5 \Delta E^* &= a_6\,\gamma\,e^{a_7\,C\,t_f}\,C - F && \text{in } Q, \\
\sigma_5 \frac{\partial E^*}{\partial n} &= 0 && \text{on } \Sigma, \\
E^*(0) &= \|E_0\|_{L^\infty(\Omega)} - E_0 && \text{in } \Omega.
\end{aligned}$$

As the right-hand sides are non-negative, we conclude from Theorem 7 (i) that $E^* \geq 0$ holds and obtain the following upper bound

$$E^M \leq \|E_0\|_{L^\infty(\Omega)} + t_f\,a_6\,\gamma\,e^{a_7\,C\,t_f}\,C.$$

To summarise, we have shown that the concentrations X^M, N^M, O^M, S^M, and E^M are bounded from below by zero and the temperature T^M is bounded from below by $\max(b_1, b_2)$. Moreover, we have $y^M \leq K$, where the upper bound is defined as follows

$$K \coloneqq \max(C, \|N_0\|_{L^\infty(\Omega)}, \|O_0\|_{L^\infty(\Omega)}, \|S_0\|_{L^\infty(\Omega)}, \|E_0\|_{L^\infty(\Omega)} + t_f\,a_6\,\gamma\,e^{a_7\,C\,t_f}\,C, e^{a_7\,C\,t_f}\gamma + b_2).$$

Notice that these bounds depend only on the parameters and the boundary and initial conditions, but not on M. We therefore conclude that $\ell \leq y^M \leq K$ for all $M > 0$.

Consequently, it holds that $\ell \leq y^K \leq K$, which implies $f^K(y^K) = f(y^K)$, as no truncation can occur. Thus y^K is the unique solution of (3.6), as it satisfies $y_t^K - D\Delta y^K = f^K(y^K) = f(y^K)$.

By the previous considerations, we have a boundedness result in the $L^\infty(Q)$-norm, i.e., there exists a function p such that

$$\|y\|_{L^\infty(Q;\mathbb{R}^6)} \leq p\left(\|y_0\|_{L^\infty(\Omega;\mathbb{R}^6)}, \|u\|_{L^\infty(0,t_f)}, \|T_{\text{ext}}\|_{L^\infty(0,t_f)}\right)$$

holds. For the estimate in the $W(0,t_f)$-norm, we use the boundedness result for the heat equation of Theorem 7 and obtain the following

$$\|y\|_{W(0,t_f)} \leq C\left(\|y_0\|_{L^\infty(\Omega;\mathbb{R}^6)} + \|u\|_{L^\infty(0,t_f)} + \|T_{\text{ext}}\|_{L^\infty(0,t_f)} + \|f(y)\|_{L^2(Q;\mathbb{R}^6)}\right).$$

As the function f is locally Lipschitz continuous for non-negative inputs, we conclude that

$$\|f(y)\|_{L^2(Q;\mathbb{R}^6)} \leq \sqrt{6\,t_f\,|\Omega|}\,L(K)\,\|y\|_{L^\infty(Q;\mathbb{R}^6)};$$

see (3.10). Hence, there exists a function q that depends on the problem data such that the desired stability result (3.11) holds. □

Having proven Theorem 16 and the unique solvability of the wine fermentation model equations (3.6), we can define the mapping S that assigns to each feasible control $u \geq \max(b_1, b_2)$ in $L^\infty(0,t_f)$ a function y in the space $W(0,t_f)$ as follows

$$\begin{aligned} S : L^\infty(0,t_f) \supset \{u \geq \max(b_1,b_2)\} &\to W(0,t_f), \\ u &\mapsto y. \end{aligned}$$

Hence, we can write $y = S(u)$ for the solution of the wine fermentation model.

To close this subsection we mention that the proof of Theorem 16 can be adjusted to a large set of biological reacting models. The essential features for the reaction function of the wine fermentation that are exploited in the proof are, on one hand, the conservation of chemical amount and, on the other hand, the limited nutrient sources. The reaction stops as soon as nitrogen, oxygen, and sugar are consumed. Hence, for other models that share the same structure similar results can be obtained.

3.3.2 An Optimal Control Problem and the Existence of Minimisers

In this section, we formulate an optimal control problem for the wine fermentation process and investigate its solution. To characterise this solution, we discuss the first-order necessary optimality conditions.

First, we define the goal for the optimisation process. We assume that desired trajectories $y_d := (X_d, N_d, O_d, S_d, E_d, T_d)^\top \in L^2(Q;\mathbb{R}^6)$ for the concentrations and for the temperature are given. Moreover, we wish to reach a desired final state that is given by $y_{t_f} := (X_{t_f}, N_{t_f}, O_{t_f}, S_{t_f}, E_{t_f}, T_{t_f})^\top \in L^2(\Omega;\mathbb{R}^6)$. In addition, technical restrictions on the control u are modelled by a set of admissible controls as follows

$$U_{\text{ad}} := \left\{u \in L^2(0,t_f) : u_a \leq u \leq u_b \text{ a.e. in } (0,t_f)\right\}. \tag{3.17}$$

The bounds are given by $u_a, u_b \in L^\infty(0,t_f)$. In addition to the assumptions given in the beginning of Subsection 3.3.1 we assume that $u_a(x) \geq \max(b_1,b_2)$ in order guarantee that

the temperature dependent terms in our model, $T - b_1$ and $T - b_2$, remain positive and the reaction kinetics are not reversed; see (3.7).

Our optimal control problem reads as follows

$$\min_{u \in U_{\text{ad}}} J(y,u) \coloneqq \sum_{i=1}^{6} \left(\frac{\alpha_i}{2} \|y_i - y_{d,i}\|^2_{L^2(Q)} + \frac{\beta_i}{2} \|y_i(\cdot, t_f) - y_{t_f,i}\|^2_{L^2(\Omega)} \right) + \frac{\lambda}{2} \|u - T_{\text{ext}}\|^2_{L^2(0,t_f)}$$
$$\text{subject to (3.6)}, \tag{3.18}$$

where α_i and β_i ($i \in \{1, \dots, 6\}$) are non-negative constants. Further, we assume $\lambda > 0$. The objective functional J in (3.18) penalises control temperatures u, which deviate from the external temperature T_{ext} and therefore it takes into account the energy requirement of the heat regulation. The following theorem addresses the existence of optimal controls.

Theorem 17 *There exists at least one globally optimal solution to the optimal control problem* (3.18)*.*

We prove this theorem following standard arguments [Lio71, Chapter III.15], [Trö10, Chapter 4.3] and emphasise the weak continuity of the control-to-state operator.

Proof. We denote by $y(u)$ the unique solution to (3.6) for a given $u \in U_{\text{ad}}$; see Theorem 16. As J is bounded from below, there exists $j \coloneqq \inf_{u \in U_{\text{ad}}} J(y(u), u)$ and a sequence $(u_n) \subset U_{\text{ad}}$ such that $\lim_{n\to\infty} J(y(u_n), u_n) = j$. The sequence (u_n) is bounded in $L^2(0, t_f)$, as U_{ad} is a bounded set. By Theorem 11 there exists a subsequence, which we also denote by u_n, with a weak limit $\overline{u} \in L^2(0, t_f)$ such that $u_n \rightharpoonup \overline{u}$ weakly in $L^2(0, t_f)$. U_{ad} is convex and closed in the Hilbert space $L^2(0, t_f)$ and therefore sequentially weakly closed by Theorem 12. Consequently, the limit $\overline{u} \in U_{\text{ad}}$ is admissible. Due to Theorem 16, the corresponding states $y_n \coloneqq y(u_n)$ are bounded in the Hilbert space $W(0, t_f)$; see (3.11). Again by Theorem 11, there exists a subsequence of y_n that is weakly convergent in $W(0, t_f)$, where we denote subsequences still by u_n and y_n. We denote the weak limit of y_n by $\overline{y} \in W(0, t_f)$. Further, note that the objective functional J is continuous and convex. Hence, J is sequentially weakly lower semicontinuous by Theorem 13 and it follows that

$$J(\overline{y}, \overline{u}) \leq \liminf_{n\to\infty} J(y_n, u_n) = j.$$

Therefore, $\overline{u}$ is a global solution of (3.18) provided the state $\bar{y}$ and the control $\bar{u}$ satisfy the model equations (3.6). This means that it remains to show that $\overline{y} = y(\overline{u})$ holds, which is done in the following.

We know by Theorem 16 that the sequence of states y_n is bounded in $L^\infty(Q; \mathbb{R}^6)$. Hence, the reaction term $d_n \coloneqq f(y_n)$ is also bounded in $L^\infty(Q; \mathbb{R}^6)$, since the reaction function f is locally Lipschitz continuous. Moreover, we conclude that d_n is also bounded in $L^2(Q; \mathbb{R}^6)$ and extract by Theorem 11 a weakly converging subsequence with a weak limit $\overline{d}$ in that space. The state y_n is the solution of the following heat equation

$$\begin{aligned} \frac{\partial y_n}{\partial t} - D\Delta y_n &= d_n && \text{in } Q, \\ D\frac{\partial y_n}{\partial n} + Z y_n &= g(u_n) && \text{on } \Sigma, \\ y_n(0) &= y_0 && \text{in } \Omega, \end{aligned}$$

with right-hand sides d_n and $g(u_n)$. The mapping from u_n and d_n onto the unique solution y_n of the heat equation is affine and continuous from $L^2(0, t_f) \times L^2(Q; \mathbb{R}^6)$ into $W(0, t_f)$,

and hence weakly continuous by Theorem 10. We conclude that the weak limit $\overline{y}$ is the unique solution to

$$\begin{aligned} \frac{\partial \overline{y}}{\partial t} - D\Delta \overline{y} &= \overline{d} && \text{in } Q, \\ D\frac{\partial \overline{y}}{\partial n} + Z\overline{y} &= g(\overline{u}) && \text{on } \Sigma, \\ \overline{y}(0) &= y_0 && \text{in } \Omega. \end{aligned}$$

It remains to show $\overline{d} = f(\overline{y})$, which has $\overline{y} = y(\overline{u})$ as a consequence.

Next, we show that the states y_n converge strongly in $L^2(Q;\mathbb{R}^6)$. Therefore, note that we have $H^1(\Omega;\mathbb{R}^6) \hookrightarrow L^2(\Omega;\mathbb{R}^6) \hookrightarrow H^1(\Omega;\mathbb{R}^6)^*$, where the first embedding is compact due to Theorem 3. As $H^1(\Omega;\mathbb{R}^6)$ and its dual are reflexive we conclude by Theorem 5 that the embedding $W(0,t_f) \hookrightarrow L^2(Q;\mathbb{R}^6)$ is compact. The weakly converging sequence y_n is bounded in $W(0,t_f)$. Therefore, the compact embedding yields that it contains a subsequence that is strongly convergent in $L^2(Q;\mathbb{R}^6)$. We also know from Theorem 16 that the states y_n are bounded component-wise by a constant K. Hence, this holds also for its limit $\overline{y}$ and we conclude by the local Lipschitz continuity of f that $f(\overline{y}) \in L^2(Q;\mathbb{R}^6)$. Together with the Lipschitz estimate (3.10) for f we obtain

$$\|f(y_n) - f(\overline{y})\|_{L^2(Q;\mathbb{R}^6)} \leq L(K)\|y_n - \overline{y}\|_{L^2(Q;\mathbb{R}^6)} \to 0,$$

and the strong convergence $d_n = f(y_n) \to f(\overline{y})$ in $L^2(Q;\mathbb{R}^6)$ ensues. But d_n has the weak limit $\overline{d}$. As the limit in both topologies must be the same, we find that $\overline{d} = f(\overline{y})$ and consequently, $\overline{y} = y(\overline{u})$. This completes the proof. □

3.3.3 Differentiability of the Control–to–State Operator and First-Order Necessary Optimality Conditions

Next, we discuss the characterisation of locally optimal solutions by their first-order necessary optimality conditions. For this purpose, we investigate the differentiability of the control-to-state operator. We prove the following theorem.

Theorem 18 *The mapping $S : u \mapsto y$, given by the solution of (3.6), is Fréchet differentiable from U_{ad} (endowed with the $L^\infty(0,t_f)$ topology) into $L^\infty(Q;\mathbb{R}^6)$. For $\delta u \in L^\infty(0,t_f)$ the directional derivative $\delta y = S'(u)\,\delta u$ is given by the unique solution of the following initial value problem,*

$$\begin{aligned} \frac{\partial}{\partial t}\delta y - D\Delta \delta y &= f'(y)\,\delta y && \text{in } Q, \\ D\frac{\partial}{\partial n}\delta y + Z\delta y &= g'(u)\,\delta u && \text{on } \Sigma, \\ \delta y(0) &= 0 && \text{in } \Omega, \end{aligned} \tag{3.19}$$

where $y = S(u)$ is the state of the system corresponding to the control u, and $f'(y)$ denotes the Jacobian of f.

Proof. We define the function spaces $Y := L^\infty(Q;\mathbb{R}^6)$, $U := L^\infty(0,t_f)$ and $V := L^\infty(Q;\mathbb{R}^6)$. For an arbitrary $u^* \in U_{\text{ad}}$ Theorem 16 ensures that $y^* := S(u^*) \in Y$ and $y^* \geq 0$ holds. In order to define a neighbourhood of (u^*, y^*), we choose an arbitrary open set $O_U \subset U$ such that $u^* \in O_U$. Moreover, we define $O_Y \subset \{y \in Y : y \geq -\varepsilon\}$,

where $0 < \varepsilon < \min\{c_j | j = 1, \dots, 5\}$, in order to avoid singularities of f. Hence, the nonlinearity f regarded as a Nemytskii operator for Lebesgue spaces $f : O_Y \to L^\infty(Q; \mathbb{R}^6)$ is continuously differentiable [Trö10, Lemma 4.12].

Similar to the proof in [BJT10] we define $S_Q : L^\infty(Q; \mathbb{R}^6) \to L^\infty(Q; \mathbb{R}^6)$, $S_\Sigma : L^\infty(\Sigma; \mathbb{R}^6) \to L^\infty(Q; \mathbb{R}^6)$, and $S_\Omega : L^\infty(\Omega; \mathbb{R}^6) \to L^\infty(Q; \mathbb{R}^6)$, as the linear and continuous solution operators for the heat equation

$$\begin{aligned} \frac{\partial y}{\partial t} - D\Delta y &= f \quad \text{in } Q, \\ D\frac{\partial y}{\partial n} + Zy &= g \quad \text{on } \Sigma, \\ y(0) &= h \quad \text{in } \Omega, \end{aligned}$$

in the sense that $S_Q : f \mapsto y$ with $g = h = 0$, $S_\Sigma : g \mapsto y$ with $f = h = 0$, and $S_\Omega : h \mapsto y$ with $f = g = 0$. We refer to [Cas97, Theorem 5.1] for the proof of essentially bounded solutions to the heat equation for L^∞ data.

In the following, we want to apply the implicit function theorem, see Theorem 14, to the mapping $F : O_U \times O_Y \to V$ defined by

$$F(u, y) \coloneqq y - S_Q(f(y)) - S_\Sigma(g(u)) - S_\Omega(y_0),$$

at the point (u^*, y^*). It is $F(u^*, y^*) = 0$, because $y^* = S_Q(f(y^*)) + S_\Sigma(g(u^*)) + S_\Omega(y_0)$ is equivalent to the system (3.6). F is continuously differentiable since the same holds for f and the other mappings involved are affine and continuous.

Next, we show the continuous invertibility of the partial Fréchet derivative

$$F_y(u^*, y^*) : w \mapsto w - S_Q(f'(y^*)\, w).$$

To this end, we show that for each $v \in V$ there exists a unique element $w \in Y$, such that

$$v = F_y(u^*, y^*)\, w, \tag{3.20}$$

which depends continuously on v. Equivalently, we can search for an $r \coloneqq w - v$, as $S_Q(f'(y^*)\, w) = r$ equals (3.20). The corresponding parabolic problem for r is given by

$$\begin{aligned} \frac{\partial r}{\partial t} - D\Delta r - f'(y^*)r &= f'(y^*)v \quad \text{in } Q, \\ D\frac{\partial r}{\partial n} + Zr &= 0 \qquad \text{on } \Sigma, \\ r(0) &= 0 \qquad \text{in } \Omega, \end{aligned} \tag{3.21}$$

where we used $f'(y^*)w = f'(y^*)r + f'(y^*)v$. Since y^* is the state corresponding to an admissible control, it takes values in a finite interval not including the singularities $c_1, \dots, c_5$ of f. Hence, the matrix function $f'(y^*)$ is bounded, and therefore the initial value problem (3.21) has a unique solution r in $L^\infty(Q; \mathbb{R}^6)$, which depends continuously on the data $v \in V$. We conclude that the mapping $v \mapsto r$ is continuous and bounded. The same holds true for $v \mapsto w = r + v$, which shows the continuous invertibility of $F_y(u^*, y^*)$. Therefore, the assumptions of the implicit function theorem are satisfied and it follows that there exists a continuously differentiable function $\widetilde{S}$ such that

$$\left\{(u, y) \in \widetilde{O}_U \times \widetilde{O}_Y | F(u, y) = 0\right\} = \left\{(u, y) \in \widetilde{O}_U \times \widetilde{O}_Y | y = \widetilde{S}(u)\right\} \tag{3.22}$$

in some neighbourhoods $\widetilde{O}_U$ of u^* and $\widetilde{O}_Y$ of y^*. Since $F(u, S(u)) = 0$ holds for all $u \in U_{\text{ad}}$ we have $S(u) = \widetilde{S}(u)$. This shows the continuous Fréchet differentiability of the control-to-state operator at the arbitrarily chosen point u^*.

In order to derive a formula for the derivative of S, we take into account that all mappings in the equation

$$S(u) = S_Q(f(S(u))) + S_\Sigma(g(u)) + S_\Omega(y_0), \tag{3.23}$$

are Fréchet differentiable. As the mappings S_Q and S_Σ are linear, taking the derivative with respect to u in (3.23) leads to

$$S'(u)\,\delta u = S_Q(f'(S(u))\,S'(u)\,\delta u) + S_\Sigma(g'(u)\,\delta u). \tag{3.24}$$

Due to $\delta y = S'(u)\delta u$ and $y = S(u)$ equation (3.24) is equivalent to the initial value problem (3.19), which completes the proof. □

Now, the optimal control problem (3.18) is equivalent to minimising the reduced functional $\widetilde{J}(u) \coloneqq J(S(u), u)$ over the set of feasible controls U_{ad}. Note that the optimal control of the wine fermentation process is a non-linear problem and the reduced functional is not convex. Hence, uniqueness of optimal controls cannot be proven. Moreover, the optimality conditions are also satisfied by locally optimal solutions and numerically computed results are not necessarily global optimal controls. The following theorem states the first-order necessary optimality conditions that are also instrumental to compute locally optimal controls.

Theorem 19 *Let $\overline{u}$ be a solution of the optimal control problem (3.18), $\overline{y} = S(\overline{u})$ be the corresponding state that solves the forward state equation (3.6), and $\overline{p} \in W(0, t_f)$ be the adjoint state defined as the solution to the following linear backward in time adjoint equation*

$$-\frac{\partial p}{\partial t} - D\Delta p = f'(\overline{y})^T p + \alpha\,(\overline{y} - y_d) \quad \text{in } Q, \tag{3.25a}$$

$$D\frac{\partial p}{\partial n} + Zp = 0 \quad \text{on } \Sigma, \tag{3.25b}$$

$$p(t_f) = \beta\,(\overline{y}(t_f) - y_{t_f}) \quad \text{in } \Omega, \tag{3.25c}$$

where

$$\alpha = \operatorname{diag}(\alpha_1, \ldots, \alpha_6), \qquad y_d = (X_d, N_d, O_d, S_d, E_d, T_d)^\top,$$
$$\beta = \operatorname{diag}(\beta_1, \ldots, \beta_6), \qquad y_{t_f} = (X_{t_f}, N_{t_f}, O_{t_f}, S_{t_f}, E_{t_f}, T_{t_f})^\top.$$

Then the variational inequality

$$\int_0^{t_f} \left(\lambda\,(\overline{u} - T_{\text{ext}}) + \int_{\Gamma_2} \tau_{coolant}\,\overline{p}_6 \,\mathrm{d}s \right) (u - \overline{u})\,\mathrm{d}t \geq 0 \quad \text{for all } u \in U_{\text{ad}} \tag{3.26}$$

is fulfilled.

Proof. We regard the reduced functional $\widetilde{J} : U_{\text{ad}} \to \mathbb{R}$ with respect to the L^∞ topology in U_{ad}. Theorem 18 guarantees that the control-to-state operator S is Fréchet differentiable in U_{ad}. It is even differentiable in an open neighbourhood of U_{ad}, if we assume

that the lower bound u_a in the definition of U_{ad} satisfies $\max(b_1, b_2) + \varepsilon \leq u_a$ a.e. in $(0, t_f)$ with a small number $\varepsilon > 0$. Moreover, the mapping $f : L^2(\Omega) \to \mathbb{R}$ defined by $y \to \int_\Omega y^2 \mathrm{d}x$ is Fréchet differentiable with derivative $f'(y) = (h \to 2\int_\Omega y\, h \,\mathrm{d}x)$. The function f is a fortiori differentiable defined in the smaller space $L^\infty(\Omega)$, where the domain Ω is bounded. Hence, the composition $\widetilde{J}(u) = J(S(u), u)$ is differentiable in an open set containing the convex set U_{ad}. Therefore, a solution $\overline{u}$ of Equation 3.18 satisfies, according to Theorem 15, the variational inequality

$$\widetilde{J}'(\overline{u})(u - \overline{u}) \geq 0,$$

for all $u \in U_{\text{ad}}$. It remains to show that this is equivalent to (3.26).

Note that we can write the reduced functional as $\widetilde{J}(u) = J_1(u) + J_2(S(u))$, as J is a sum of terms that are either dependent on u or on y. For the u dependent addend of the directional derivative of $\widetilde{J}$ in the direction δu we conclude by the considerations above that it is given by

$$J_1'(\overline{u})\delta u = \int_0^{t_f} \lambda(\overline{u} - T_{\text{ext}})\delta u \,\mathrm{d}t,$$

which is the first part of (3.26).

Further, we define $\widetilde{J}_2(u) = J_2(S(u))$. In the following, we investigate the derivative of $\widetilde{J}_2$ in the direction δu. We define $\delta y = S'(\overline{u})\delta u$ and remember that δy is the weak solution of (3.19). Using the chain rule we have

$$\widetilde{J}_2'(\overline{u})\delta u = J_2'(S(\overline{u}))\delta y = \int_Q (\overline{y} - y_d)^\top \,\alpha\, \delta y \,\mathrm{d}x \,\mathrm{d}t + \int_\Omega (\overline{y}(t_f) - y_{t_f})^\top \,\beta\, \delta y(t_f) \,\mathrm{d}x,$$

where the diagonal matrices α and β are defined in Theorem 19. As the adjoint state $\overline{p}$ is a weak solution of (3.25) and by Definition 6 of weak solutions we have

$$\frac{\mathrm{d}}{\mathrm{d}t}\int_\Omega -\overline{p}^\top v \,\mathrm{d}x + \int_\Omega \nabla\overline{p}^\top D\,\nabla v - \overline{p}^\top f'(\overline{y})^\top v \,\mathrm{d}x + \int_\Gamma \overline{p}^\top Z\, v \,\mathrm{d}s = \int_\Omega f^\top v \,\mathrm{d}x + \int_\Gamma g^\top v \,\mathrm{d}s$$

with $f = \alpha\,(\overline{y} - y_d)$ and $g = 0$ for all $v \in H^1(\Omega)$. Using $v = \delta y$ and recalling $\frac{\mathrm{d}}{\mathrm{d}t}\int_\Omega \overline{p}^\top v \,\mathrm{d}x = \langle \overline{p}', v\rangle_{H^1(\Omega;\mathbb{R}^6)^*, H^1(\Omega;\mathbb{R}^6)}$ we compute

$$\begin{aligned}
\widetilde{J}_2'(\overline{u})\delta u &= \int_0^{t_f} \langle -\overline{p}', \delta y\rangle_{H^1(\Omega)^*, H^1(\Omega)} \,\mathrm{d}t + \int_Q \nabla\overline{p}^\top D\nabla\delta y - \overline{p}^\top f'(\overline{y})^\top \delta y \,\mathrm{d}x\,\mathrm{d}t + \int_\Sigma \overline{p}^\top Z\delta y \,\mathrm{d}s\,\mathrm{d}t \\
&\quad + \int_\Omega \overline{p}(t_f)^\top \delta y(t_f)\,\mathrm{d}x \\
&= \int_0^{t_f} \langle \delta y', \overline{p}\rangle_{H^1(\Omega)^*, H^1(\Omega)} \,\mathrm{d}t + \int_Q \nabla\delta y^\top D\nabla\overline{p} - \delta y^\top f'(\overline{y})\,\overline{p}\,\mathrm{d}x\,\mathrm{d}t + \int_\Sigma \delta y^\top Z\overline{p}\,\mathrm{d}s\,\mathrm{d}t \\
&= \int_\Sigma (g'(\overline{u})\delta u)^\top \overline{p}\,\mathrm{d}s\,\mathrm{d}t,
\end{aligned}$$

where we used the integration by parts formula of Theorem 4 and the zero initial condition for δy. Note that $g'(\overline{u})\delta u$ equals $(0, 0, 0, 0, 0, \tau_{\text{coolant}}\,\delta u)^\top$ on Σ_2 and is zeros elsewhere.

Hence, we have shown the equality

$$\begin{aligned}\widetilde{J}'(\overline{u})(u-\overline{u}) &= \int_0^{t_f} \lambda(\overline{u}-T_{\text{ext}})(u-\overline{u})\,\mathrm{d}t + \int_\Sigma \left(g'(\overline{u})(u-\overline{u})\right)^\top \overline{p}\,\mathrm{d}s\,\mathrm{d}t \\ &= \int_0^{t_f} \left(\lambda\,(\overline{u}-T_{\text{ext}}) + \int_{\Gamma_2} \tau_{\text{coolant}}\,\overline{p}_6\,\mathrm{d}s\right)(u-\overline{u})\,\mathrm{d}t,\end{aligned}$$

and this completes the proof. □

Note that for differentiable real-valued functions $\widetilde{J}$, defined in a Hilbert space U, there exists a gradient $\nabla\widetilde{J} \in U$ such that $\widetilde{J}'(u)\delta u = (\nabla\widetilde{J}, \delta u)_U$ holds. It is well-known that the negative gradient is the direction of steepest descent. Therefore, gradient-based optimisation methods can be applied by searching for a suitable step length and add to a current approximation of the optimal control the negative gradient multiplied by the step length. This result due to the Riesz representation theorem cannot be used in our case as we work with $L^\infty(0,t_f)$. Hence, the derivative of $\widetilde{J}$ is in the dual space of $L^\infty(0,t_f)$. Nevertheless, the computations in the proof of Theorem 19 show that the gradient of $\widetilde{J}$ at an arbitrary point in U_{ad} can be represented as $\widetilde{J}'(u)\delta u = (\nabla\widetilde{J}, \delta u)_{L^2(0,t_f)}$, where the gradient is given by $\nabla\widetilde{J}(u) = \lambda\,(u - T_{\text{ext}}) + \int_{\Gamma_2} \tau_{\text{coolant}}\,p_6\,\mathrm{d}s$. Assume that $T_{\text{ext}} \in L^\infty(0,t_f)$, $y_d \in L^\infty(Q;\mathbb{R}^6)$, and $y_{t_f} \in L^\infty(\Omega;\mathbb{R}^6)$, which is not restrictive for the industrial application of the optimal control framework. Then we obtain an adjoint state p that is essentially bounded as it is the solution of a linear parabolic problem with L^∞ data; see [Cas97, Theorem 5.1]. Hence, we observe that the gradient $\nabla\widetilde{J}$ is an element of $L^\infty(0,t_f)$ and we have with $-\nabla\widetilde{J}$ a direction of steepest descent. These considerations are used in the following section, where the optimal control of the wine fermentation process is computed by a quasi-Newton BFGS method.

3.4 Numerical Validation

In this section, we discuss the numerical solution of the optimality system, consisting of the forward model (3.6), the adjoint model (3.25), and the variational inequality (3.26). Specifically, we illustrate a suitable discretisation scheme for the forward and backward equations, and employ a BFGS quasi-Newton optimisation method to solve this system in reduced formulation for the wine fermentation model. We follow here an optimise–then–discretise approach.

The purpose of this section is to explore the potential of temperature controls on the amount of sugar converted. The numerical examples that are presented in this section use realistic model parameters. Under these conditions, it turns out that neither the lower bound (depending on the stagnation temperatures b_1 and b_2) nor the technological upper bound for the control became active in the solution. We therefore describe the BFGS optimisation algorithm for solving the unconstrained problem, for which (3.26) is replaced by the equation

$$\lambda\,(u - T_{\text{ext}}) + \int_{\Gamma_2} \tau_{\text{coolant}}\,p_6\,\mathrm{d}s = 0 \quad \text{a.e. in } [0,t_f].$$

3.4.1 Discretisation Schemes and Optimisation Algorithm

We discretise the forward equation and the adjoint backward equation with different schemes. Both numerical discretisations are presented in the following and we give reasons

for this specific choice. Moreover, the BFGS optimisation algorithm is presented.

Discretisation of the Forward State Equation

We discuss the discretisation of the reaction-diffusion system (3.6). Since these equations are non-linear, any scheme implicit in time would incur the need to solve non-linear algebraic equations. On the other hand, it is well known that an explicit scheme is only conditionally stable and would incur the need to use very small time steps. In order to avoid both difficulties, we discretise the equation with an IMEX Runge-Kutta scheme, proposed in [ARS97], whose stability and convergence properties were examined in [Kot08].

In order to illustrate this scheme in detail, we semi-discretise (3.6) in space by a finite difference scheme ([JS14]) to obtain

$$\mathbf{y}' = L_h\mathbf{y} + \varphi_h(u) + f_h(\mathbf{y}). \tag{3.27}$$

The matrix L_h contains contributions from the Laplacian and $\varphi(u)$ accounts for the boundary conditions. For the solution of this ordinary differential equation, we divide the time interval $[0, t_f]$ into M equidistant subintervals and the vector $\mathbf{y}^m$ represents the approximation of the solution of equation (3.27) at time $t^m := m\,\delta t$, where $\delta t = \frac{t_f}{M}$. On this time grid the discretisation of the resulting system of ordinary differential equations by the IMEX Runge-Kutta scheme can be written with one intermediate step $\mathbf{y}^\omega$ as follows

$$\begin{aligned}
\mathbf{y}^\omega &= \mathbf{y}^m + \delta t\,\omega\,(L_h\mathbf{y}^\omega + \varphi_h(u(t^m + \omega\,\delta t))) + \delta t\,\omega f(\mathbf{y}^m),\\
\mathbf{y}^{m+1} &= \mathbf{y}^m + \delta t\,(1-\omega)\,(L_h\mathbf{y}^\omega + \varphi_h(u(t^m + \omega\,\delta t))) + \delta t\,\kappa f(\mathbf{y}^m)\\
&\quad + \delta t\,\omega\left(L_h\mathbf{y}^{m+1} + \varphi_h(u(t^{m+1}))\right) + \delta t\,(1-\kappa) f(\mathbf{y}^\omega),
\end{aligned}$$

where $\omega = \frac{2-\sqrt{2}}{2}$ and $\kappa = 1 - \frac{1}{2\omega}$. This scheme is second-order accurate in time and possesses a larger stability region compared to the slightly simpler IMEX trapezoidal scheme [Kot08].

Discretisation of the Backward Adjoint Equation

At this point, it would seem natural to use the discrete adjoint scheme for the backward equation. However, numerical tests show that the discrete adjoint scheme results in an explicit treatment of the reaction part of the adjoint equation, given by

$$-\frac{\partial p}{\partial t} - D\Delta p = f'(y)^T p + \alpha\,(y - y_d). \tag{3.28}$$

The resulting scheme is, however, not able to recover the actual behavior, due to large eigenvalues of the Jacobian $f'(y)$ of the reaction function. We therefore implement the (implicit) Crank-Nicolson scheme for (3.28), i.e.,

$$\begin{aligned}
-\frac{\mathbf{p}^m - \mathbf{p}^{m-1}}{\delta t} &= \frac{1}{2}\left(L_h\mathbf{p}^m + f_h'(\mathbf{y}^m)^T\mathbf{p}^m + \alpha\,(\mathbf{y}^m - y_d(t^m))\right)\\
&\quad + \frac{1}{2}\left(L_h\mathbf{p}^{m-1} + f_h'(\mathbf{y}^{m-1})^T\mathbf{p}^{m-1} + \alpha\,(\mathbf{y}^{m-1} - y_d(t^{m-1}))\right).
\end{aligned} \tag{3.29}$$

We remark that this numerical scheme has second-order convergence in time as well [HV03, Chapter I. 4.2].

The BFGS Optimisation Algorithm

For the optimisation problem (3.18), we employ the matrix-free quasi-Newton BFGS scheme; see, e.g., [NW06, Algorithm 7.4] or [BS12, Chapter 4.2.2]. Given a control u, we evaluate the gradient w.r.t. the $L^2(0,t_f)$-topology of the reduced cost functional $\widetilde{J}$ at this point in the following way:

1. Solve the state equation (3.6) for y with the given control u;
2. Solve the adjoint equation (3.25) for the adjoint state p, inserting the state function y into the reaction part and terminal condition;
3. Compute the gradient $\nabla\widetilde{J}$ by the following formula,

$$\nabla\widetilde{J}(u) = \lambda\,(u - T_{\text{ext}}) + \int_{\Gamma_2} \tau_{\text{coolant}}\, p_6 \,\mathrm{d}s \in L^2(0,t_f). \tag{3.30}$$

The BFGS optimisation algorithm reads as follows

1: Choose an initial approximation u_0 and compute $g_0 = \nabla\widetilde{J}(u_0)$.
2: Choose tolerance tol and set $k = 0$
3: **while** $k < k_{\max}$ **do**
4: Compute search direction $v_k = -g_k - \sum_{i=0}^{k-1} \varrho_i\,[(s_i, g_k)\, r_i - (z_i, g_k)\, s_i]$.
5: Compute step length $\alpha_k \approx \min_{\alpha>0} \widetilde{J}(u_k + \alpha\, v_k)$.
6: Stop if $\|\alpha_k\, v_k\|_{L^\infty(0,t_f)} < \text{tol}$
7: Compute new approximation $u_{k+1} = u_k + \alpha_k\, p_k$ and $g_{k+1} = \nabla\widetilde{J}(u_{k+1})$.
8: Compute

$$y_k = g_{k+1} - g_k, \quad s_k = \alpha_k v_k = u_{k+1} - u_k, \quad \varrho_k = (y_k, s_k)^{-1},$$
$$z_k = y_k + \sum_{i=0}^{k-1} \varrho_i\,[(s_i, y_k)\, r_i - (z_i, y_k)\, s_i], \quad d_k = 1 + \varrho_k(y_k, z_k), \quad r_k = d_k\, s_k - z_k$$

9: Set $k = k + 1$.
10: **end while**

Notice that the scalar product $(\cdot,\cdot)$ denotes the $L^2(0,t_f)$ inner product. The auxiliary variables y_k, s_k, ϱ_k, z_k, d_k and r_k in step 8 of the optimisation algorithm are necessary to calculate the action of the approximate Hessian of $\widetilde{J}$, taken as an operator $L^2(0,t_f) \to L^2(0,t_f)$. This approximation is initialised with the identity.

For the line search in Step 5, we utilise Algorithm 3.5 in [NW06], which generates step lengths such that the strong Wolfe conditions

$$\widetilde{J}(u_k + \alpha_k\, v_k) \le \widetilde{J}(u_k) + \delta_1\, \alpha_k (\nabla\widetilde{J}(u_k), v_k) \tag{3.31a}$$
$$|(\nabla\widetilde{J}(u_k + \alpha_k\, v_k), v_k)| \ge \delta_2 (\nabla\widetilde{J}(u_k), v_k) \tag{3.31b}$$

are satisfied. These conditions (3.31) are sufficient to maintain positive definiteness of the quasi-Newton operator.

$\sigma_1 = 10^{-9}\ \frac{m^2}{s}$	$\sigma_2 = 10^{-9}\ \frac{m^2}{s}$	$\sigma_3 = 10^{-9}\ \frac{m^2}{s}$
$\sigma_4 = 10^{-9}\ \frac{m^2}{s}$	$\sigma_5 = 10^{-9}\ \frac{m^2}{s}$	$\sigma_6 = 0.144 \cdot 10^{-3}\ \frac{m^2}{s}$
$\tau_{\text{coolant}} = 4 \cdot 10^{-7}\ \frac{m}{s}$	$\tau_{\text{air}} = 8 \cdot 10^{-4}\ \frac{m}{s}$	
$a_1 = 1 \cdot 10^{-5}\ \frac{1}{Ks}$	$a_2 = 5 \cdot 10^{-8}\ \frac{1}{Ks}$	$a_3 = 1 \cdot 10^{-9}\ \frac{1}{Ks}$
$a_4 = 1 \cdot 10^{-7}\ \frac{1}{Ks}$	$a_5 = 1 \cdot 10^{-6}\ \frac{1}{Ks}$	$a_6 = 0.511\ a_5$
$a_7 = 2\ a_5$	$b_1 = 9\ ^\circ\text{C}$	$b_2 = 9\ ^\circ\text{C}$
$c_1 = 0.05\ \frac{kg}{m^3}$	$c_2 = 0.001\ \frac{kg}{m^3}$	$c_3 = 50\ \frac{kg}{m^3}$
$c_4 = 5\ \frac{kg}{m^3}$	$c_5 = 34\ \frac{kg}{m^3}$	$E_{\text{tol}} = 70\ \frac{kg}{m^3}$
$k_1 = 10\ \frac{m^3}{kg}$	$k_2 = 6 \cdot 10^{-9}\ \left(\frac{m^3}{kg}\right)^2 \frac{1}{s}$	$T_{\text{ext}} = 12\ ^\circ\text{C}$

Table 3.1: Parameter values that were used in numerical experiments.

3.4.2 Numerical Results

In this section, we focus on the numerical validation of our optimal control formulation. In particular, we compare the simulation of the fermentation process with constant control temperature and with optimised control temperature. For convenience, we choose a two-dimensional spatial domain $\Omega = (0, 0.5) \times (0, 1)$, which represents a fermenter of 50 cm width and 1 m height. We consider tank with a cooling mantle on the lateral boundary. Therefore, we define the control boundary as $\Gamma_2 = \{(x_1, x_2) \in \Gamma : 0.3 \leq x_2 \leq 0.7\}$. We have the following initial conditions

$$\begin{array}{lll} X_0 = 0.5\ \frac{g}{l}, & N_0 = 0.2\ \frac{g}{l}, & O_0 = 0.004\ \frac{g}{l}, \\ S_0 = 200\ \frac{g}{l}, & E_0 = 0\ \frac{g}{l}, & T_0 = 16\ ^\circ\text{C}, \end{array} \tag{3.32}$$

and integrate the differential equations for $t_f = 30$ days, or 2 592 000 seconds. In our numerical experiments, whose results are reported in Figure 3.1 and Figure 3.2, we work on a grid of 41×81 points in space and 401 points in time. Further, we choose realistic diffusion coefficients and reaction parameter values that are shown in Table 3.1. In fact, these parameters depend strongly on the actual experimental setting, and we have not applied a parameter estimation for a special yeast culture and fermenter. We rather want to show the general ability of the optimal control framework presented in this work to optimise the fermentation process. Therefore, we use parameters that result in qualitatively good simulation results (private communication with Dr. Christian von Wallbrunn, Departments of Microbiology & Biochemistry, Geisenheim University). With this setting and a constant control temperature $u = 16\ ^\circ\text{C}$, we obtain the fermentation results plotted in blue color in Figure 3.1. We see that the yeast population cannot consume all of the sugar before dying out. This phenomenon is called stagnation, and it results in a great loss of quality of the fermented wine. The reason is that additional yeast cells would have be added at a very late stage of the fermentation process in order to obtain a dry wine with almost zero sugar concentration. These additional yeast cultures change the taste of the wine, and the product will be not as good as desired. Therefore stagnation must be avoided. Our control objective is to maximise the sugar consumption in the fermentation process. Moreover, the working temperature T should not deviate too much from an ideal fermentation temperature of 16 °C, as thermal stress applied to the yeast culture results in compounds that influence the taste in a negative way. Therefore, we set the objective coefficients in (3.18) to zero except for

$$\alpha_T = 10^{-5}, \qquad \beta_S = 10, \qquad \lambda = 10^{-7}.$$

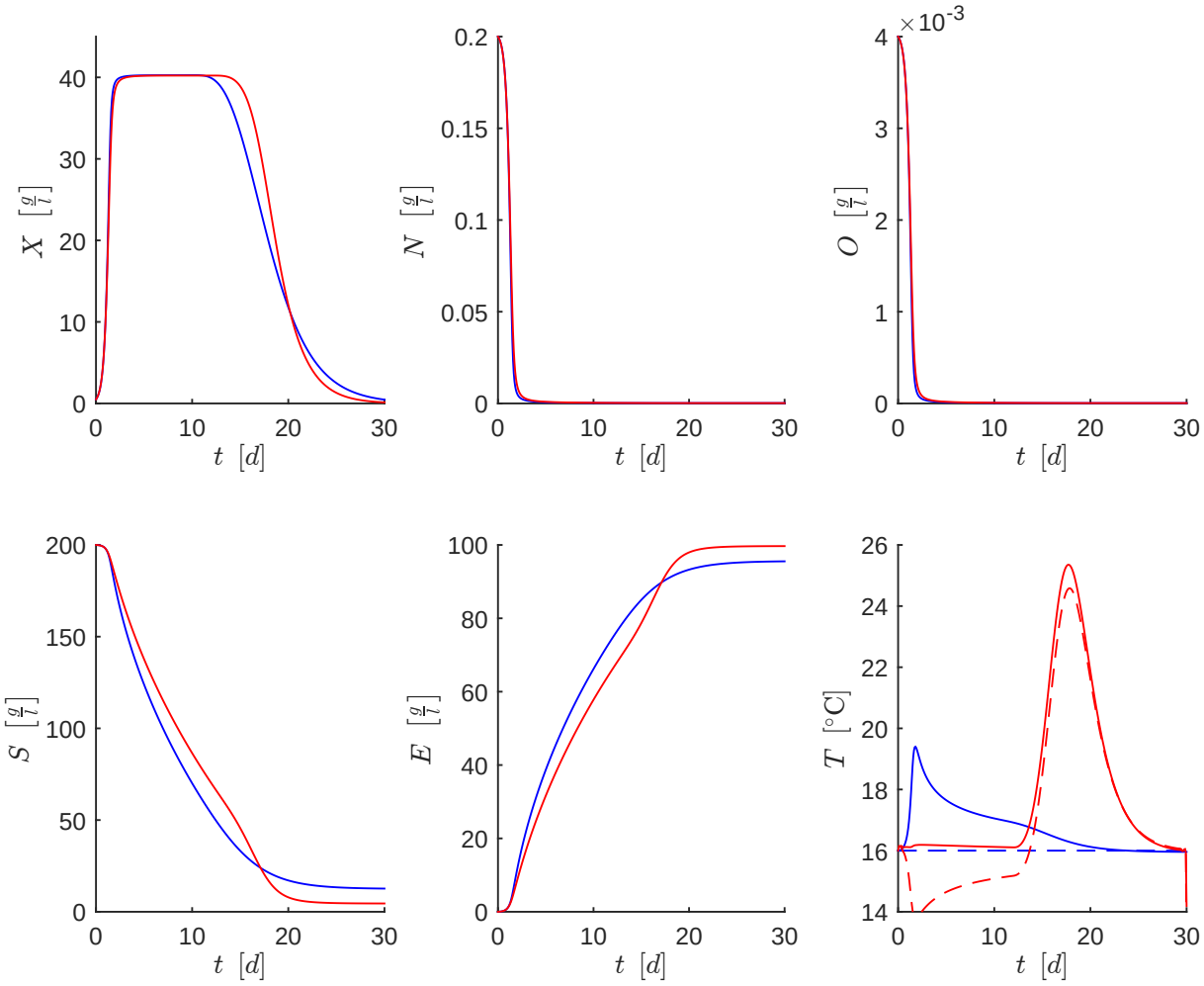

Figure 3.1: Space-averaged values of X, N, O, S, E and T over 30 days of fermentation. The two different control functions u correspond to the dashed lines in the lower right plot. Results for constant control in blue and for optimised control in red.

Furthermore, we define the following desired trajectory for temperature and final state for sugar

$$T_d(t) = 16\ ^\circ\text{C}, \qquad S_{t_f} = 0\ \frac{g}{l}.$$

With this setting, we apply the optimisation scheme starting from an initial guess $u = 16\ ^\circ$C. The results of the optimisation process are shown in red color in Figure 3.1. We see that, in the optimally controlled fermentation process, the amount of sugar left after 30 days is significantly lower. Moreover, one can observe that the mean temperature is near 16 °C, except for the late stage of the fermentation process, where the lack of yeast must be compensated by high temperatures to ensure a sufficiently large reaction rate.

The temperature distribution in the fermenter is shown in Figure 3.2. In the first stage of the fermentation the yeast produces much heat, and the tank must be cooled. The temperature within the vessel can differ up to one degree Celsius. In contrast, there is almost no activity during the last days, and there is a fairly homogeneous temperature.

Furthermore, we want to give some evidence that the proposed optimality system is correct. We discretise the partial differential equation along with the corresponding objective functional, which results in a discretised optimisation problem with control $u \in$

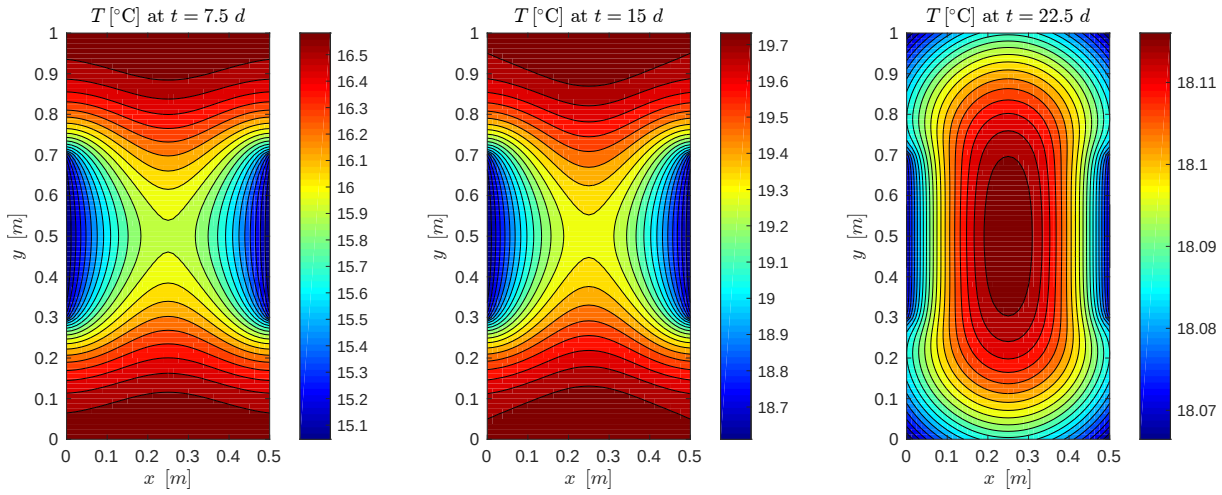

Figure 3.2: Distribution of temperature at three different time points.

N_x	N_y	M	relative error (eoc)
5	9	201	0.3896
9	17	201	0.1853 (1.07)
17	33	201	0.0875 (1.08)
33	65	201	0.0402 (1.12)
65	129	201	0.0175 (1.20)

Table 3.2: Experimental order of convergence (eoc) of the relative error of the optimise–before–discretise gradient (3.30) given by $\|\nabla\widetilde{J}(u) - \nabla\widetilde{J}_{disc}(u)\|_{L^2_{\delta t}} / \|\nabla\widetilde{J}(u)\|_{L^2_{\delta t}}$ computed with N_x, N_y and M grid points in x-, y- and t-direction, respectively.

$\mathbb{R}^{M+1}$. The gradient $\nabla\widetilde{J}(u)$ of the reduced functional can be approximated componentwise by a finite difference approach as follows

$$(\nabla\widetilde{J}_{disc}(u))_j := \frac{J(u + \alpha\, e_j) - J(u - \alpha\, e_j)}{2\,\alpha}. \tag{3.33}$$

The j-th unit vector is denoted by e_j. Hence, with substantial computational effort (solving the forward equation $2\,(M+1)$ times) we can approximate the discrete gradient $\nabla\widetilde{J}_{disc}(u)$. Afterwards, we solve the forward and backward equation and obtain an approximation of the gradient $\nabla\widetilde{J}(u)$ by discretising the continuous optimality system. When refining the mesh, we see in Table 3.2 the difference between these two gradients at the control $u = 16$ °C decreases to zero and we have a numerical verification that the derived optimality system for our proposed optimal control problem is correct.

Moreover, we compute the optimal solution on different grids and the difference between the optimal control, its corresponding state, and adjoint state of two subsequent grids. The results in Table 3.3 indicate the convergence of the solution of the optimality system.

Conclusion

The formulation of an optimal control of the wine fermentation process was investigated. The system of reaction-diffusion equations modelling the wine fermentation process was theoretically investigated proving existence and uniqueness of solutions. Further, an optimal control problem with thermal boundary control was formulated. Existence of optimal

N_x, N_y, M	21,41,401	41,81,401 (eoc)
X	$8.76 \cdot 10^{-6}$	$2.44 \cdot 10^{-6}$ (1.84)
N	$4.29 \cdot 10^{-5}$	$1.68 \cdot 10^{-5}$ (1.35)
O	$4.29 \cdot 10^{-5}$	$1.68 \cdot 10^{-5}$ (1.35)
S	$5.51 \cdot 10^{-6}$	$1.39 \cdot 10^{-6}$ (1.97)
E	$1.98 \cdot 10^{-6}$	$4.99 \cdot 10^{-7}$ (1.99)
T	$3.31 \cdot 10^{-6}$	$1.09 \cdot 10^{-6}$ (1.61)
p_1	$7.65 \cdot 10^{-5}$	$2.35 \cdot 10^{-5}$ (1.70)
p_2	$9.87 \cdot 10^{-5}$	$2.87 \cdot 10^{-5}$ (1.78)
p_3	$9.87 \cdot 10^{-5}$	$2.87 \cdot 10^{-5}$ (1.78)
p_4	$1.15 \cdot 10^{-5}$	$4.95 \cdot 10^{-6}$ (1.21)
p_5	$2.32 \cdot 10^{-5}$	$9.72 \cdot 10^{-6}$ (1.25)
p_6	$5.40 \cdot 10^{-3}$	$1.88 \cdot 10^{-3}$ (1.60)
u	$7.14 \cdot 10^{-6}$	$2.46 \cdot 10^{-6}$ (1.54)

Table 3.3: Convergence rates of the optimal solution, its state and adjoint state. The error measures the difference of the solutions of two subsequent grids by $\|C_h - C_{2h}\|_{L^2_{h,\delta t}} / \|C_{2h}\|_{L^2_{h,\delta t}}$, where the finer grid is specified in the top row of the table. The mesh width parameter is denoted by h.

solutions and its characterisation as solutions to the corresponding optimality system was discussed. Results of numerical experiments were presented to demonstrate the effectiveness of the proposed control framework.

Chapter 4

A Function Identification Method

Mathematical models of dynamical systems of physical, biological, and chemical nature usually contain parameters, which describe the dependencies of the state variables and their time derivatives. These model parameters allow to use one model for many situations by choosing a different set of parameters, which is calibrated to the desired application. We can think of, for example, yeast strains that convert sugar into ethanol very fast while other strains need more time. Hence, the parameters a_5, a_6, and a_7 of the wine fermentation model (2.8) would be larger in the case of fast fermenting yeast strains. By developing mathematical models, the relationship between state variables, their time derivatives, and the parameters is derived by arguments or at least heuristics. But sometimes our understanding of the underlying process is so poor that a parametrised function cannot be given for such a relationship. Moreover, the underlying phenomena could be highly non-linear and have many regimes with different behaviours. In these cases, it is beneficial to work with a general function with no constraints about its shape. For a specific application, one has to find an element out of a function space, which fits best in the current context. Allowing arbitrary variations of a function and not restricting ourselves to a parametrised shape is the central idea of this chapter.

For clarifying our concept we consider a simple biological model of an enzymatic reaction [Mur93, Chapter 6.1]. Let $y(t)$ denote the concentration of a substrate at time t, which is converted to a product with the aid of an enzyme. In [MM13, JG11], the authors argue that a model that describes the evolution of the function y is given by the following differential equation

$$\frac{\mathrm{d}y}{\mathrm{d}t} = p_1 \frac{y}{p_2 + y}.$$

In this case, we know the shape of the right-hand side function $F(y, p_1, p_2) \coloneqq p_1 \frac{y}{p_2+y}$ and, by varying the parameter p_1 and p_2, we can model many different enzymatic reactions.

An example for a model with unknown dynamics function is the process of decaying yeast cell concentrations in the wine fermentation due to high ethanol concentrations. In Chapter 2, the following differential equation is given

$$\frac{\mathrm{d}X}{\mathrm{d}t} = -\Psi(E)X,$$

where the shape of the function Ψ is unknown; see (2.6).

Therefore, we investigate the problem of identifying a function that participates in a dynamical system. We distinguish two cases. First, we discuss the identification problem with a deterministic model, which is given by the following one dimensional differential

equation

$$\frac{\mathrm{d}y}{\mathrm{d}t} = f(y).$$

The proposed function identification method is considered for this deterministic case in Section 4.1.

Further, we consider stochastic models, as uncertainties in biology are very high. The mathematical framework for stochastic differential equations is discussed later, but to get the idea behind these concepts one can think of the following differential equation

$$\frac{\mathrm{d}y}{\mathrm{d}t} = f(y) + \xi,$$

where ξ represents a random disturbance for the evolution of the state variable y. The function identification method for this kind of stochastic models is addressed in Section 4.2.

4.1 The Deterministic Case

This section deals with a method for the identification of an unknown function that is involved in an ordinary differential equation. For this purpose we consider the following minimisation problem

$$\min_{f \in H^m(\mathbb{R})} J(y, f) = \frac{1}{2} \|y - y_d\|^2_{L^2(0,t_f)} + \frac{\lambda}{2} \|f - f_p\|^2_{H^m(\mathbb{R})}, \tag{4.1a}$$

$$\text{subject to} \quad \dot{y}(t) = f(y(t)) \quad \text{for } t \in [0, t_f], \tag{4.1b}$$

$$y(0) = y_0, \tag{4.1c}$$

where we denote the time derivative of y by $\dot{y}(t)$. Here, the functional J depends on a function f in the function space $H^m(\mathbb{R})$ and on the state y of a differential equation. The minimisation of J is done with an initial value problem as a constraint. The ordinary differential equation (4.1b) together with the corresponding initial condition (4.1c), where $y_0 \in \mathbb{R}$ is given, describe the connection between the function f and the state y. We choose the Sobolev space $H^m(\mathbb{R})$ as the function space where the unknown function f is sought. With this setting, we can exploit the Hilbert space structure of $H^m(\mathbb{R})$ and adjust the differentiability properties of f by increasing the degree m.

The differential equation (4.1b) is an example of a dynamical system modelling a physical, chemical, or biological process, where a part of the dynamics is unknown, namely the function f. We restrict ourselves to this model problem in order to ease the notation. Nevertheless, the given proofs in this work are also valid for a more general class of problems and we apply the proposed method to the wine fermentation model (2.8) in Subsection 4.1.6.

The motivation for investigating the minimisation problem (4.1) is as follows. We have a physical system in mind whose state $y(t)$ at time $t \in [0, t_f]$ evolves according to the differential equation (4.1b), where $t_f > 0$ is the final time. We assume that we have poor a priori knowledge f_p of the function f, which describes the relationship between the state of the system and its change in time $\dot{y}$. Given some measurement $y_d \in L^2(0, t_f)$ of the evolving state, we want to identify the function f based on these measurements. This can be done by minimising the objective functional J, as its first term measures the deviation of a simulation result y subject to a certain function f from the measurements

y_d. J also includes the $H^m(\mathbb{R})$–norm of $f - f_p$, as this often used Tikhonov–regularisation gives us the possibility to prove the existence of a unique minimiser of J provided the regularisation parameter λ is sufficiently large. Moreover, by minimising $\|f - f_p\|^2_{H^m(\mathbb{R})}$, we obtain an optimal $f \in H^m(\mathbb{R})$ that is close to f_p.

This section is organised as follows. First, we comment on the similarities and differences of the parameter estimation problem compared to the function identification. Further, we analyse the mapping that assigns to each trial function $f \in H^m(\mathbb{R})$ the solution y of the initial value problem (4.1b–4.1c). Its differentiability properties are proven and we present the adjoint operators of its derivatives. Moreover, the minimisation problem is analysed. We prove its unique solvability and define the mapping that assigns a measurement set to the optimal function, which reproduces these data as good as possible. The sensitivity of the identification of the unknown function with respect to deviations for the given data can be quantified by means of the derivative of the "data–to–function" mapping. Finally, the proposed identification method is applied to the logistic growth equation as well as to the toxicity function of the wine fermentation model (2.8). Numerical results for these identification problems are presented.

4.1.1 Similarities and Differences to Parameter Identification

The function identification method is connected to the problem of parameter estimation. The analogy between these methods is as follows. For the function identification problem (4.1) we use a set of functions, namely $H^m(\mathbb{R})$, as a trial space to model the dependence between the state variable y of a differential equation and its time derivative.

For a parameter estimation problem, the shape of the right-hand side of (4.1b) is known by means of a given parametrised function $F(y, a)$, where $a \in \mathbb{R}^n$ is a set of parameters. The corresponding minimisation problem is as follows

$$\begin{aligned} \min_{a \in \mathbb{R}^n} J(y, a) &= \frac{1}{2} \|y - y_d\|^2_{L^2(0,t_f)} + \frac{\lambda}{2} \|a - a_p\|^2_{\mathbb{R}^n}, \\ \text{subject to} \quad \dot{y}(t) &= F(y(t), a) \quad \text{for } t \in [0, t_f], \\ y(0) &= y_0, \end{aligned}$$

where a_p is a known good guess of the optimal parameters. See [Bar74, Boc87, BDB86, LOP05] for more information on the parameter estimation problem.

Note that a similar minimisation problem is obtained, if we exchange the trial space $H^m(\mathbb{R})$ in (4.1a) by the set $\{y \mapsto F(y, a) \,|\, a \in \mathbb{R}^n\}$. But there is one very important difference. The regularisation term in the function identification framework (4.1) measures the distance of the function f to the guessed optimal function f_p in the $H^m(\mathbb{R})$ norm. Hence, it takes all derivative up to order m into account and enhances the smoothness of the solution of the minimisation problem.

In contrast, the distance of the parameters to the guess a_p is measured in the Euclidean norm. This means that deviations are counted for each parameter to the same extend, regardless which impact on the shape of the right-hand side function $F(y, a)$ they have. This can be very problematic as it is likely the case that some parameters are more important than others. Moreover, they can differ by several magnitudes, which leads to a weighting of the corresponding parameters, which has nothing to do with their impact on the shape of the right-hand side function. Although this can be overcome by the definition of a different norm for the parameter space, which is then used for the regularisation term, the choice of a good norm is not obvious and it must be adjusted for different applications.

In the case of the function identification problem (4.1), the choice of the norm is more natural, as it is inherited from the infinite dimensional space $H^m(\mathbb{R})$. Moreover, we have to discretise the space $H^m(\mathbb{R})$ in order to approximate the optimal function numerically as it is unlikely that this minimisation problem can be solved analytically. Hence, we exchange the infinite dimensional trial space $H^m(\mathbb{R})$ by suitable chosen finite dimensional function space V_h. This casts the infinite dimensional minimisation problem to a finite dimensional one. But now we obtain a norm that is reasonably defined, as it is still the $H^m(\mathbb{R})$ norm restricted to the approximation space V_h. To summarise, the disretised function identification problem can be seen as an parameter estimation problem with a suitably defined norm of the parameter space.

Finally, we mention that the minimisation problem (4.1) is set in an infinite dimensional vector space. Hence, its analysis is more involved compared to the finite dimensional parameter estimation problem. In the following we present theoretical results concerning the function identification problem.

4.1.2 The Solution Operator of the Differential Equation

Before we turn our attention to the analysis of the solution operator of the ordinary differential equation (4.1b), we provide the following Lemma due to Grönwall; see [Eva10, Appendix B.2.j].

Lemma 1 *Let y be a non-negative, absolutely continuous function on $[0, t_f]$, which satisfies for a.e. t the differential inequality*

$$\dot{y}(t) \leq \alpha(t)y(t) + \beta(t),$$

where α and β are non-negative, integrable functions on $[0, t_f]$. Then the inequality

$$y(t) \leq \exp\left(\int_0^t \alpha(s)\,\mathrm{d}s\right)\left(y(0) + \int_0^t \beta(s)\,\mathrm{d}s\right)$$

holds for all $0 \leq t \leq t_f$.

Proof. We compute

$$\begin{aligned}\frac{\mathrm{d}}{\mathrm{d}s}\left(y(s)\exp\left(-\int_0^s \alpha(x)\mathrm{d}x\right)\right) &= \exp\left(-\int_0^s \alpha(x)\mathrm{d}x\right)\left(y'(s) - \alpha(s)y(s)\right)\\ &= \exp\left(-\int_0^s \alpha(x)\mathrm{d}x\right)\beta(s)\end{aligned}$$

for a.e. $s \in [0, t_f]$. Hence, we have for each $0 \leq t \leq t_f$

$$\begin{aligned}y(t)\exp\left(-\int_0^t \alpha(x)\mathrm{d}x\right) &= y(0) + \int_0^t \frac{\mathrm{d}}{\mathrm{d}s}\left(y(s)\exp\left(-\int_0^s \alpha(x)\mathrm{d}x\right)\right)\,\mathrm{d}s\\ &\leq y(0) + \int_0^t \exp\left(-\int_0^s \alpha(x)\mathrm{d}x\right)\beta(s)\,\mathrm{d}s\\ &\leq y(0) + \int_0^t \beta(s)\,\mathrm{d}s,\end{aligned}$$

as α is assumed to be non-negative. This completes the proof. □

We investigate the solution operator of the initial value problem (4.1b–4.1c), as we want to convert the constrained minimisation problem as stated in (4.1) into an unconstrained one. Therefore, we prove the next theorem, where differentiability properties of our model are shown. In contrast to the derivative with respect to time $\dot{y}$, we use the notation $f'(y) = \frac{\mathrm{d}f}{\mathrm{d}y}(y)$ for elements of $H^m(\mathbb{R})$.

Theorem 20 *Assume that $m \geq 2$. Then the solution operator $S : H^m(\mathbb{R}) \to L^2(0, t_f)$, which maps a function $f \in H^m(\mathbb{R})$ to the solution y of the initial value problem (4.1b–4.1c), is well-defined and of class C^{m-2}.*

In particular, the first derivative $S'(f) : H^m(\mathbb{R}) \to L^2(0, t_f)$ is given by the solution of

$$\dot{v} = f'(y)v + h(y) \quad \text{for } t \in [0, t_f], \tag{4.2a}$$
$$v(0) = 0, \tag{4.2b}$$

where $y = S(f)$ and $v = S'(f)h$ with $h \in H^m(\mathbb{R})$.

Moreover, the second derivative $S''(f) : H^m(\mathbb{R}) \times H^m(\mathbb{R}) \to L^2(0, t_f)$ is given by the solution of

$$\dot{w} = f'(y)w + f''(y)v_h v_k + h'(y)v_k + k'(y)v_h \quad \text{for } t \in [0, t_f], \tag{4.3a}$$
$$w(0) = 0, \tag{4.3b}$$

where $y = S(f)$, $v_h = S'(f)h$, $v_k = S'(f)k$, and $w = S''(f)(h, k)$ with $h, k \in H^m(\mathbb{R})$.

Proof. Notice that due to Theorem 2, we have the embeddings $H^m(\mathbb{R}) \hookrightarrow C^{m-1,\frac{1}{2}}(\mathbb{R})$ and $H^1(\mathbb{R}) \hookrightarrow L^\infty(\mathbb{R})$; see [AF03, Theorem 4.12] for the additional results on embeddings into spaces of continuous functions. Therefore, every function $f \in H^m(\mathbb{R})$ has Lipschitz-continuous derivatives up to order $m-2$ for which the mean value theorem holds. Hence, by the Picard-Lindelöf theorem [Hal09, Theorem 3.1], there exists a unique solution y to the initial value problem (4.1b–4.1c). A fortiori $y \in L^2(0, t_f)$ holds. We conclude that the operator S is well-defined. Next, we show the continuity of S.

Denoting $y_1 = S(f_1)$ and $y_2 = S(f_2)$ the following initial value problem

$$\dot{z} = f_1(y_1) - f_2(y_2),$$
$$z(0) = 0,$$

is solved by $z = y_1 - y_2$. Moreover, we estimate

$$\begin{aligned} |\dot{z}| &\leq |f_1(y_1) - f_1(y_2) + f_1(y_2) - f_2(y_2)| \\ &\leq |f_1'(\xi)|\,|y_1 - y_2| + |(f_1 - f_2)(y_2)| \\ &\leq \|f_1'\|_{L^\infty(\mathbb{R})}\,|z| + \|f_1 - f_2\|_{L^\infty(\mathbb{R})}, \end{aligned}$$

where we use the mean value theorem for f_1. By Lemma 1, we conclude that

$$|z| \leq t\|f_1 - f_2\|_{L^\infty(\mathbb{R})} \exp\left(t\|f_1'\|_{L^\infty(\mathbb{R})}\right)$$

holds. Hence, we have the following estimate

$$\|z\|_{L^2(0,t_f)} \leq \sqrt{t_f}\|z\|_{L^\infty(\mathbb{R})} \leq (t_f)^{\frac{3}{2}}\,\|f_1 - f_2\|_{L^\infty(\mathbb{R})} \exp\left(t_f\|f_1'\|_{L^\infty(\mathbb{R})}\right).$$

Using the embeddings mentioned above and a generic constant C, that does not depend on f_1 and f_2, we arrive at the estimate

$$\|S(f_1) - S(f_2)\|_{L^2(0,t_f)} \leq C \exp\left(C \|f_1\|_{H^m(\mathbb{R})}\right) \|f_1 - f_2\|_{H^m(\mathbb{R})}, \tag{4.4}$$

and hence we have proven the continuity of S.

In order to show the differentiability of S, we first show that the linear operator $S'(f)$ as defined in (4.2) is bounded. As

$$|\dot{v}| \leq |f'(y)||v| + |h(y)| \leq \|f'\|_{L^\infty(\mathbb{R})}|v| + \|h\|_{L^\infty(\mathbb{R})}$$

holds, we conclude by Lemma 1

$$|v| \leq t\|h\|_{L^\infty(\mathbb{R})} \exp\left(t\|f'\|_{L^\infty(\mathbb{R})}\right),$$

which results in

$$\|S'(f)h\|_{L^2(0,t_f)} \leq C \exp\left(C \|f\|_{H^m(\mathbb{R})}\right) \|h\|_{H^m(\mathbb{R})}. \tag{4.5}$$

Hence, $S'(f)$ is bounded.

Next, we show that $S'(f)$ is the Fréchet derivative of S. Therefore, let $f, h \in H^m(\mathbb{R})$ be arbitrary and define $\overline{y} = S(f+h)$, $y = S(f)$, $v = S'(f)h$, and $z = \overline{y} - y - v$. Hence,

$$\begin{aligned} \dot{z} &= (f+h)(\overline{y}) - f(y) - f'(y)v - h(y), \\ z(0) &= 0. \end{aligned}$$

We compute

$$\begin{aligned} |\dot{z}| &\leq |f(\overline{y}) + h(\overline{y}) - f(y) - f'(y)v - h(y)| \\ &\leq |f'(y)(\overline{y} - y - v)| + |f'(\xi)(\overline{y} - y) - f'(y)(\overline{y} - y)| + |h'(\zeta)||\overline{y} - y| \\ &\leq |f'(y)||z| + |f'(\xi) - f'(y)||\overline{y} - y| + |h'(\zeta)||\overline{y} - y| \\ &\leq |f'(y)||z| + |f''(\theta)||\overline{y} - y|^2 + |h'(\zeta)||\overline{y} - y| \\ &\leq \|f'\|_{L^\infty(\mathbb{R})}|z| + \|f''\|_{L^\infty(\mathbb{R})}\|\overline{y} - y\|^2_{L^\infty(\mathbb{R})} + \|h'\|_{L^\infty(\mathbb{R})}\|\overline{y} - y\|_{L^\infty(\mathbb{R})} \\ &\leq \|f'\|_{L^\infty(\mathbb{R})}|z| + C \exp\left(C \|f\|_{H^m(\mathbb{R})}\right) \|h\|^2_{H^m(\mathbb{R})}, \end{aligned}$$

where we use (4.4) for the last estimate and the mean value theorem for f and f'. Due to Lemma 1, we conclude

$$|z| \leq C \exp\left(C \|f\|_{H^m(\mathbb{R})}\right) \|h\|^2_{H^m(\mathbb{R})} \exp\left(C \|f'\|_{L^\infty(\mathbb{R})}\right),$$

and therefore

$$\lim_{\|h\|_{H^m(\mathbb{R})} \to 0} \frac{\|S(f+h) - S(f) - S'(f)h\|_{L^2(0,t_f)}}{\|h\|_{H^m(\mathbb{R})}} = 0,$$

which completes the proof for the Fréchet differentiability of S.

In order to estimate the norm of $S'(f_1) - S'(f_2)$ to show the continuity of S' we define $y_1 = S(f_1)$, $y_2 = S(f_2)$, and $z = v_1 - v_2 = S'(f_1)h - S'(f_2)h$. The function z solves

$$\begin{aligned} \dot{z} &= f_1'(y_1)v_1 + h(y_1) - f_2'(y_2)v_2 - h(y_2), \\ z(0) &= 0. \end{aligned}$$

Using the mean value theorem, embedding results, (4.4), and (4.5), we estimate

$$\begin{aligned}
|\dot{z}| &\leq |f_1'(y_1)v_1 + h(y_1) - f_2'(y_2)v_2 - h(y_2)| \\
&\leq |f_1'(y_1)v_1 - f_1'(y_1)v_2| + |f_1'(y_1)v_2 - f_2'(y_2)v_2| + |h'(\zeta)(y_1 - y_2)| \\
&\leq |f_1'(y_1)||v_1 - v_2| + |f_1'(y_1) - f_2'(y_2)||v_2| + |h'(\zeta)(y_1 - y_2)| \\
&\leq |f_1'(y_1)||z| + (|f_1'(y_1) - f_1'(y_2)| + |f_1'(y_2) - f_2'(y_2)|)\,|v_2| + |h'(\zeta)(y_1 - y_2)| \\
&\leq |f_1'(y_1)||z| + (|f_1''(\xi)||y_1 - y_2| + |(f_1' - f_2')(y_2)|)\,|v_2| + |h'(\zeta)(y_1 - y_2)| \\
&\leq \|f_1'\|_{L^\infty(\mathbb{R})}|z| + C\|h\|_{H^m(\mathbb{R})}\|f_1 - f_2\|_{H^m(\mathbb{R})}.
\end{aligned}$$

Due to Lemma 1, we conclude

$$|z| \leq tC\|h\|_{H^m(\mathbb{R})}\|f_1 - f_2\|_{H^m(\mathbb{R})} \exp\left(t\|f_1'\|_{L^\infty(\mathbb{R})}\right),$$

and therefore

$$\|S'(f_1) - S'(f_2)\|_{\mathcal{L}(H^m(\mathbb{R}),L^2(0,t_f))} \leq C \exp\left(C\,\|f_1\|_{H^m(\mathbb{R})}\right)\|f_1 - f_2\|_{H^m(\mathbb{R})}, \tag{4.6}$$

which proves the continuity of the first derivative of S.

Finally, in order to show that S is k-times continuously differentiable, we need to assume that, on one hand, the mean value theorem holds for the k-th derivatives of the elements of the underlying function space and that, on the other hand, we can bound the $L^\infty(\mathbb{R})$-norm of their $(k+1)$-th derivative as follows

$$\|f^{(k+1)}\|_{L^\infty(\mathbb{R})} \leq C\|f\|_{H^m(\mathbb{R})}.$$

This means that for $f \in H^m(\mathbb{R})$ we can at least prove that S is of class C^{m-2}.

In order to compute the governing differential equations for derivatives of S one must take derivatives of (4.1b) with respect to f taking into account that y is also dependent on f. Let us denote by D_h the directional derivative operator with respect to f in the direction $h \in H^m(\mathbb{R})$. Define $v := D_h(y) = D_h(S(f)) = S'(f)h$. For the time derivative of v, we compute by exchanging the order of differentiation the following

$$\dot{v} = \frac{\mathrm{d}}{\mathrm{d}t}D_h(y) = D_h(\dot{y}) = D_h(f(y)) = f'(y)D_h(y) + h(y) = f'(y)v + h(y).$$

For the second summand, we use fact that for a function w that is independent of f the operator $f \mapsto f(w)$ is linear and we have $D_h(f(w)) = h(w)$. Hence, we have shown (4.2a). Moreover, denoting $w = D_k(D_h(y))$, $v_h = D_h(y)$, $v_k = D_k(y)$ for $h, k \in H^m(\mathbb{R})$, we compute

$$\begin{aligned}
\dot{w} &= \frac{\mathrm{d}}{\mathrm{d}t}D_k(D_h(y)) = D_k\left(\frac{\mathrm{d}}{\mathrm{d}t}D_h(y)\right) = D_k\left(\dot{v}_h\right) = D_k\left(f'(y)v_h + h(y)\right) \\
&= D_k(f'(y))v_h + f'(y)D_k(v_h) + D_k(h(y)) \\
&= \left(k'(y) + f''(y)D_k(y)\right)v_h + f'(y)w + h'(y)D_k(y) \\
&= f'(y)w + f''(y)v_kv_h + h'(y)v_k + k'(y)v_h,
\end{aligned}$$

which shows (4.3a). □

The first derivative of S is a linear operator between Hilbert spaces. Hence, there exists an adjoint operator. As we use this adjoint operator in the next section, we present the following theorem, which provides a computational formula for this operator and its derivative.

Theorem 21 *Let $m \geq 4$. For a fixed $f \in H^m(\mathbb{R})$, the adjoint operator*

$$S'(f)^* : L^2(0,t_f) \to H^m(\mathbb{R})$$

maps an element $x \in L^2(0,t_f)$ on the Riesz representative $S'(f)^*(x)$ of the $H^m(\mathbb{R})$–functional

$$k \mapsto \int_0^{t_f} p\, k(y) \mathrm{d}t \quad \text{for } k \in H^m(\mathbb{R}), \tag{4.7}$$

where $y = S(f)$ and p solves the following adjoint equation

$$-\dot{p} = f'(y)p + x \quad \text{for } t \in [0,t_f], \tag{4.8a}$$

$$p(t_f) = 0. \tag{4.8b}$$

Moreover, given a fixed $x \in L^2(0,t_f)$ the first derivative of the adjoint operator

$$S'(\cdot)^*(x) : H^m(\mathbb{R}) \to H^m(\mathbb{R})$$

with respect to f in the direction h is given by the Riesz representative $[S'(f)^*(x)]'h$ of the $H^m(\mathbb{R})$–functional

$$k \mapsto \int_0^{t_f} z\, k(y) + p\, k'(y)\, v \,\mathrm{d}t \quad \text{for } k \in H^m(\mathbb{R}), \tag{4.9}$$

where $y = S(f)$, $v = S'(f)h$, p solves (4.8), and z solves the following terminal value problem

$$-\dot{z} = f'(y)z + (f''(y)v + h'(y))\, p \quad \text{for } t \in [0,t_f], \tag{4.10a}$$

$$z(t_f) = 0. \tag{4.10b}$$

Proof. First, note that the terminal value problem (4.8) is a linear problem and its solution is given by

$$p(t) = -\int_t^{t_f} \exp\left(\int_t^s f'(y(\tau))\mathrm{d}\tau\right) x(s)\,\mathrm{d}s.$$

As $x \in L^2(0,t_f)$ and $f' \in L^\infty(\mathbb{R})$ holds, we have $p \in L^\infty(0,t_f) \hookrightarrow L^2(0,t_f)$ and conclude that the mapping $x \mapsto S'(f)^*(x)$ is well-defined. Moreover, the linear mapping (4.7) is bounded, as

$$\left|\int_0^{t_f} p\, k(y)\,\mathrm{d}t\right| \leq t_f \|p\|_{L^\infty(0,t_f)} \|k\|_{L^\infty(\mathbb{R})} \leq C\|p\|_{L^\infty(0,t_f)} \|k\|_{H^m(\mathbb{R})} \tag{4.11}$$

holds.

Further, for arbitrary $k \in H^m(\mathbb{R})$ and $x \in L^2(0,t_f)$

$$\begin{aligned}
(S'(f)^*(x), k)_{H^m(\mathbb{R})} &= \int_0^{t_f} p\, k(y)\,\mathrm{d}t = \int_0^{t_f} p\,(\dot{v} - f'(y)v)\,\mathrm{d}t \\
&= \int_0^{t_f} (-\dot{p} - f'(y)p)\, v\,\mathrm{d}t + p(t_f)v(t_f) - p(0)v(0) \\
&= \int_0^{t_f} x\, v\,\mathrm{d}t = (x, S'(f)k)_{L^2(0,t_f)},
\end{aligned}$$

where we used integration by parts, $v(0) = p(t_f) = 0$, and $k(y) = \dot{v} - f'(y)v$ for $v = S'(f)k$. This shows that (4.7) together with (4.8) is indeed the adjoint mapping.

In order to prove the differentiability of the adjoint mapping, we take a closer look on the second derivative of S. Fixing the first argument of this bilinear mapping it becomes the linear, bounded operator $k \mapsto S''(f)(h,k)$, where $h \in H^m(\mathbb{R})$ is given. Hence, there exists an adjoint operator

$$[S''(f)(h,\cdot)]^* : L^2(0,t_f) \to H^m(\mathbb{R}).$$

Now, consider the following computation

$$\begin{aligned}
&(x, S''(h,k))_{L^2(0,t_f)} = \int_0^{t_f} x\, w \,\mathrm{d}t = \int_0^{t_f} (-\dot{p} - f'(y)p)\, w \,\mathrm{d}t \\
&= \int_0^{t_f} p\,(\dot{w} - f'(y)w)\,\mathrm{d}t = \int_0^{t_f} p\,(f''(y)v_h v_k + h'(y)v_k + k'(y)v_h)\,\mathrm{d}t \\
&= \int_0^{t_f} (-\dot{z} - f'(y)z)\, v_k + p\,k'(y)\, v_h \,\mathrm{d}t = \int_0^{t_f} z\,(\dot{v}_k - f'(y)\, v_k) + p\,k'(y)\, v_h \,\mathrm{d}t \\
&= \int_0^{t_f} z\,k(y) + p\,k'(y)\, v_h \,\mathrm{d}t = \left([S'(f)^*(x)]'\, h, k\right)_{H^m(\mathbb{R})}.
\end{aligned}$$

It follows that

$$[S''(f)(h,\cdot)]^*(x) = [S'(f)^*(x)]'\, h. \tag{4.12}$$

Finally, for a fixed $x \in L^2(0,t_f)$, the estimate

$$\begin{aligned}
&\left|\left(S'(f+h)^*(x) - S'(f)^*(x) - [S'(f)^*(x)]'\, h, k\right)_{H^m(\mathbb{R})}\right| \\
&= \left|(x, S'(f+h)k - S'(f)k - S''(f)(h,k))_{L^2(0,t_f)}\right| \\
&\le \|x\|_{L^2(0,t_f)}\, \|S'(f+h) - S'(h) - S''(f)(h,\cdot)\|_{\mathcal{L}(H^m(\mathbb{R}),L^2(0,t_f))}\, \|k\|_{H^m(\mathbb{R})} \\
&\le C\, \|k\|_{H^m(\mathbb{R})}\, \|h\|^2_{H^m(\mathbb{R})}
\end{aligned}$$

proves that the mapping corresponding to (4.9) is the derivative of $f \mapsto S'(f)^*(x)$. □

4.1.3 Existence and Uniqueness of Minimisers

The existence of a solution to the minimisation problem (4.1) is addressed in the following. In the corresponding proof, we show that the states of a minimising sequence are converging not only weakly but also strongly. This is proven by utilising the following theorem. It states the necessary and sufficient conditions for a bounded set in an L^p space to be pre-compact and can be found in [AF03, Theorem 2.32].

Theorem 22 *Let $\Omega \subset \mathbb{R}^n$ be an open set and further let $1 \le p < \infty$. A bounded subset $C \in L^p(\Omega)$ is pre-compact in $L^p(\Omega)$ if and only if for every number $\varepsilon > 0$ there exists a $\delta > 0$ and a compact subset G of Ω such that for every $y \in C$ and $h \in \mathbb{R}^n$ with $\|h\|_2 \le \delta$*

the following inequalities hold:

$$\int_{\Omega} |y(x+h) - y(x)|^p \mathrm{d}x \leq \varepsilon^p,$$

$$\int_{\Omega \setminus G} |y(x)|^p \mathrm{d}x \leq \varepsilon^p,$$

where $y(x+h)$ is defined to be zero for $x + h \notin \Omega$.

The following theorem states the existence of a solution to problem (4.1). The proof of the uniqueness of a minimiser cannot be given for an arbitrary regularisation parameter λ, but only for a λ that is large enough; see Theorem 25.

Theorem 23 *Let $y_d \in L^2(0,t_f)$, $f_p \in H^m(\mathbb{R})$, $m \geq 2$ and $\lambda > 0$ be given. Then there exists a solution to the constrained minimisation problem* (4.1)*.*

Proof. The objective functional J is bounded from below by zero. As the norms of y and f are included in J, a pair of minimising sequences (y_n) and (f_n) exists and is bounded in $L^2(0,t_f)$ and $H^m(\mathbb{R})$. Hence, there exists a bound $M > 0$ such that $\|y_n\|_{L^2(0,t_f)} \leq M$ and $\|f_n\|_{H^m(\mathbb{R})} \leq M$ holds for all $n \in \mathbb{N}$. Moreover, we have $y_n = S(f_n)$. Bounded sequences in a Hilbert space contain weakly convergent subsequences due to Theorem 11. Hence, we have $y_n \rightharpoonup \overline{y}$ in $L^2(0,t_f)$ and $f_n \rightharpoonup \overline{f}$ in $H^m(\mathbb{R})$, where use the same notation for subsequences. Recall that J is sequentially weakly lower semicontinuous due to Theorem 13. Hence, we have $J(\overline{y},\overline{f}) \leq \liminf_{n\to\infty} J(y_n, f_n)$ and it remains to show that $\overline{y}$ and $\overline{f}$ satisfies the constraint of the minimisation problem (4.1), which can be written as $\overline{y} = S(\overline{f})$.

First, we show that the sequence (y_n) converges even strongly in $L^2(0,t_f)$. The state y_n is a solution for the initial value problem (4.1b–4.1c) with right-hand side function f_n and we conclude that

$$y_n(t) = y_0 + \int_0^t f_n(y_n(s))\mathrm{d}s$$

holds. Hence, we conclude

$$|y_n(t)| \leq |y_0| + t\|f_n\|_{L^\infty(\mathbb{R})} \leq |y_0| + t_f M,$$

and, therefore, $\|y_n\|_{L^\infty(0,t_f)} \leq M'$ holds for $M' = |y_0| + t_f M$.

We use Theorem 22 in order to prove that the set $\{y_n | n \in \mathbb{N}\} \subset L^2(0,t_f)$ is precompact in $L^2(0,t_f)$. Therefore, let $\varepsilon > 0$ be arbitrary. First, we choose $\delta := \frac{\varepsilon}{\sqrt{t_f} M}$ and compute

$$\begin{aligned}\int_0^{t_f} |y_n(t+h) - y_n(t)|^2 \,\mathrm{d}t = \int_0^{t_f} \left| \int_t^{t+h} f_n(y_n(s))\,\mathrm{d}s \right|^2 \mathrm{d}t &\leq \int_0^{t_f} \left| h\,\|f_n\|_{L^\infty(\mathbb{R})} \right|^2 \mathrm{d}t \\ &\leq t_f\, h^2\, M^2 \leq \varepsilon^2,\end{aligned}$$

for all $|h| \leq \delta$. Further, we choose $G := [\frac{\varepsilon^2}{2M'^2}, t_f - \frac{\varepsilon^2}{2M'^2}]$, which is a compact interval in $[0,t_f]$, and compute

$$\int_{(0,t_f)\setminus G} |y_n(t)|^2 \,\mathrm{d}t \leq \int_{(0,t_f)\setminus G} \|y_n\|^2_{L^\infty(0,t_f)} \,\mathrm{d}t \leq \frac{\varepsilon^2}{M'^2} \|y_n\|^2_{L^\infty(0,t_f)} \leq \varepsilon^2.$$

Both proven inequalities hold for all $n \in \mathbb{N}$. Hence, we conclude by Theorem 22 that the set $\{y_n | n \in \mathbb{N}\}$ is pre-compact in $L^2(0,t_f)$ and there exists a strongly convergent subsequence, which we again denote by (y_n). Due to Theorem 9 the strong limit of the sequence (y_n) is its weak limit $\overline{y}$.

Further, we show that the sequence of the states y_n converges point-wise to y_* defined by

$$y_*(t) = y_0 + \int_0^t \overline{f}(\overline{y}(s))\,\mathrm{d}s.$$

We have

$$\begin{aligned}
|y_n(t) - y_*(t)| &= \left| \int_0^t f_n(y_n(s)) - \overline{f}(\overline{y}(s))\,\mathrm{d}s \right| \\
&\leq \int_0^t |f_n(y_n(s)) - \overline{f}(y_n(s))|\mathrm{d}s + \int_0^t |\overline{f}(y_n(s)) - \overline{f}(\overline{y}(s))|\mathrm{d}s \\
&\leq t\|f_n - \overline{f}\|_{L^\infty(\mathbb{R})} + \int_0^t |\overline{f}'(\xi_k)||y_n(s) - \overline{y}(s)|\mathrm{d}s \\
&\leq t_f\|f_n - \overline{f}\|_{L^\infty(\mathbb{R})} + \|\overline{f}'\|_{L^\infty(\mathbb{R})} \left(\int_0^t 1\mathrm{d}s \right)^{\frac{1}{2}} \left(\int_0^t |y_n(s) - \overline{y}(s)|^2\mathrm{d}s \right)^{\frac{1}{2}} \\
&\leq t_f\|f_n - \overline{f}\|_{L^\infty(\mathbb{R})} + \|\overline{f}'\|_{L^\infty(\mathbb{R})}\sqrt{t_f}\|y_n - \overline{y}\|_{L^2(0,t_f)},
\end{aligned}$$

where we use the mean value theorem and the Cauchy-Schwarz inequality. The derivative of $f \in H^m(\mathbb{R})$ is essentially bounded for $m \geq 2$; see Theorem 2. Moreover, (f_n) converges strongly to $\overline{f}$ in $L^\infty(\mathbb{R})$, as the embedding $H^m(\mathbb{R}) \hookrightarrow H^{m-1}(\mathbb{R})$ is compact and the embedding $H^{m-1}(\mathbb{R}) \hookrightarrow L^\infty(\mathbb{R})$ is continuous; see Theorem 3 and Theorem 2. Recall that $\{y_n\}$ converges strongly to $\overline{y}$ in $L^2(0,t_f)$. Hence, we conclude $y_n(t) \to y_*(t)$ as n tends to infinity for all $t \in [0,t_f]$. As $\overline{y}$ is the limit of $\{y_n\}$ in $L^2(0,t_f)$, we have

$$\overline{y}(t) = y_*(t) = y_0 + \int_0^t \overline{f}(\overline{y}(s))\,\mathrm{d}s,$$

which proves $\overline{y} = S(\overline{f})$ and completes the proof. □

In order to prove also uniqueness of solutions to the minimisation problem (4.1), we omit the constraint by using the solution operator S of the previous section and define the following reduced objective functional

$$\widetilde{J}(f) = \frac{1}{2}\left\|S(f) - y_d\right\|^2_{L^2(0,t_f)} + \frac{\lambda}{2}\left\|f - f_p\right\|^2_{H^m(\mathbb{R})}. \tag{4.13}$$

The next theorem states the differentiability properties of $\widetilde{J}(f)$ and gives the explicit form of the first and second derivative.

Theorem 24 *Assume that $m \geq 4$. Then, the reduced functional $\widetilde{J}$ is of class C^{m-2}. In particular, its gradient $\widetilde{J}'(f) \in H^m(\mathbb{R})$ and the second derivative $\widetilde{J}''(f) : H^m(\mathbb{R}) \to H^m(\mathbb{R})$ are given by*

$$\widetilde{J}'(f) = S'(f)^*(S(f) - y_d) + \lambda\,(f - f_p)\,, \tag{4.14a}$$

$$\widetilde{J}''(f) = [S'(f)^*(x)]'\Big|_{x=S(f)-y_d} + S'(f)^*S'(f) + \lambda I, \tag{4.14b}$$

where I is the identity operator in $H^m(\mathbb{R})$.

Proof. In every Hilbert space X the function $x \mapsto \|x\|_X^2$ is of class C^∞, where the first derivative is given by $\widetilde{x} \mapsto 2(x, \widetilde{x})_X$. Hence, as S is of class C^{m-2} the same is true for $\widetilde{J}$. The explicit form (4.14) is easily computed by utilising the linearity of the adjoint operator of S', Theorem 20, and Theorem 21.

Let us mention that the first Fréchet derivative of the operator $\widetilde{J} : H^m(\mathbb{R}) \to \mathbb{R}$ is an element of the dual space $H^m(\mathbb{R})^*$. Hence, the second derivative of $\widetilde{J}$ at the point f is a linear operator between the spaces $H^m(\mathbb{R})$ and $H^m(\mathbb{R})^*$. By identifying $H^m(\mathbb{R})^*$ with $H^m(\mathbb{R})$ due to the Riesz respresentation theorem we consider $\widetilde{J}''(f)$ as a linear operator from $H^m(\mathbb{R})$ to $H^m(\mathbb{R})$. □

Note that the adjoint state p defined by (4.8), which is often defined in optimal control problems, is not equal to $S'(f)^*(S(f) - y_d)$ as it is an element of the space $L^2(0, t_f)$ and not $H^m(\mathbb{R})$. Hence, it is not possible to just sum the adjoint state p and the function $f - f_p$ in order to get the derivative of $\widetilde{J}$ as it is done for the optimal control problem of the wine fermentation process in Theorem 19. We rather have to find the Riesz representative of the functional (4.7) corresponding to p in order to compute $\widetilde{J}'$.

In preparation for the next section, we prove that the reduced functional $\widetilde{J}$ has a unique global minimum.

Theorem 25 *Provided that $\lambda > 0$ is big enough, there exists a unique global minimiser $\overline{f}$ of the reduced functional $\widetilde{J}$ given by* (4.13) *and the following estimate holds*

$$\left\|\overline{f} - f_p\right\|_{H^m(\mathbb{R})} \leq \frac{1}{\sqrt{\lambda}} \left\|y_p - y_d\right\|_{L^2(0,t_f)}, \tag{4.15}$$

where $y_p = S(f_p)$.

Proof. We know that $\min_{f \in H^m(\mathbb{R})} \widetilde{J}(f) \leq \widetilde{J}(f_p) = \frac{1}{2} \|y_p - y_d\|_{L^2(0,t_f)}^2$. Hence, we conclude that the global minimum - if it exists - must be inside the ball $B_{r(\lambda)}$ with center f_p with radius $r(\lambda) = \frac{1}{\sqrt{\lambda}} \|y_p - y_d\|_{L^2(0,t_f)}$, as for all $f \notin B_{r(\lambda)}$ the following holds

$$\widetilde{J}(f) \geq \frac{\lambda}{2} \|f - f_p\|_{H^m(\mathbb{R})}^2 > \frac{\lambda}{2} r(\lambda)^2 = \widetilde{J}(f_p).$$

Therefore, we conclude (4.15) for all global minima of $\widetilde{J}$.

In the following, we show that $\widetilde{J}$ is strictly convex in $B_{r(\lambda)}$ provided that λ is big enough. Convexity together with continuity of $\widetilde{J}$ yields its sequential weak lower semi-continuity; see [Cia13, Theorem 9.2-3]. Choose a minimising sequence (f_n) of $\widetilde{J}$. It is bounded and has due to Theorem 11 a weakly converging sequence $\overline{f} \in H^m(\mathbb{R})$. Hence, we have

$$\widetilde{J}(\overline{f}) \leq \liminf_{n \to \infty} \widetilde{J}(f_n) = \min_{f \in H^m(\mathbb{R})} \widetilde{J}(f),$$

and the existence of a minimiser follows. Strict convexity guarantees the uniqueness of the minimiser, as for two global minimisers $\overline{f}_1$ and $\overline{f}_2$ the following

$$\widetilde{J}\left(\frac{1}{2}\overline{f}_1 + \frac{1}{2}\overline{f}_2\right) < \frac{1}{2}\widetilde{J}(\overline{f}_1) + \frac{1}{2}\widetilde{J}(\overline{f}_2) = \min_{f \in H^m(\mathbb{R})} \widetilde{J}(f)$$

holds. This contradicts the assumption that f_1 and f_2 are global minima.

In order to prove strict convexity of $\widetilde{J}$ in $B_{r(\lambda)}$, we show that $\widetilde{J}'$ is strictly monotone in $B_{r(\lambda)}$; see [Kos10, Theorem 3.12.1]. For arbitrary $f_1, f_2 \in B_{r(\lambda)}$, we have

$$\begin{aligned}
&\left(\widetilde{J}'(f_1) - \widetilde{J}'(f_2), f_1 - f_2\right)_{H^m(\mathbb{R})} \\
=&(S'(f_1)^*(S(f_1) - y_d), f_1 - f_2)_{H^m(\mathbb{R})} + \lambda(f_1 - f_p, f_1 - f_2)_{H^m(\mathbb{R})} \\
&- (S'(f_2)^*(S(f_2) - y_d), f_1 - f_2)_{H^m(\mathbb{R})} - \lambda(f_2 - f_p, f_1 - f_2)_{H^m(\mathbb{R})} \\
=&\lambda \|f_1 - f_2\|^2_{H^m(\mathbb{R})} + (S(f_1) - y_d, (S'(f_1) - S'(f_2))(f_1 - f_2))_{L^2(0,t_f)} \\
&+ (S(f_1) - S(f_2), S'(f_2)(f_1 - f_2))_{L^2(0,t_f)}\,.
\end{aligned}$$

On one hand, we estimate with a generic constant C the following

$$\begin{aligned}
&\left|(S(f_1) - y_d, (S'(f_1) - S'(f_2))(f_1 - f_2))_{L^2(0,t_f)}\right| \\
\leq& \|S(f_1) - y_d\|_{L^2(0,t_f)} \|S'(f_1) - S'(f_2)\|_{\mathcal{L}(H^m(\mathbb{R}),L^2(0,t_f))} \|f_1 - f_2\|_{H^m(\mathbb{R})} \\
\leq& \left(\|S(f_1)\|_{L^2(0,t_f)} + \|y_d\|_{L^2(0,t_f)}\right) C \exp\left(C \|f_1\|_{H^m(\mathbb{R})}\right) \|f_1 - f_2\|^2_{H^m(\mathbb{R})} \\
\leq& \left(C \exp\left(C \|f_1\|_{H^m(\mathbb{R})}\right) + \|y_d\|_{L^2(0,t_f)}\right) C \exp\left(C \|f_1\|_{H^m(\mathbb{R})}\right) \|f_1 - f_2\|^2_{H^m(\mathbb{R})}\,,
\end{aligned}$$

where we use (4.4) and (4.6). Note that $\|f_1\|_{H^m(\mathbb{R})} \leq \|f_p\|_{H^m(\mathbb{R})} + r(\lambda)$ is decreasing for an increasing parameter λ. Therefore, we have

$$\left|(S(f_1) - y_d, (S'(f_1) - S'(f_2))(f_1 - f_2))_{L^2(0,t_f)}\right| \leq K_1(\lambda) \|f_1 - f_2\|^2_{H^m(\mathbb{R})}\,,$$

where K_1 is a non-negative, decreasing function. On the other hand, we estimate with a generic constant C

$$\begin{aligned}
&\left|(S(f_1) - S(f_2), S'(f_2)(f_1 - f_2))_{L^2(0,t_f)}\right| \\
\leq& \|S(f_1) - S(f_2)\|_{L^2(0,t_f)} \|S'(f_2)(f_1 - f_2)\|_{L^2(0,t_f)} \\
\leq& C \exp\left(C \|f_1\|_{H^m(\mathbb{R})}\right) \exp\left(C \|f_2\|_{H^m(\mathbb{R})}\right) \|f_1 - f_2\|^2_{H^m(\mathbb{R})}\,,
\end{aligned}$$

where we use (4.4) and (4.5). Hence, there is a non-negative, decreasing function K_2 such that

$$\left|(S(f_1) - S(f_2), S'(f_2)(f_1 - f_2))_{L^2(0,t_f)}\right| \leq K_2(\lambda) \|f_1 - f_2\|^2_{H^m(\mathbb{R})}$$

holds.

We conclude that there exists a $\lambda^* > 0$ such that

$$\left(\widetilde{J}'(f_1) - \widetilde{J}'(f_2), f_1 - f_2\right)_{H^m(\mathbb{R})} \geq (\lambda - K_1(\lambda) - K_2(\lambda)) \|f_1 - f_2\|^2_{H^m(\mathbb{R})} > 0,$$

for all $\lambda > \lambda^*$ and $f_1, f_2 \in B_{r(\lambda)}$. This proves the strict convexity of $\widetilde{J}$ in $B_{r(\lambda)}$ and therefore the existence of a unique minimiser of $\widetilde{J}$. □

Remark 1 *The functions K_1 and K_2 depend on the data y_d. Nevertheless, one can easily prove that there exists an $\lambda^* > 0$ such that $\widetilde{J}$ corresponding to $\lambda > \lambda^*$ and data y_d in a bounded neighbourhood of a fixed $y_D \in L^2(0, t_f)$ has a unique minimiser. From now on we will assume that the regularisation parameter λ is big enough and the minimisation problem* (4.1) *has a unique global solution for all data y_d in an open neighbourhood.*

4.1.4 Sensitivity with Respect to Measurements

We have seen in Subsection 4.1.3 that the minimisation problem (4.1) has a unique solution. In this section, we are interested in the dependence of the minimiser $\overline{f}$ on the data $y_d \in L^2(0,t_f)$. Therefore, we choose an $\lambda > 0$ big enough such that (4.1) has a unique solution for all measurement data from an open neighbourhood U of a fixed $y_d \in L^2(0,t_f)$ and define the mapping

$$H : U \to H^m(\mathbb{R}) \tag{4.16a}$$
$$\widetilde{y}_d \mapsto f \tag{4.16b}$$

that assigns to measurements $\widetilde{y}_d \in U$ the optimal right-hand side function $f \in H^m(\mathbb{R})$, which is the unique solution of (4.1).

Theorem 26 *Let $m \geq 4$. Provided that the regularisation parameter $\lambda > 0$ is big enough, the mapping H is Fréchet–differentiable and its derivative $H'(y_d)$ is given by*

$$H'(y_d) = \left[\widetilde{J}''(H(y_d))\right]^{-1} S'(H(y_d))^*. \tag{4.17}$$

Its image $h = H'(y_d)\widetilde{y}_d$ for $\widetilde{y}_d \in L^2(0,t_f)$ is the solution of the variational problem

$$\begin{aligned}(S''(f)(h,k), y - y_d)_{L^2(0,t_f)} + (S'(f)h, S'(f)k)_{L^2(0,t_f)} + \lambda\,(h,k)_{H^m(\mathbb{R})} \\ = (\widetilde{y}_d, S'(f)k)_{L^2(0,t_f)}\,,\end{aligned} \tag{4.18}$$

for all $k \in H^m(\mathbb{R})$, where $f = H(y_d)$ and $y = S(f)$.

Proof. To prove this theorem, we will employ the implicit function theorem; see Theorem 14. Therefore, we define the mapping

$$\begin{aligned}F : L^2(0,t_f) \times H^m(\mathbb{R}) &\to H^m(\mathbb{R}) \\ (y_d, f) &\mapsto S'(f)^*(S(f) - y_d) + \lambda f.\end{aligned}$$

F is linear in y_d and equals $\widetilde{J}'$ for a fixed $y_d \in L^2(0,t_f)$. Hence, due to Theorem 24 F is of class C^{m-3}. Let $y_d \in L^2(0,t_f)$ be given. We define $\overline{f} = H(y_d)$ and conclude $F(y_d, \overline{f}) = 0$, as $\overline{f}$ is a minimum of $\widetilde{J}$ and F is its gradient.

Moreover, we prove that $\frac{\partial F(y_d,\overline{f})}{\partial f}$ is self-adjoint as follows

$$\begin{aligned}&\left(\frac{\partial F(y_d,\overline{f})}{\partial f}h, k\right)_{H^m(\mathbb{R})} = \left(\widetilde{J}''(\overline{f})h, k\right)_{H^m(\mathbb{R})} \\ &= \left(\left[S'(\overline{f})^*(x)\right]'\Big|_{x=S(\overline{f})-y_d} h + S'(\overline{f})^*S'(\overline{f})h + \lambda h, k\right)_{H^m(\mathbb{R})} \\ &= \left(S(\overline{f}) - y_d, S''(\overline{f})(h,k)\right)_{L^2(0,t_f)} + \left(S'(\overline{f})h, S'(\overline{f})k\right)_{L^2(0,t_f)} + \lambda\,(h,k)_{H^m(\mathbb{R})} \\ &= \left(h, \frac{\partial F(y_d,\overline{f})}{\partial f}k\right)_{H^m(\mathbb{R})},\end{aligned}$$

where we use (4.12) and the symmetry of $S''(\overline{f})$.

Next, we prove that, provided λ is big enough, there exists a $\delta > 0$ such that

$$\left(\frac{\partial F(y_d, \overline{f})}{\partial f} h, h\right)_{H^m(\mathbb{R})} \geq \delta \|h\|^2_{H^m(\mathbb{R})} \tag{4.19}$$

holds for all $h \in H^m(\mathbb{R})$. Therefore, we estimate with a generic constant C

$$\begin{aligned}
&\left|\left(S(\overline{f}) - y_d, S''(\overline{f})(h,h)\right)_{L^2(0,t_f)}\right| \\
&\leq \left\|S(\overline{f}) - y_d\right\|_{L^2(0,t_f)} \left\|S''(\overline{f})(h,h)\right\|_{L^2(0,t_f)} \\
&\leq \left(C\left\|\overline{f}\right\|_{H^m(\mathbb{R})} + \|y_d\|_{L^2(0,t_f)}\right) C \exp\left(C\left\|\overline{f}\right\|_{H^m(\mathbb{R})}\right) \|h\|^2_{H^m(\mathbb{R})} \\
&\leq \left(C(\|f_p\|_{H^m(\mathbb{R})} + r(\lambda)) + \|y_d\|_{L^2(0,t_f)}\right) C \exp\left(C(\|f_p\|_{H^m(\mathbb{R})} + r(\lambda))\right) \|h\|^2_{H^m(\mathbb{R})},
\end{aligned}$$

where we use (4.4), the estimate (4.15) for the minimiser, and the boundedness of $S''(\overline{f})$, which can be proven in a similar fashion as (4.6). Hence, we arrive at

$$\left(\frac{\partial F(y_d, \overline{f})}{\partial f} h, h\right)_{H^m(\mathbb{R})} \geq (\lambda - K(\lambda)) \|h\|^2_{H^m(\mathbb{R})} + \left\|S'(\overline{f})h\right\|^2_{H^m(\mathbb{R})},$$

where K is a non-negative, decreasing function. We conclude the existence of $\lambda^* > 0$ and $\delta > 0$ such that for all $\lambda \geq \lambda^*$ the inequality (4.19) holds. Hence, we conclude as a consequence of the Banach closed range theorem, see [Cia13, Problem 5.11-5]), that $\frac{\partial F(y_d,\overline{f})}{\partial f}$ is bijective. Furthermore, it has a bounded inverse, which is shown by using $k = \left(\frac{\partial F(y_d,\overline{f})}{\partial f}\right)^{-1} h$ and (4.19) as follows

$$\begin{aligned}
\|h\|_{H^m(\mathbb{R})} \left\|\left(\frac{\partial F(y_d, \overline{f})}{\partial f}\right)^{-1} h\right\|_{H^m(\mathbb{R})} &\geq \left(h, \left(\frac{\partial F(y_d, \overline{f})}{\partial f}\right)^{-1} h\right)_{H^m(\mathbb{R})} \\
&= \left(\frac{\partial F(y_d, \overline{f})}{\partial f} k, k\right)_{H^m(\mathbb{R})} \\
&\geq \delta \|k\|^2_{H^m(\mathbb{R})} \\
&= \delta \left\|\left(\frac{\partial F(y_d, \overline{f})}{\partial f}\right)^{-1} h\right\|^2_{H^m(\mathbb{R})},
\end{aligned}$$

which is equivalent to

$$\left\|\left(\frac{\partial F(y_d, \overline{f})}{\partial f}\right)^{-1} h\right\|_{H^m(\mathbb{R})} \leq \frac{1}{\delta} \|h\|_{H^m(\mathbb{R})}.$$

Finally, we apply the implicit function theorem and conclude that there is an implicit function that must be equal to H such that

$$F(\widetilde{y}_d, H(\widetilde{y}_d)) = 0,$$

for all $\widetilde{y}_d$ in a neighborhood of y_d. Furthermore, H is differentiable and

$$\frac{\partial F(y_d, H(y_d))}{\partial f} H'(y_d) + \frac{\partial F(y_d, H(y_d))}{\partial y_d} = 0$$

holds, which is equivalent to (4.17). Finally, (4.18) follows by using the adjoint operators and (4.12). □

Remark 2 *Although* (4.18) *is difficult to compute, we can restrict h and k to a finite-dimensional subspace of $H^m(\mathbb{R})$ and this variational problem reduces to a system of linear equations, which is uniquely solvable for a regularisation parameter λ that is large enough.*

Remark 3 *The results of Theorem 26, in particular* (4.17) *and* (4.18)*, are not only valid for a global minimum, but also for a local minimum and for arbitrary λ as long as the second derivative of $\widetilde{J}$ is strictly positive at this point. Hence, also in this situations it is possible to compute the sensitivity of the identified function f with respect to measurement errors.*

4.1.5 Discretisation with Radial Basis Functions

In this section, we approximate the infinite dimensional function space $H^m(\mathbb{R})$ by a finite dimensional subspace $V_h \subset H^m(\mathbb{R})$ that depends on a discretisation parameter h. All theorems and computations done up to now are still valid for $f \in V_h$, as functions in this subspace have the same differentiability properties as functions in $H^m(\mathbb{R})$. It is in general not clear how a good approximation of an infinite dimensional function space can be constructed. For our purpose the range of the optimal state $\overline{y}$ is important, as we have only information of the function to be identified in this interval. Hence, the approximation of a function $f \in H^m(\mathbb{R})$ by the finite dimensional space V_h should be reasonably good in this interval. Radial basis functions are appropriate for this task, as we show next.

Radial basis functions have been originally analyzed in the context of multivariate interpolation problems, where values of an unknown function f are given for finitely many points and one seeks to construct an interpolant. In particular, given finitely many nodal points $x_i \in \mathbb{R}^d$ $(i = 1, \dots, N)$ and corresponding values $f(x_i) \in \mathbb{R}$, the interpolant s should satisfy the equalities

$$s(x_i) = f(x_i), \qquad \text{for } 1 \leq i \leq N. \tag{4.20}$$

Now, consider a shape function $\varphi : [0, \infty) \to \mathbb{R}$ and define the radially symmetric, multivariate function

$$\begin{aligned} \Phi(x) : \mathbb{R}^d &\to \mathbb{R}, \\ x &\mapsto \varphi(\|x\|_2), \end{aligned}$$

which is called radial basis function. Next, we use shifts of Φ to construct the RBF interpolant as follows

$$s(x) = \sum_{j=1}^{N} u_j \Phi(x - x_j). \tag{4.21}$$

The conditions (4.20) translate to the following system of linear equations

$$\sum_{j=1}^{N} u_j \Phi(x_i - x_j) = f(x_i), \qquad \text{for } 1 \leq i \leq N. \tag{4.22}$$

For a wide class of shape functions φ, it has been proven that the system matrix $(\Phi(x_i - x_j))_{i,j}$ is invertible for an arbitrary distribution of distinct nodal points x_i. Hence, there is a unique interpolant. For further information and an introduction to the theory of radial basis functions see [Buh03] and references therein.

For our purpose, we want to mention that most results on the convergence order of this interpolation are valid only for functions f contained in the so-called "native space"

corresponding to the shape function φ. It has been shown that this space is smaller for smooth shape functions and vice versa, as it is defined via the Fourier transform of Φ. Hence, for our work, we must choose such a shape function whose native space coincides with $H^m(\mathbb{R})$, where we search for the unknown right-hand side function of the differential equation. Fortunately, Wendland's piecewise polynomial, positive definite, and compactly supported radial functions of minimal degree $\varphi_{d,k}$, see [Wen95], have exactly this property, which is shown in [Wen98]. Within their support $r \in [0,1]$ they are defined as follows

$$\varphi_{d,k}(r) = \sum_{n=0}^{k} \beta_{n,k} r^n (1-r)^{l+2k-n}, \tag{4.23}$$

where d is the space dimension, $l = \lfloor d/2 \rfloor + k + 1$, and the coefficients $\beta_{n,k}$ are computed by the recursion formula

$$\beta_{i,j+1} = \sum_{a=\max\{i-1,0\}}^{j} \beta_{a,j} \frac{(i+1)_{a-i+1}}{(l+2j-a+1)_{a-i+2}} \qquad \text{for } 0 \le i \le j+1,$$

with $\beta_{0,0} = 1$ and the Pochhammer symbol $(q)_k = q(q+1)\dots(q+k-1)$. $\Phi_{d,k} = \varphi_{d,k}(\|\cdot\|_2)$ is $2k$-times continuously differentiable with compact support and, therefore, belongs at least to $H^{2k}(\mathbb{R}^d)$.

According to [Wen98] the native space for $\varphi_{d,k}$ is $H^{k+\frac{d+1}{2}}(\mathbb{R}^d)$. Hence, we will use $\varphi_{1,m-1}$ in our work as we minimise in $H^m(\mathbb{R})$. We cite from [Wen98] the following theorem regarding the convergence order of the interpolation problem.

Theorem 27 *Let $m = k + \frac{d+1}{2}$ and $k \ge 1$ for $d = 1, 2$. For every $f \in H^m(\mathbb{R}^d)$ and every compact subset $\Omega \subset \mathbb{R}^d$ satisfying a uniform interior cone condition the interpolant s defined by (4.21) and (4.22) on $\{x_1, \dots, x_N\} \subset \Omega$ using $\varphi_{d,k}$ satisfies the estimate*

$$\|f - s\|_{L^\infty(\Omega)} \le C \|f\|_{H^m(\mathbb{R}^d)} h^{m-\frac{d}{2}}, \tag{4.24}$$

provided $h = \sup_{x\in\Omega} \min_{1\le i\le N} \|x - x_i\|_2$ is sufficiently small.

Next, we define the finite dimensional subspace V_h. Let $y_d \in L^2(0, t_f)$ and a sufficiently large regularisation parameter $\lambda > 0$ be given. Then there is a unique minimiser $\overline{f}$ of (4.1). Its relevant domain $I = \overline{y}([0, t_f])$ is given by the range of the corresponding state $\overline{y} = S(\overline{f})$. As $\overline{y}$ is continuous, its range is an interval $I = [a, b]$. For $h > 0$ we define $x_i = a + i\,h$ for $0 \le i \le N = \lceil \frac{b-a}{h} \rceil$. Using these nodal points the finite dimensional subspace is defined as follows

$$V_h = \operatorname{span}\left\{ x \mapsto \Phi_i(x) = \varphi_{1,m-1}(|x - x_i|) \,\middle|\, 0 \le i \le N \right\}.$$

By Theorem 27, we know that there is a function $s \in V_h$ such that

$$|s(x) - \overline{f}(x)| \le C \left\|\overline{f}\right\|_{H^m(\mathbb{R})} h^{m-\frac{1}{2}},$$

for all $x \in I$. Though we only have the above estimate on I, we can show with a small change in the proof of the continuity of S that

$$\begin{aligned} \left\|S(s) - S(\overline{f})\right\|_{L^2(0,t_f)} &\le C \exp\left(C \|s'\|_{L^\infty(I)}\right) \|s - \overline{f}\|_{L^\infty(I)} \\ &\le C \exp\left(C \left\|\overline{f}\right\|_{H^m(\mathbb{R})}\right) h^{m-\frac{1}{2}}, \end{aligned}$$

where $\|s'\|_{L^\infty(I)}$ is replaced by $\left\|\overline{f}\right\|_{H^m(\mathbb{R})}$. This can be done, as

$$\left\|(s-\overline{f})'\right\|_{L^\infty(I)} \leq C \left\|\overline{f}\right\|_{H^m(\mathbb{R})} h^{m-\frac{3}{2}}$$

holds by the results of [WS93], where a similar estimate as in (4.24) are given also for the derivatives up to order $m-1$. As one expects the convergence order reduces by 1 for each further derivative. We summarise these consideration in the following

Theorem 28 *There exists a family of functions $s_h \in H^m(\mathbb{R})$ with $s_h \in V_h$ for $h > 0$ such that the corresponding simulation results $y_h = S(s_h)$ converge to $\overline{y} = S(\overline{f})$ in $L^2(0,t_f)$, i.e.*

$$\|y_h - \overline{y}\|_{L^2(0,t_f)} \to 0 \quad as \quad h \to 0.$$

Remark 4 *The great benefit of radial basis functions is that they can be used in each space dimension. Hence, a generalisation of* (4.1) *to a function identification in a system of ordinary differential equations is possible and the results given here are still valid.*

4.1.6 Numerical Application

In this section, we first apply our results on the logistic equation and identify its right-hand side function for computationally generated data. Afterwards, we identify the toxicity function in a system of ordinary differential equations modelling the wine fermentation process using real-life measurements. For both problems, we use the shape function $\varphi_{1,3}(r) = (1-r)^7(21r^3+19r^2+7r+1)$ for the radial basis functions and its native space $H^4(\mathbb{R})$ in the definition of the minimisation problem (4.1). Hence, the resulting mappings S and $\widetilde{J}$ are of class C^2.

Identifying a growth dynamic

Consider the following logistic equation [Mur93, Chapter 1.1]

$$\dot{y} = ry\left(1-\frac{y}{K}\right). \tag{4.25}$$

It models the evolution of the population number of a species. For small populations the dynamic in (4.25) exhibits an exponential growth. The greater the population becomes, the smaller the reproduction rate $r\left(1-\frac{y}{K}\right)$ gets, due to resource restrictions and a higher death probability. Therefore, the solution of (4.25) converges to the stable population number K.

Fixing the parameters as $r = 0.1$, $K = 1$, and the initial value as $y(0) = 0.1$ the exact solution of (4.25) is given by $y_d(t) = 1 - \frac{9}{9+\mathrm{e}^{t/10}}$. Moreover, we set the prior knowledge as $f_p = 0$, the regularisation parameter as $\lambda = 10^{-6}$, and the final observation time as $t_f = 8$. We generate three different measurements $y_{d,j}(t) = y_d(t) + \widetilde{y}_j(t)$, $t \in [0,t_f]$, $j \in \{1,2,3\}$, by adding to the exact solution y_d error functions $\widetilde{y}_j(t)$, $j \in \{1,2,3\}$. These error functions $\widetilde{y}_j(t)$ are linear interpolations of uniformly distributed errors with mean zero at 50 equally spaced sampling points. The magnitude of the error is taken from $\{0, 0.1, 0.2\}$. They are shown as dashed lines in the upper plot of Figure 4.1. The optimal function $\overline{f}_j = H(y_{d,j})$ subject to these three different measurements were computed with the BFGS optimisation algorithm, see Subsection 3.4.1, and can be seen in the lower plot of Figure 4.1. Despite the errors in the measurements, the resulting optimal functions

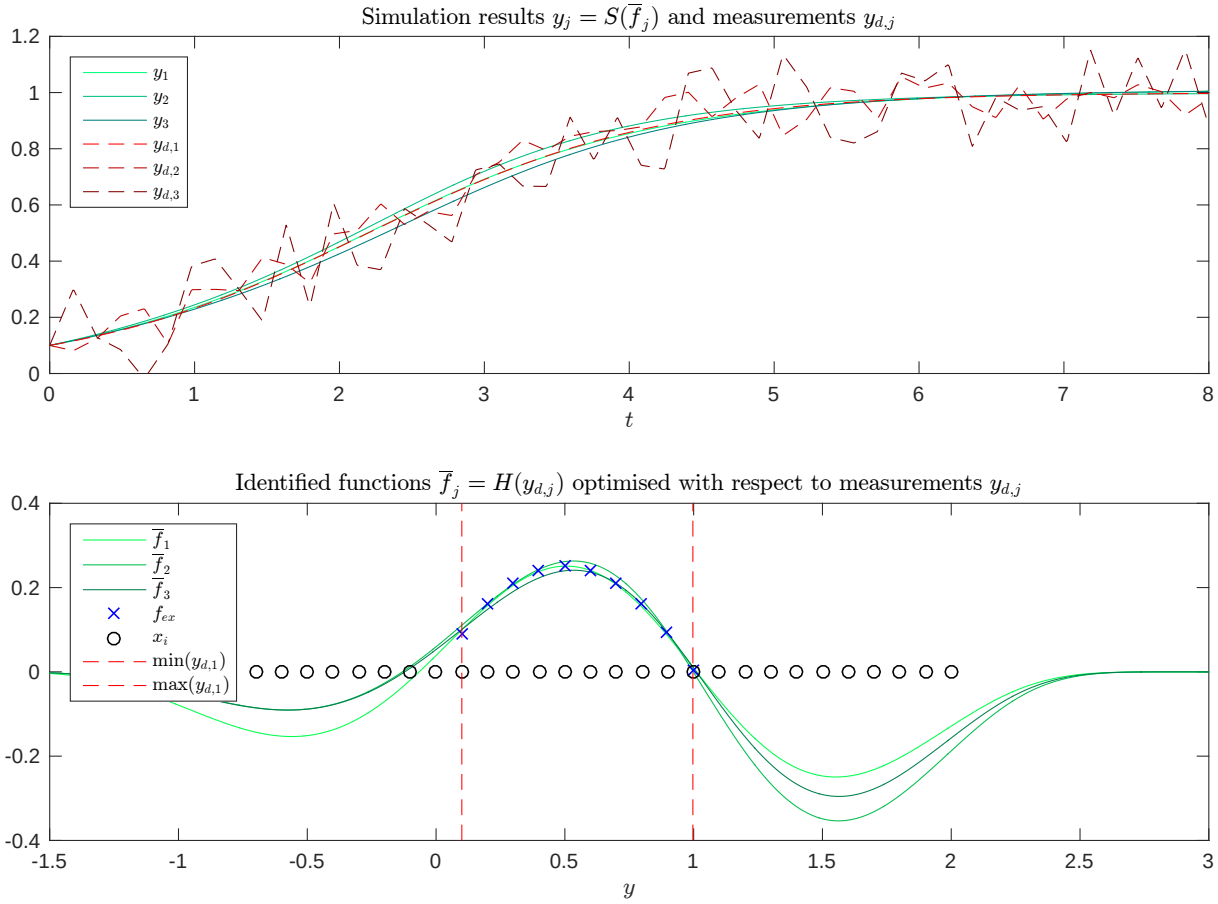

Figure 4.1: Three different measurements $y_{d,j}$ (top) are used to find optimal right-hand side functions $\overline{f}_j = H(y_{d_j})$ (bottom) such that the corresponding simulations $y_j = S(\overline{f}_j)$ (top) match them as good as possible. Circles (bottom) indicate the nodal points x_i of the radial basis functions in use. The image I of $y_{d,1}$ is indicated by the red dashed vertical lines (bottom).

are in a good agreement with the exact function $f_{ex}(y) = ry\left(1 - \frac{y}{K}\right)$ (crosses) within the interval of the measurements indicated by the two dashed vertical lines. For the finite dimensional subspace V_h of $H^4(\mathbb{R})$ we use the linear span of the RBFs defined in Subsection 4.1.5, where the nodal points are given by $x_i = -1 + 0.1\,i$ $(i = 0, \ldots, 30)$ and can be seen as circles in the lower plot of Figure 4.1. As the range of the optimal state is a priori unknown, we discretise with x_i a large interval that contains the measurements values. Also the corresponding simulation results $y_j = S(\overline{f}_j)$ follow the exact trajectory y_d quite well; compare the solid lines in the upper plot of Figure 4.1.

The quality of the resulting $\overline{f}_j$ can be estimated by the use of the derivative of the "data–to–function" mapping H at y_d as follows. The best approximation to the exact right-hand side function f_{ex} is given by $\overline{f}_1 = H(y_{d,1})$, as $y_{d,1} = y_d$ is the solution of (4.25) with respect to f_{ex} and we have no measurement errors. We estimate its distance of the identified functions $\overline{f}_j$ $(j = 2, 3)$, where measurement errors are present as follows

$$\begin{aligned}\left\|\overline{f}_1 - \overline{f}_j\right\|_{H^m(\mathbb{R})} &= \|H(y_d) - H(y_d + \widetilde{y}_j)\|_{H^m(\mathbb{R})} \\ &\leq \|H'(y_d)\|_{\mathcal{L}(L^2(0,t_f),H^m(\mathbb{R}))}\,\|\widetilde{y}_j\|_{L^2(0,t_f)} + O\left(\|\widetilde{y}_j\|^2_{L^2(0,t_f)}\right).\end{aligned}$$

Moreover, as we are now dealing with the finite dimensional space V_h, there are func-

j	$\left\|\overline{f}_j\right\|_{H^m(\mathbb{R})}$	$\left\|\overline{f}_1 - \overline{f}_j\right\|_{H^m(\mathbb{R})}$	$\|H'(y_d)\|_{\mathcal{L}(L^2(0,t_f),H^m(\mathbb{R}))} \|\widetilde{y}_{d,j}\|_{L^2(0,t_f)}$
1	30.77	0	0
2	39.42	17.40	≤ 58.1
3	34.09	13.25	≤ 118.7

Table 4.1: Comparison between the distances of $\overline{f}_j$ and its estimate based on the derivative of H.

tions z_i in $L^2(0,t_f)$ such that

$$H'(y_d)\widetilde{y}_d = \sum_{i=0}^{N} (z_i, \widetilde{y}_d)_{L^2(0,t_f)} \Phi_i.$$

This is due to the fact that restricting the linear mapping $H'(y_d)$ to the one dimensional subspace $\operatorname{span}\{\Phi_i\}$ yields a linear bounded functional, where Φ_i are the RBFs that we use. Hence, there exists a Riesz representative z_i. Therefore, we can estimate

$$\begin{aligned}
\|H'(y_d)\|_{\mathcal{L}(L^2(0,t_f),H^m(\mathbb{R}))} &= \sup_{\widetilde{y}_d \in L^2(0,t_f)} \frac{\|H'(y_d)\widetilde{y}_d\|_{H^m(\mathbb{R})}}{\|\widetilde{y}_d\|_{L^2(0,t_f)}} \\
&= \sup_{\widetilde{y}_d \in L^2(0,t_f)} \frac{\left(\sum\limits_{i,j=1}^{N} \left(\int\limits_0^{t_f} z_i \widetilde{y}_d \mathrm{d}t\right)\left(\int\limits_0^{t_f} z_j \widetilde{y}_d \mathrm{d}s\right)(\Phi_i,\Phi_j)_{H^m(\mathbb{R})}\right)^{\frac{1}{2}}}{\|\widetilde{y}_d\|_{L^2(0,t_f)}} \\
&= \sup_{\widetilde{y}_d \in L^2(0,t_f)} \frac{\left(\int\limits_0^{t_f}\int\limits_0^{t_f}\left(\sum\limits_{i,j=1}^{N}(\Phi_i,\Phi_j)_{H^m(\mathbb{R})} z_i(s) z_j(t)\right)\widetilde{y}_d(s)\widetilde{y}_d(t)\mathrm{d}s\mathrm{d}t\right)^{\frac{1}{2}}}{\|\widetilde{y}_d\|_{L^2(0,t_f)}} \\
&\leq \left(\int_0^{t_f}\int_0^{t_f}\left(\sum_{i,j=1}^{N}(\Phi_i,\Phi_j)_{H^m(\mathbb{R})} z_i(s) z_j(t)\right)^2 \mathrm{d}s\mathrm{d}t\right)^{\frac{1}{4}},
\end{aligned}$$

where we use the Cauchy–Schwarz inequality.

Computing the Riesz representatives z_i and evaluating the double integral in the case of the logistic equation we get the estimate

$$\|H'(y_d)\|_{\mathcal{L}(L^2(0,t_f),H^m(\mathbb{R}))} \leq 443.44\ldots \tag{4.26}$$

and can compare the distance between optimised function f_j^* with respect to different data $y_{d,j}$ as well as its estimate. We can see in Table 4.1 that the norm of $H'(y_d)$ multiplied by the norm of the data y_d is an upper bound of the actual norm of $f_1^* - f_j^*$.

Identifying a toxicity function

In the second part of this section, we apply the proposed function identification technique to a more complex model. We identify the toxicity function for the wine fermentation model (2.8) on the basis of measurements of a fermentation experiment. We cordially thank Dr. Christian von Wallbrunn and his team at the Departments of Microbiology & Biochemistry of the Geisenheim University, Germany for providing us measured concentrations of yeast cell numbers, sugar, and ethanol for a fermentation process that was performed at 17 °C.

As the experimental conditions were isothermal, we discard both the temperature equation and the factors $(T-b_1)$ and $(T-b_2)$ in the fermentation model (2.8). Therefore, we consider the following system of five coupled ordinary differential equations

$$\dot{X} = a_1 \frac{N}{a_7+N}\frac{O}{a_8+O}\frac{S}{a_9+S}X - \Psi(E)X, \tag{4.27a}$$

$$\dot{N} = -a_2 \frac{N}{a_7+N}\frac{O}{a_8+O}\frac{S}{a_9+S}X, \tag{4.27b}$$

$$\dot{O} = -a_3 \frac{N}{a_7+N}\frac{O}{a_8+O}\frac{S}{a_9+S}X, \tag{4.27c}$$

$$\dot{S} = -a_4 \frac{N}{a_7+N}\frac{O}{a_8+O}\frac{S}{a_9+S}X - a_5 \frac{S}{a_{10}+S}\frac{a_{11}}{a_{11}+E}X, \tag{4.27d}$$

$$\dot{E} = a_6 \frac{S}{a_{10}+S}\frac{a_{11}}{a_{11}+E}X, \tag{4.27e}$$

as a model for the wine fermentation experiment. This model contains eleven unknown parameters a_j and the unknown function $\Psi : \mathbb{R} \to \mathbb{R}$, that models the toxic influence of ethanol on the reproduction rate of the yeast.

The toxicity function Ψ is of special interest as it is not known how its shape can be parametrised. Therefore, we define the following minimisation problem in order to identify the toxicity function Ψ. We have

$$\min_{\Psi\in H^4(\mathbb{R}),\, a\in\mathbb{R}^{11}} J(y,\Psi,a) = \sum_{i=1}^{5} \frac{\lambda_i}{2} \left\|y_i - y_{i,d}\right\|^2_{L^2(0,t_f)} + \frac{\lambda_\Psi}{2} \left\|\Psi\right\|^2_{H^4(\mathbb{R})} + \frac{\lambda_a}{2} \left\|a - a_p\right\|^2_{\mathbb{R}^{11}},$$
$$\text{subject to (4.27) and } y(0) = y_0, \tag{4.28}$$

where we collect the model variables as $y = (X, N, O, S, E)^\top$. The measurements are represented by the vector $y_d = (X_d, N_d, O_d, S_d, E_d)^\top$. Note that the parameters for the specific yeast strain in use are unknown and we have to estimate them during the function identification. In this case, the objective function J includes also a regularisation term for the parameter vector $a \in \mathbb{R}^{11}$, where $a_p \in \mathbb{R}^{11}$ is an a priori known guess. The non-negative weights λ_i $(i = 1, \ldots, 5)$, λ_Ψ, and λ_a can be used to change the importance of the corresponding terms in the objective functional.

We can write the system (4.27) also in the form

$$\dot{y} = F(t, y, \Psi(y), a). \tag{4.29}$$

Note that the results given in this chapter can be generalised to differential equations of the form (4.29) with mild assumptions on F.

Figure 4.2 shows the results of the simultaneous parameter and function identification, where measured cell numbers of the yeast population X_d and the concentrations of sugar S_d and ethanol E_d of a wine fermentation experiment are used. As it can be seen in the left and middle plot of Figure 4.2, the simulation results with respect to the identified optimal parameters and optimal toxicity function Ψ coincide with the measurements quite well. The deviations are due to the measurement errors. They are most severe for the cell numbers, as it is a difficult task to count all yeast cells in a small portion of the must and to extrapolate for the whole fermentation vessel. Errors of up to 30 % are usual in this case. The right plot of Figure 4.2 shows the identified toxicity function Ψ. It seems that the toxic influence of the ethanol on the yeast cells is such that it is negligible for concentrations below approximately $40\,\frac{g}{l}$, increases rapidly up to a value of about

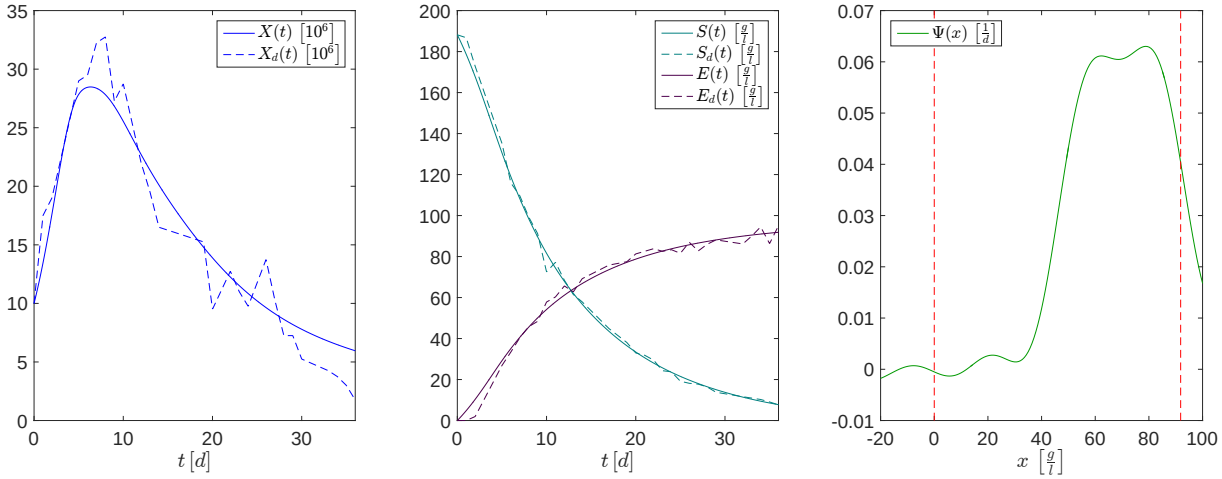

Figure 4.2: Experimental data for yeast cell numbers X_d (left) and sugar S_d and ethanol E_d concentrations (middle) compared to simulation results X, S, E subject to the identified optimal parameters and optimal function Ψ (right).

$0.06\,\frac{1}{d}$, and stays nearly constant at this value for increasing ethanol concentrations. This behaviour in the interval of measurement values, which is indicated by the vertical dashed lines in the right plot of Figure 4.2, can be described by a smoothed step function. Hence, our identification scheme allows us to identify the shape of the unknown toxicity function. Our results suggest that it would be convenient to model toxicity functions for different yeast strains by a parametrised step function.

Conclusion

The problem of identifying an unknown function from given measurement data was discussed. A framework was established, where this identification problem was formulated as a minimisation problem in an infinite dimensional function space. The analysis of the reduced problem was carried out by proving that for a regularisation parameter that is bigger than a threshold there is a unique function that minimises the objective. With this result, it was possible to define the "data–to–function" mapping and compute its derivative in order to estimate the dependence of the identified function subject to measurement errors. Furthermore, Wendland's compactly supported radial basis functions of minimal degree were used to discretise the infinite dimensional space to be able to use this framework for real-life applications. The proposed function identification method was applied to a representative dynamical model and to a system of ODEs modelling the wine fermentation process.

4.2 The Stochastic Case

In contrast to the previous section, where the identification of a function involved in an ordinary differential equation is presented, we now turn our attention in this section to models with stochastic differential equations. Mathematical modelling with stochastic differential equations is being applied for physical or biological system. Whenever a system is disturbed by effects that cannot be described in detail and appear to be random, a stochastic model is appropriate as a first modelling attempt. One example could be the changing environment for an organism in a biological model. In this case the exponential growth of the population of a species, which is observed for small population numbers, undergoes a stochastic disturbance, as the environmental conditions are varying. Hence, we aim to extend the wine fermentation model by stochastic perturbations in order to cope with uncertainties. Therefore, we analyse the problem of identifying a function belonging to a stochastic differential model. Hereby, we assume that this function is included in the deterministic part. Likewise in Section 4.1, we restrict the presentation of the proposed function identification method with stochastic differential equations to the one dimensional case. Nevertheless, the extension to higher dimensions in straightforward.

We proceed as follows. In Subsection 4.2.1, we introduce the concept of stochastic differential equations of Itô type. This includes the definition of the Itô integral and the presentation of Itô's lemma. In Subsection 4.2.2, we present how the Fokker-Planck equation, which under certain assumptions describes the statistics of the solution of a stochastic differential equation, is derived. Moreover, the unique solvability of the Fokker-Planck equation and its continuous dependence on the data is presented. In Subsection 4.2.3, we state the minimisation problem, which we solve in order to identify the unknown function. Further, the existence of a solution to this problem is proven. In Subsection 4.2.4, we derive the optimality system that characterises local minima of the objective functional. In Subsection 4.2.5, the Chang-Cooper finite difference scheme for the discretisation of a Fokker-Planck equation is presented. Following a discretise–before–optimise approach we also compute the gradient of the discretised reduced objective functional. Finally, we apply in Subsection 4.2.6 the discussed framework to the problem of identifying the toxicity function of the wine fermentation model and present numerical results.

4.2.1 Stochastic Differential Equations

In the following, we introduce the necessary terminology to discuss stochastic differential equations and to derive the corresponding Fokker-Planck partial differential equation. This exposition is mainly based on [Gar83, Chapter 4].

Itô Calculus

We assume in the following that the reader is familiar with the basics of probability theory. In order to define stochastic differential equations, we need the definition of the Wiener process.

Definition 10 *A real-valued stochastic process on a probability space $(\Omega, \mathcal{F}, \mathcal{P})$ is a collection of real-valued random variables X_t for $t \in [0, t_f]$. The* ***Wiener process*** *W_t is a continuous stochastic process with the following properties:*

- $W_0 = 0$ *with probability 1,*

- *for every* $0 \leq t_0 < t_1 < \ldots < t_n \leq t_f$ *the random variables* $W_{t_1} - W_{t_0}$, ... , $W_{t_n} - W_{t_{n-1}}$ *are stochastically independent,*
- *for every* $0 \leq t < s \leq t_f$ *the random variable* $W_s - W_t$ *is normally distributed with mean 0 and variance* $s - t$.

The existence of a Wiener process is shown in [KS91, Chapter 2.2] and goes beyond the scope of this thesis.

Stochastic differential equations are defined as integral equations, where the non-deterministic part is given by an integral with respect to the Wiener process. Therefore, we define such an integral, which is called Itô integral.

Definition 11 *Let* X_t *be a stochastic process. The Itô integral of* X_t *is defined as*

$$\int_0^t X_s \mathrm{d}W_s = \underset{n\to\infty}{\text{ms-lim}} \sum_{i=0}^{n-1} X_{t_i} \left(W_{t_{i+1}} - W_{t_i} \right), \tag{4.30}$$

where $0 = t_0 < t_1 < \ldots t_n = t$ *is a partition of* $[0, t]$.

The right-hand side in (4.30) is a mean square limit $\underset{n\to\infty}{\text{ms-lim}}\, X_n = X$, which exists if

$$\lim_{n\to\infty} \mathbf{E}[(X_n - X)^2] = 0$$

holds.

Remark 5 *The definition of the Itô integral* (4.30) *uses the left end* t_i *of the subinterval* $[t_i, t_{i+1}]$ *to evaluate* X_t *for the partial sums. This is consistent with the definition of a Markov process. The value of the integral is not independent of the choice of the intermediate point* $\tau_i \in [t_i, t_{i+1}]$. *Choosing the midpoint* $\tau_i = \frac{1}{2}(t_i + t_{i+1})$ *corresponds to the integral called Stratonovich integral. Nevertheless, stochastic differential equations defined with the Stratonovich integral instead of the Itô integral can be reformulated as stochastic differential equations of Itô type. Moreover, there is also a correspondence between the derived Fokker-Planck equations with respect to the different definitions of a stochastic integral. See [Gar83, Chapter 4] for more information. Therefore, we restrict our presentation to stochastic differential equation of Itô type.*

It can be shown that the Itô integral exists provided X_t is continuous and non-anticipating, that is X_s is stochastically independent of $W_\tau - W_s$ for all s, τ such that $0 \leq s < \tau \leq t$; see [Arn74, Chapter 4.3]. Moreover, we conclude that the mean of the Itô integral of a non-anticipating function X_t is zeros. Note that X_{t_i} and $W_{t_{i+1}} - W_{t_i}$ are independent. Hence, we compute

$$E\left[\int_0^t X_s \mathrm{d}W_s\right] = \underset{n\to\infty}{\text{ms-lim}} \sum_{i=0}^{n-1} E\left[X_{t_i}\right] E\left[W_{t_{i+1}} - W_{t_i}\right] = 0, \tag{4.31}$$

as the mean of $W_{t_{i+1}} - W_{t_i}$ is zero.

Stochastic Differential Equations

As indicated at the beginning of this chapter, we aim to extend an ordinary differential equation

$$\frac{\mathrm{d}y}{\mathrm{d}t} = f(y)$$

by a random disturbance ξ, which results in a formal differential equation of the form

$$\frac{\mathrm{d}y}{\mathrm{d}t} = f(y) + \xi.$$

This equation is known as the Langevin equation; see [Gar83]. A rigorous mathematical definition is given by a stochastic differential equation of Itô type. We are changing now the notation in order to adapt it to that usually used for stochastic differential equations. In the following, the stochastic process X_t, which is the state of a stochastic differential equation, is the analogue for the state $y(t)$ of an ordinary differential equation, which is analysed in Section 4.1. Moreover, the unknown function we seek to identify is denoted by f in Section 4.1. As f is usually use for the probability density function in stochastics, we denote in this section by b the unknown function for the stochastic function identification method.

Let $b : \mathbb{R} \times [0, t_f] \to \mathbb{R}$, which is called drift, and $\sigma : \mathbb{R} \times [0, t_f] \to \mathbb{R}$, which is called diffusion, be given. Then the stochastic process X_t is a solution of the following stochastic differential equation

$$dX_t = b(X_t, t)\,\mathrm{d}t + \sigma(X_t, t)\,\mathrm{d}W_t, \tag{4.32}$$

if X_t satisfies the following integral equation

$$X_t = X_0 + \int_0^t b(X_s, s)\,\mathrm{d}s + \int_0^t \sigma(X_s, s)\mathrm{d}W_s, \tag{4.33}$$

where the initial value X_0 is a given random variable independent of W_t. It is known that a stochastic differential equation admits exactly one strong solution, if the functions b and σ are measurable in $\mathbb{R} \times [0, t_f]$ and there exists a $K > 0$ such that

$$|b(x,t) - b(y,t)| + |\sigma(x,t) - \sigma(y,t)| \leq K|x - y|$$

and

$$|b(x,t)|^2 + |\sigma(x,t)|^2 \leq K(1 + |x|^2)$$

holds for all $t \in [0, t_f]$ and $x, y \in \mathbb{R}$. See [Arn74, Chapter 6.2] for the proof, where an iteration based on the integral equation (4.33), which is similar to the one used in the proof of the Picard-Lindelöf theorem, is defined and its convergence to the solution is shown.

The next theorem states the so-called Itô formula. For a stochastic process X_t that satisfies a stochastic differential equation we define a second stochastic process by a functional relationship $h(X_t, t)$, where h is a known function. The question arises whether $h(X_t, t)$ satisfies also a stochastic differential equation and how it looks like. The following theorem answers this question and is used to derive the Fokker-Planck equation later.

Theorem 29 *Let the function $h : \mathbb{R} \times [0, t_f] \to \mathbb{R}, (x, t) \mapsto h(x, t)$ be continuously differentiable up to order 1 with respect to the time variable t and up to order 2 with respect to the space variable x. Let X_t be the solution of the stochastic differential equation* (4.32).

Then the stochastic process $h(X_t, t)$ is the solution of the following stochastic differential equation

$$\begin{aligned}\mathrm{d}h(X_t,t) = &\left(\frac{\partial h}{\partial t}(X_t,t) + b(X_t,t)\frac{\partial h}{\partial x}(X_t,t) + \frac{1}{2}\sigma(X_t,t)^2\frac{\partial^2 h}{\partial x^2}(X_t,t)\right)\mathrm{d}t \\ &+ \sigma(X_t,t)\frac{\partial h}{\partial x}(X_t,t)\mathrm{d}W_t,\end{aligned}$$

with the initial value $h(X_0, 0)$.

The proof is given in [Arn74, Chapter 5.3]. A heuristic argument can be carried out by expanding the differential $\mathrm{d}h(X_t, t)$ in a Taylor series and discard all terms, which have a higher order that $\mathrm{d}t$. Hereby, the stochastic differential $\mathrm{d}W_t$ is treated like $\sqrt{\mathrm{d}t}$, as the equality

$$\int_0^t X_s \left[\mathrm{d}W_s\right]^2 = \int_0^t X_s \,\mathrm{d}s$$

can be proven.

4.2.2 Derivation and Analysis of the Fokker-Planck Equation

Let X_t be a stochastic process, which satisfies the stochastic differential equation (4.32). Denote by $f(x, t)$ the probability density function of the process to be at the point x at time t. In the following, we derive a partial differential equation that governs the evolution of f. As the probability density f describes the process X_t completely, this casts the stochastic problem of solving a stochastic differential equation to a deterministic problem of solving a partial differential equation.

Let $h : \mathbb{R} \to \mathbb{R}$ be an arbitrary function that is smooth enough to guarantee the following computations. We compute the time derivative of the expected value of $h(X_t)$

$$\frac{\mathrm{d}}{\mathrm{d}t}\mathbf{E}[h(X_t)] = \frac{\mathrm{d}}{\mathrm{d}t}\int_{\mathbb{R}} h(x) f(x,t)\,\mathrm{d}x = \int_{\mathbb{R}} h(x)\frac{\partial f}{\partial t}(x,t)\,\mathrm{d}x,$$

where we exchange integration and differentiation. Using Theorem 29 and the fact that the expected value of an Itô integral is zero, see (4.31), we have

$$\begin{aligned}&\frac{\mathrm{d}}{\mathrm{d}t}\mathbf{E}[h(X_t)] \\ &= \frac{\mathrm{d}}{\mathrm{d}t}\mathbf{E}\left[h(X_0) + \int_0^t b(X_s,s)h'(X_s) + \frac{1}{2}\sigma(X_s,s)^2 h''(X_s)\mathrm{d}t + \int_0^t \sigma(X_s)h'(X_s)\mathrm{d}W_s\right] \\ &= \mathbf{E}\left[b(X_t,t)h'(X_t) + \frac{1}{2}\sigma(X_t,t)^2 h''(X_t)\right] = \int_{\mathbb{R}}\left(b(x,t)h'(x) + \frac{1}{2}\sigma(x,t)^2 h''(x)\right) f(x,t)\,\mathrm{d}x \\ &= \int_{\mathbb{R}} h(x)\left(-\frac{\partial}{\partial x}\left(b(x,t)f(x,t)\right) + \frac{\partial^2}{\partial x^2}\left(\frac{1}{2}\sigma(x,t)^2 f(x,t)\right)\right)\mathrm{d}x,\end{aligned}$$

where we use integration by parts for the last equality. As h was arbitrarily chosen, we identify the following partial differential equation for the probability density function f

$$\frac{\partial f}{\partial t}(x,t) - \frac{\partial^2}{\partial x^2}\left(\frac{1}{2}\sigma(x,t)^2 f(x,t)\right) + \frac{\partial}{\partial x}\left(b(x,t)\,f(x,t)\right) = 0,$$

which is know as the Fokker-Planck or forward Kolmogorov equation.

For diffusion functions σ that are bounded from below by a positive constant it can be shown that the probability density function has global support on the whole real line $\mathbb{R}$. Moreover, also an initial condition with range $\mathbb{R}$ causes a non-compact support of f. Therefore, one has to solve the Fokker-Planck equation on the whole real line $\mathbb{R}$. Another approach is to assume that the process approximately stays in a bounded domain $\Omega \subset \mathbb{R}$ and to describe what happens when the process touches the boundary. The most often boundary conditions used in literature are absorbing and reflecting boundaries; see [Gar83, Chapter 5.2.1]. We stick to the concept of reflecting boundary conditions, where the probability flux across the domain boundary is zero. Note that initial conditions are often prescribed to be Gaussian and, therefore, its probability density function tends to zero very quickly for $x \to \pm\infty$. Hence, the computational solution of a Fokker-Planck equation with reflecting boundary conditions in a large domain containing the initial probability density is a good approximation for the case of an unbounded domain, as in this case the probability at the boundary is below machine precision.

For the identification of an unknown function b in a stochastic differential equation we consider the following Fokker-Planck equation. It is stated in a bounded domain Ω and for the time horizon $[0, t_f]$ and is given by

$$\frac{\partial f}{\partial t} - \frac{1}{2}\frac{\partial^2}{\partial x^2}\left(\sigma^2 f\right) + \frac{\partial}{\partial x}(b f) = 0 \qquad \text{in } Q = \Omega \times [0, t_f], \tag{4.34a}$$

$$F = 0 \qquad \text{on } \Sigma = \Gamma \times [0, t_f], \tag{4.34b}$$

$$f(0) = f_0 \qquad \text{in } \Omega, \tag{4.34c}$$

where the flux at the boundary $\Gamma = \partial\Omega$ is defined by $F = \frac{1}{2}\frac{\partial}{\partial x}(\sigma^2 f) - b f$. The initial distribution f_0 is the probability density of the stochastic process at time $t = 0$.

In order to formulate a minimisation problem whose solution aims to identify the drift function b, we have to guarantee that the Fokker-Planck equation has a unique solution for each possible choice for b. Hence, we present the following theorem, where a right-hand side functional is included, as this will be necessary later to prove the differentiability of the solution operator.

Theorem 30 *Assume that σ^2 is differentiable and is bounded from below by $\bar{\sigma}^2 > 0$. Further, assume that $\sigma^2, \frac{\partial \sigma^2}{\partial x}, b \in L^\infty(\Omega)$. Moreover, let $f_0 \in L^2(\Omega)$ and $g \in L^2(Q)$. Then the following weak formulation of the Fokker-Planck equation* (4.34) *with right-hand side g*

$$\frac{\mathrm{d}}{\mathrm{d}t}\int_\Omega f v \,\mathrm{d}x + \int_\Omega \frac{1}{2}\sigma^2 \frac{\partial f}{\partial x}\frac{\partial v}{\partial x} + \left(\frac{1}{2}\frac{\partial \sigma^2}{\partial x} - b\right) f \frac{\partial v}{\partial x}\,\mathrm{d}x = \int_\Omega g \frac{\partial v}{\partial x}\,\mathrm{d}x \tag{4.35}$$

for all $v \in H^1(\Omega)$ and almost all $t \in [0, t_f]$ with the initial condition $f(0) = f_0$ has a unique weak solution $f \in W(0, t_f)$ and the following holds

(i) If $f_0 \geq 0$ and $g = 0$, then $f \geq 0$ holds.

(ii) If $\int_\Omega f_0(x)\,\mathrm{d}x = 1$ and $g = 0$, then for all $t \in [0, t_f]$ it holds that $\int_\Omega f(x,t)\,\mathrm{d}x = 1$.

(iii) There exists a function q such that

$$\|f\|^2_{W(0,t_f)} \leq q(\|b\|_{L^\infty(\Omega)})\left(\|f_0\|^2_{L^2(\Omega)} + \|g\|^2_{L^2(Q)}\right)$$

holds.

Proof. Note that for $g = 0$ and strong solutions of the Fokker-Planck equation (4.34) the above given variational problem is satisfied, as we have

$$\int_\Omega \left(-\frac{1}{2}\frac{\partial^2}{\partial x^2}\left(\sigma^2 f\right) + \frac{\partial}{\partial x}\left(b f\right)\right) v \,\mathrm{d}x = -\int_\Omega \left(-\frac{1}{2}\frac{\partial}{\partial x}\left(\sigma^2 f\right) + b f\right)\frac{\partial v}{\partial x}\,\mathrm{d}x,$$

due to vanishing boundary integrals because of the zero flux condition. In contrast to the results of Theorem 7 for diffusion equations there is a convection term present in (4.34) now. Defining the bilinear form a by

$$a(t,f,v) = \int_\Omega \frac{1}{2}\sigma^2 \frac{\partial f}{\partial x}\frac{\partial v}{\partial x} + \left(\frac{1}{2}\frac{\partial \sigma^2}{\partial x} - b\right) f \frac{\partial v}{\partial x}\,\mathrm{d}x,$$

we prove that it is continuous as follows

$$\begin{aligned}
|a(t,f,v)| \leq & \frac{1}{2}\left\|\sigma^2\right\|_{L^\infty(\Omega)} \left\|\frac{\partial f}{\partial x}\right\|_{L^2(\Omega)} \left\|\frac{\partial v}{\partial x}\right\|_{L^2(\Omega)} \\
& + \left(\frac{1}{2}\left\|\frac{\partial \sigma^2}{\partial x}\right\|_{L^\infty(\Omega)} + \|b\|_{L^\infty(\Omega)}\right)\|f\|_{L^2(\Omega)} \left\|\frac{\partial v}{\partial x}\right\|_{L^2(\Omega)} \\
\leq & \left(\frac{1}{2}\left\|\sigma^2\right\|_{L^\infty(\Omega)} + \frac{1}{2}\left\|\frac{\partial \sigma^2}{\partial x}\right\|_{L^\infty(\Omega)} + \|b\|_{L^\infty(\Omega)}\right)\|f\|_{H^1(\Omega)}\|v\|_{H^1(\Omega)}.
\end{aligned}$$

Moreover, we have the following estimate

$$\begin{aligned}
a(t,f,f) \geq & \frac{1}{2}\bar{\sigma}^2 \left\|\frac{\partial f}{\partial x}\right\|^2_{L^2(\Omega)} - \left(\frac{1}{2}\left\|\frac{\partial \sigma^2}{\partial x}\right\|_{L^\infty(\Omega)} + \|b\|_{L^\infty(\Omega)}\right)\|f\|_{L^2(\Omega)} \left\|\frac{\partial f}{\partial x}\right\|_{L^2(\Omega)} \\
\geq & \frac{1}{4}\bar{\sigma}^2 \left\|\frac{\partial f}{\partial x}\right\|^2_{L^2(\Omega)} - \frac{1}{\bar{\sigma}^2}\left(\frac{1}{2}\left\|\frac{\partial \sigma^2}{\partial x}\right\|_{L^\infty(\Omega)} + \|b\|_{L^\infty(\Omega)}\right)^2 \|f\|^2_{L^2(\Omega)} \\
\geq & \frac{1}{4}\bar{\sigma}^2 \|f\|^2_{H^1(\Omega)} - \left(\frac{1}{\bar{\sigma}^2}\left(\frac{1}{2}\left\|\frac{\partial \sigma^2}{\partial x}\right\|_{L^\infty(\Omega)} + \|b\|_{L^\infty(\Omega)}\right)^2 + \frac{1}{4}\bar{\sigma}^2\right)\|f\|^2_{L^2(\Omega)},
\end{aligned} \tag{4.36}$$

where we use the Cauchy inequality $ab \leq \frac{a^2}{4\varepsilon} + \varepsilon b^2$ for $\varepsilon = \frac{1}{4}\bar{\sigma}^2$. Finally, we define

$$G(t,v) \coloneqq \int_\Omega g \frac{\partial v}{\partial x}\,\mathrm{d}x,$$

and conclude $|G(t,v)| \leq \|g(t)\|_{L^2(\Omega)}\|v\|_{H^1(\Omega)}$ and, hence, $G \in L^2(0,t_f;H^1(\Omega)^*)$. Therefore, we can use Theorem 6 to prove the existence of a unique weak solution in $W(0,t_f)$ and we have

$$\frac{\mathrm{d}}{\mathrm{d}t}\int_\Omega f(x,t)v(x)\,\mathrm{d}x + a(t;f(t),v) = G(t,v)$$

for all $v \in H^1(\Omega)$.

In order to prove (i) and (ii) assume that $G = 0$. By choosing the test function v as $f^- \coloneqq \min(0,f)$, we prove the non-negativity of solutions for non-negative initial

conditions as follows

$$\begin{aligned}\frac{1}{2}\frac{\mathrm{d}}{\mathrm{d}t}\int_\Omega \left(f^-\right)^2 \,\mathrm{d}x &\le -a(t,f^-,f^-)\\ &\le -\frac{1}{2}\bar\sigma^2\left\|\frac{\partial f^-}{\partial x}\right\|^2_{L^2(\Omega)} + \left(\frac{1}{2}\left\|\frac{\partial\sigma^2}{\partial x}\right\|_{L^\infty(\Omega)} + \|b\|_{L^\infty(\Omega)}\right)\left\|f^-\right\|_{L^2(\Omega)}\left\|\frac{\partial f^-}{\partial x}\right\|_{L^2(\Omega)}\\ &\le \frac{1}{2\bar\sigma^2}\left(\frac{1}{2}\left\|\frac{\partial\sigma^2}{\partial x}\right\|_{L^\infty(\Omega)} + \|b\|_{L^\infty(\Omega)}\right)^2\left\|f^-\right\|^2_{L^2(\Omega)},\end{aligned}$$

where we use the Cauchy inequality with $\varepsilon = \frac{1}{2}\bar\sigma^2$. By the Grönwall inequality, see Lemma 1, we get

$$\left\|f^-(t)\right\|^2_{L^2(\Omega)} \le \exp\left(\frac{1}{\bar\sigma^2}\left(\frac{1}{2}\left\|\frac{\partial\sigma^2}{\partial x}\right\|_{L^\infty(\Omega)} + \|b\|_{L^\infty(\Omega)}\right)^2 t\right)\left\|f^-(0)\right\|^2_{L^2(\Omega)},$$

and the prove of (i) is complete, as $\|f^-(0)\|^2_{L^2(\Omega)} = 0$ holds.

In order to prove (ii), we choose $v \equiv 1$ in the weak formulation and deduce that $a(t,f,v) = 0$ holds. Therefore, we have

$$\frac{\mathrm{d}}{\mathrm{d}t}\int_\Omega f(x,t)\,\mathrm{d}x = 0,$$

and (ii) follows.

In literature, estimates as in (iii) are proven for a fixed second-order elliptic operator with given diffusion coefficients and convection term; see [Eva10, DL92]. Notice that, the dependence on its coefficients is not explicitly described, but is hidden in a generic constant. As in our case the dependence on the drift function b is important, we present the necessary estimates.

The first estimate is done in the $C([0,t_f];L^2(\Omega))$ norm. From (4.36), we deduce

$$\begin{aligned}\frac{1}{2}\frac{\mathrm{d}}{\mathrm{d}t}\|f\|^2_{L^2(\Omega)} = -a(t,f,f) + G(t,f) &\le \frac{\theta_1}{2}\|f\|^2_{L^2(\Omega)} + \|g\|_{L^2(\Omega)}\|f\|_{L^2(\Omega)}\\ &\le \frac{\theta_1+1}{2}\|f\|^2_{L^2(\Omega)} + \|g\|^2_{L^2(\Omega)},\end{aligned}$$

where $\theta_1 = \left(\frac{2}{\bar\sigma^2}\left(\frac{1}{2}\left\|\frac{\partial\sigma^2}{\partial x}\right\|_{L^\infty(\Omega)} + \|b\|_{L^\infty(\Omega)}\right)^2 + \frac{1}{2}\bar\sigma^2\right)$. The Grönwall inequality yields

$$\|f(t)\|^2_{L^2(\Omega)} \le \exp\left((\theta_1+1)\,t\right)\left(\|f_0\|^2_{L^2(\Omega)} + \int_0^t 2\,\|g(s)\|^2_{L^2(\Omega)}\,\mathrm{d}s\right),$$

which proves

$$\|f\|^2_{C([0,t_f];L^2(\Omega))} \le \exp\left((\theta_1+1)\,t_f\right)\left(\|f_0\|^2_{L^2(\Omega)} + 2\,\|g\|^2_{L^2(Q)}\right).$$

For the estimate in the $L^2(0,t_f;H^1(\Omega))$ norm, we integrate

$$\frac{1}{2}\frac{\mathrm{d}}{\mathrm{d}t}\|f\|^2_{L^2(\Omega)} + \frac{1}{4}\bar\sigma^2\|f\|^2_{H^1(\Omega)} \le \frac{\theta_1+1}{2}\|f\|^2_{L^2(\Omega)} + \|g\|^2_{L^2(\Omega)}$$

from 0 to t_f and obtain

$$\begin{aligned}
&\|f(t_f)\|^2_{L^2(\Omega)} + \frac{1}{2}\bar{\sigma}^2 \int_0^{t_f} \|f(s)\|^2_{H^1(\Omega)} \,\mathrm{d}s \\
&\leq (\theta_1 + 1) \int_0^{t_f} \|f(s)\|^2_{L^2(\Omega)} \,\mathrm{d}s + 2\|g\|^2_{L^2(Q)} + \|f_0\|^2_{L^2(\Omega)} \\
&\leq (\theta_1 + 1) \int_0^{t_f} \exp\left((\theta_1 + 1)\, s\right) \left(\|f_0\|^2_{L^2(\Omega)} + 2\|g\|^2_{L^2(Q)}\right) \mathrm{d}s + 2\|g\|^2_{L^2(Q)} + \|f_0\|^2_{L^2(\Omega)} \\
&\leq \left((\theta_1 + 1)\frac{\exp\left((\theta_1 + 1)\, t_f\right) - 1}{\theta_1 + 1} + 1\right) \left(\|f_0\|^2_{L^2(\Omega)} + 2\|g\|^2_{L^2(Q)}\right).
\end{aligned}$$

We deduce

$$\|f\|^2_{L^2(0,t_f;H^1(\Omega))} \leq \frac{2}{\bar{\sigma}^2} \exp\left((\theta_1 + 1)\, t_f\right) \left(\|f_0\|^2_{L^2(\Omega)} + 2\|g\|^2_{L^2(Q)}\right).$$

For the $L^2(0, t_f; H^1(\Omega)^*)$ norm of $\frac{\mathrm{d}}{\mathrm{d}t} f$ we estimate with an arbitrary $v \in H^1(\Omega)$ as follows

$$\begin{aligned}
\left|\left\langle \frac{\mathrm{d}}{\mathrm{d}t} f, v \right\rangle_{H^1(\Omega)^*, H^1(\Omega)}\right| &= |a(t, f, v)| + |G(t, v)| \\
&\leq \theta_2 \|f\|_{H^1(\Omega)} \|v\|_{H^1(\Omega)} + \|g(t)\|_{L^2(\Omega)} \|v\|_{H^1(\Omega)},
\end{aligned}$$

where $\theta_2 = \frac{1}{2}\|\sigma^2\|_{L^\infty(\Omega)} + \frac{1}{2}\left\|\frac{\partial \sigma^2}{\partial x}\right\|_{L^\infty(\Omega)} + \|b\|_{L^\infty(\Omega)}$ and conclude

$$\begin{aligned}
\left\|\frac{\mathrm{d}}{\mathrm{d}t} f\right\|^2_{L^2(0,t_f;H^1(\Omega)^*)} &\leq 2\theta_2^2 \|f\|^2_{L^2(0,t_f;H^1(\Omega))} + 2\|g\|^2_{L^2(Q)} \\
&\leq 2\theta_2^2 \frac{2}{\bar{\sigma}^2} \exp\left((\theta_1 + 1)\, t_f\right) \left(\|f_0\|^2_{L^2(\Omega)} + 2\|g\|^2_{L^2(Q)}\right) + 2\|g\|^2_{L^2(Q)}.
\end{aligned}$$

Finally, we have proven that (iii) holds for

$$q(\|b\|_{L^\infty(\Omega)}) \coloneqq \left(2\theta_2^2 + 1\right) \frac{4}{\bar{\sigma}^2} \exp\left((\theta_1 + 1)\, t_f\right) + 2,$$

where we suppressed the quadratic and linear dependence of θ_1 and θ_2 on the norm of the drift $\|b\|_{L^\infty(\Omega)}$, respectively. This completes the proof. □

4.2.3 Identification of the Drift of a Fokker-Planck Equation

In the following, we describe a function identification method for a stochastic differential equation. We assume that some measurements of a stochastic process X_t, which is governed by the stochastic differential equation

$$dX_t = b(X_t)\,\mathrm{d}t + \sigma(X_t, t)\,\mathrm{d}W_t,$$

are available. In our case we assume that the time independent drift b is unknown and the diffusion σ is known. In particular, let (τ_l, ξ_l) for $l = 1, \ldots, L$ be given such that a realisation of X_t takes the value ξ_l at time τ_l.

We define the same objective functional as in [GSAB] and the corresponding minimisation problem is used to identify a suitable approximation of the unknown function b in the Sobolev space $H^1(\Omega)$. We have

$$\min_{b\in H^1(\Omega)} J(f,b) = \sum_{l=1}^{L} \frac{1}{2}\left(\int_\Omega x\, f(x,\tau_l)\,\mathrm{d}x - \xi_l\right)^2 + \frac{\lambda}{2}\,\|b\|^2_{H^1(\Omega)}\,, \tag{4.37a}$$

$$\text{subject to (4.34).} \tag{4.37b}$$

The objective functional J defined in (4.37a) measures the distance between the mean value of the stochastic process X_t at time τ_l and the measured value ξ_l. The mean value is evaluated by solving a Fokker-Planck equation that governs the probability density function f of the stochastic process X_t.

Note that in a one dimensional domain, we have the embedding $H^1(\Omega) \hookrightarrow L^\infty(\Omega)$ and, hence, the Fokker-Planck equation admits a unique solution due to Theorem 30. For a generalisation to higher dimensional stochastic processes, we need to enlarge the differentiability degree m such that we obtain a similar embedding $H^m(\Omega) \hookrightarrow L^\infty(\Omega)$.

Theorem 31 *Let σ^2 be differentiable, bounded from below by $\bar\sigma^2 > 0$, and assume that $\sigma^2, \frac{\partial\sigma^2}{\partial x} \in L^\infty(\Omega)$ holds. Moreover, assume $f_0 \in L^2(\Omega)$ and $\lambda > 0$. Then the minimisation problem* (4.37) *admits a solution.*

Proof. The functional $J : W(0,t_f) \times H^1(\Omega) \to \mathbb{R}$ is bounded from below and takes the norm of b into account. Hence, there exists a bounded minimising sequence b_n and the corresponding state f_n exists and is bounded in $W(0,t_f)$ due to Theorem 30. Exploiting the Hilbert space structure of $W(0,t_f)$ and $H^1(\Omega)$ we can assume that these sequences have a weak limit $\overline{f}$ and $\overline{b}$ in $W(0,t_f)$ and $H^1(\Omega)$, respectively. The functional J is sequentially weakly lower semicontinuous, as it is convex and continuous. Hence, $(\overline{b},\overline{f})$ is a solution of (4.37), provided it is feasible. Hence, it remains to show that $\overline{f}$ is the solution of (4.34) with respect to the drift $\overline{b}$. First, we observe that f_n converges strongly to $\overline{f}$ in $L^2(0,t_f;L^2(\Omega))$, as $W(0,t_f)$ is compactly embedded in this space due to Theorem 5. For fixed $v \in H^1(\Omega)$ and $t \in [0,t_f]$ the bilinear form $(b,f) \to \int_\Omega b\, f(t)\, \frac{\partial v}{\partial x}\,\mathrm{d}x$ from $H^1(\Omega)\times L^2(\Omega)$ to $\mathbb{R}$ is continuous due to the embedding $H^1(\Omega) \hookrightarrow L^\infty(\Omega)$. As b_n is weakly convergent and f_n is strongly convergent in $L^2(0,t_f;L^2(\Omega))$ we have

$$\int_\Omega b_n\, f_n(t)\, \frac{\partial v}{\partial x}\,\mathrm{d}x \to \int_\Omega \overline{b}\,\overline{f}(t)\, \frac{\partial v}{\partial x}\,\mathrm{d}x$$

for all $t \in [0,t_f]$ and $v \in H^1(\Omega)$ due to [Cia13, Theorem 5.12-4 (c)]. Moreover, we know that $\frac{\mathrm{d}}{\mathrm{d}t} f_n$ converges weakly to $\frac{\mathrm{d}}{\mathrm{d}t}\overline{f}$ in $L^2(0,t_f;H^1(\Omega)^*)$. Hence, we can apply the limit to all terms in

$$\frac{\mathrm{d}}{\mathrm{d}t}\int_\Omega f_n\, v\,\mathrm{d}x + \int_\Omega \frac{1}{2}\sigma^2 \frac{\partial f_n}{\partial x}\frac{\partial v}{\partial x} + \left(\frac{1}{2}\frac{\partial\sigma^2}{\partial x} - b_n\right) f_n\, \frac{\partial v}{\partial x}\,\mathrm{d}x = 0$$

and conclude that $\overline{f}$ solves the Fokker-Planck equation (4.34) with respect to $\overline{b}$. This completes the proof. □

4.2.4 Differentiability of the Solution Operator and the Optimality System

Having established a proof for the existence of a solution for the minimisation problem (4.37), we are now interested in the first-order necessary optimality conditions that characterise locally optimal solutions. For preparation, we state the next theorem.

Theorem 32 *The solution operator $S : H^1(\Omega) \to W(0,t_f)$ of the Fokker-Planck equation (4.34) is Fréchet differentiable and the directional derivative $y = S'(b)h$ for $h \in H^1(\Omega)$ is given by the solution of*

$$\frac{\partial y}{\partial t} - \frac{1}{2}\frac{\partial^2}{\partial x^2}\left(\sigma^2 y\right) + \frac{\partial}{\partial x}(b\,y) = -\frac{\partial}{\partial x}(h\,f) \qquad \text{in } Q, \tag{4.38a}$$

$$F = h\,f \qquad \text{on } \Sigma, \tag{4.38b}$$

$$y(0) = 0 \qquad \text{in } \Omega, \tag{4.38c}$$

where $f = S(b)$.

Proof. Note that for the strong formulation (4.38) the corresponding weak formulation is given by (4.35) with $g = -h\,f$. Due to the embedding $H^1(\Omega) \hookrightarrow L^\infty(\Omega)$ the product $h\,f$ is an element of $L^2(Q)$. Hence, we conclude by the use of Theorem 30 that (4.38) admits a unique solution. Denote $f_1 = S(b+h)$, $f_2 = S(b)$, $y = S'(b)h$, and $z = f_1 - f_2 - y$. Then z solves the corresponding weak formulation of the following equation

$$\begin{aligned}
\frac{\partial z}{\partial t} - \frac{1}{2}\frac{\partial^2}{\partial x^2}\left(\sigma^2 z\right) + \frac{\partial}{\partial x}(b\,z) &= -\frac{\partial}{\partial x}(h(f_1 - f_2)) && \text{in } Q,\\
F &= h(f_1 - f_2) && \text{on } \Sigma,\\
z(0) &= 0 && \text{in } \Omega.
\end{aligned}$$

Hence, by Theorem 30 we conclude the following

$$\|z\|^2_{W(0,t_f)} \le q(\|b\|_{L^\infty(\Omega)})\|h(f_1 - f_2)\|^2_{L^2(Q)}.$$

Moreover, we argue that

$$\|f_1 - f_2\|^2_{L^2(Q)} \le C\|f_1 - f_2\|^2_{W(0,t_f)} \le Cq(\|b\|_{L^\infty(\Omega)})\|hf_1\|^2_{L^2(Q)},$$

as $f_1 - f_2$ solves a Fokker-Planck equation with drift b, zero initial conditions, and right-hand side $g = -hf_1$. Here, C denotes the embedding constant of $W(0,t_f) \hookrightarrow L^2(Q)$. Finally, we combine the latter two estimates to prove

$$\|z\|^2_{W(0,t_f)} \le \widetilde{q}(\|b\|_{L^\infty(\Omega)})\|h\|^2_{H^1(\Omega)},$$

with an h independent function $\widetilde{q}$. This proves the Fréchet differentiability of S. □

Note that due to the above theorem, the reduced objective functional $\widetilde{J}(b) = J(S(b), b)$ is also Fréchet differentiable, as the mapping $f \mapsto \int_\Omega x\,f(x,\tau_l)\,\mathrm{d}x$ is linear, the real-valued function $x \mapsto x^2$ is differentiable, and the square of the norm $b \mapsto \|b\|^2_{H^1(\Omega)}$ is also differentiable. Finally, we are now able to prove the following theorem that characterises the local minima of the minimisation problem (4.37).

Theorem 33 *Let $\overline{b} \in H^1(\Omega)$ be a locally optimal solution of the function identification problem (4.37). Let the corresponding state $\overline{f} = S(\overline{b})$ be given by the solution of (4.34) and the corresponding adjoint state be given by the following adjoint equation*

$$-\frac{\partial p}{\partial t} - \frac{1}{2}\sigma^2\frac{\partial^2 p}{\partial x^2} - \overline{b}\frac{\partial p}{\partial x} = 0 \qquad \text{in } Q, \tag{4.40a}$$

$$\frac{\partial p}{\partial n} = 0 \qquad \text{on } \Sigma, \tag{4.40b}$$

$$p(t_f) = 0 \qquad \text{in } \Omega, \tag{4.40c}$$

$$p(x,\tau_l) = p(x,\tau_l^+) + \left(\int_\Omega x\,\overline{f}(x,\tau_l)\,\mathrm{d}x - \xi_l\right) x \qquad \text{for } l = 1,\dots,L, \tag{4.40d}$$

where $p(x,\tau_l^+) = \lim\limits_{t\searrow\tau_l} p(x,t)$. Then the following holds true

$$\lambda\left(\overline{b},h\right)_{H^1(\Omega)} - \int_Q h\,\overline{f}\,\frac{\partial\overline{p}}{\partial x}\,\mathrm{d}x\,\mathrm{d}t = 0, \tag{4.41}$$

for all $h \in H^1(\Omega)$.

Proof. First, we define the following functional

$$\begin{aligned} j : H^1(\Omega) &\to \mathbb{R} \\ b &\mapsto \frac{1}{2}\left(\int_\Omega x\,f(x,\tau)\,\mathrm{d}x - \xi\right)^2, \end{aligned}$$

where $f = S(b)$ is given by (4.34), and show that a corresponding optimality condition as (4.41) is satisfied. The gradient of j at $b \in H^1(\Omega)$ applied to an arbitrary $h \in H^1(\Omega)$ is given by

$$(\nabla j(b),h)_{H^1(\Omega)} = \left(\int_\Omega x\,f(x,\tau)\,\mathrm{d}x - \xi\right)\int_\Omega x\,y(x,\tau)\,\mathrm{d}x,$$

where $y = S'(b)h$. Let p be defined on $\Omega\times[0,\tau]$ by the solution of the following adjoint equation

$$-\frac{\partial p}{\partial t} - \frac{1}{2}\sigma^2\frac{\partial^2 p}{\partial x^2} - b\frac{\partial p}{\partial x} = 0 \qquad \text{in } \Omega\times[0,\tau],$$

$$\frac{\partial p}{\partial n} = 0 \qquad \text{on } \Gamma\times[0,\tau],$$

$$p(\tau) = \left(\int_\Omega x\,f(x,\tau)\,\mathrm{d}x - \xi\right) x \qquad \text{in } \Omega.$$

The existence of a unique weak solution for this problem given by the following variational equality

$$-\frac{\mathrm{d}}{\mathrm{d}t}\int_\Omega p\,v\,\mathrm{d}x + \int_\Omega \frac{1}{2}\sigma^2\frac{\partial p}{\partial x}\frac{\partial v}{\partial x} + \left(\frac{1}{2}\frac{\partial\sigma^2}{\partial x} - b\right)\frac{\partial p}{\partial x}\,v\,\mathrm{d}x = 0$$

is shown with slight adjustments of the proof for Theorem 30. Using the terminal condition of p, we compute

$$\begin{aligned}(\nabla j(b), h)_{H^1(\Omega)} &= \int_\Omega p(x,\tau)\, y(x,\tau)\,\mathrm{d}x \\ &= \int_0^\tau \left\langle \frac{\mathrm{d}p}{\mathrm{d}t}, y \right\rangle_{H^1(\Omega)^*, H^1(\Omega)} + \left\langle \frac{\mathrm{d}y}{\mathrm{d}t}, p \right\rangle_{H^1(\Omega)^*, H^1(\Omega)} \mathrm{d}t,\end{aligned}$$

where we use the zero initial condition $y(x,0) = 0$. As y and p are weak solutions of the corresponding parabolic problems, we have that for the test functions p and y, respectively, the following equalities

$$\begin{aligned}\left\langle \frac{\mathrm{d}y}{\mathrm{d}t}, p \right\rangle_{H^1(\Omega)^*, H^1(\Omega)} &= -\int_\Omega \frac{1}{2}\sigma^2 \frac{\partial y}{\partial x}\frac{\partial p}{\partial x} + \left(\frac{1}{2}\frac{\partial \sigma^2}{\partial x} - b\right) y \frac{\partial p}{\partial x}\,\mathrm{d}x + \int_\Omega -h\, f \frac{\partial p}{\partial x}\,\mathrm{d}x, \\ \left\langle \frac{\mathrm{d}p}{\mathrm{d}t}, y \right\rangle_{H^1(\Omega)^*, H^1(\Omega)} &= \int_\Omega \frac{1}{2}\sigma^2 \frac{\partial p}{\partial x}\frac{\partial y}{\partial x} + \left(\frac{1}{2}\frac{\partial \sigma^2}{\partial x} - b\right) \frac{\partial p}{\partial x}\, y\,\mathrm{d}x\end{aligned}$$

hold. Hence, we arrive at

$$(\nabla j(b), h)_{H^1(\Omega)} = -\int_0^\tau \int_\Omega h\, f \frac{\partial p}{\partial x}\,\mathrm{d}x\,\mathrm{d}t.$$

In the case of the general objective functional

$$j(b) = \frac{1}{2}\sum_{l=1}^{L} \left(\int_\Omega x\, f(x,\tau_l)\,\mathrm{d}x - \xi_l \right)^2,$$

we define p_l by the corresponding terminal values problem in $[0,\tau_l]$ with respect to ξ_l. Furthermore, extend p_l on the interval $[0,t_f]$ by zero for $t > \tau_l$. Then the following holds true

$$(\nabla j(b), h)_{H^1(\Omega)} = -\int_0^{t_f} \int_\Omega h\, f \frac{\partial p}{\partial x}\,\mathrm{d}x\,\mathrm{d}t.$$

for $p = \sum_{l=1}^{L} p_l$. Note that in this case p satisfies (4.40), as the adjoint equation is linear in p.

Finally, we note that $\lambda(b,h)_{H^1(\Omega)}$ equals the derivative of $b \mapsto \frac{\lambda}{2}\|b\|^2_{H^1(\Omega)}$ applied to h. Hence, we conclude that the left-hand side of (4.41) equals the derivative of the reduced functional $\widetilde{J}$ applied to h. Due to Theorem 15, a local minimum $\overline{b}$ of $\widetilde{J}$ satisfies the condition $\widetilde{J}'(\overline{b})h = 0$ for all $h \in H^1(\Omega)$, which is equivalent to (4.41). This completes the proof. □

Theorem 33 enables us to compute candidates for the solution of the minimisation problem (4.37). On one hand, it is possible to discretise the whole optimality system and compute its solutions in order to identify the unknown function. On the other hand, it is now clear how the action of the gradient of the reduced functional $\widetilde{J}$ at an arbitrary point $b \in H^1(\Omega)$ on an arbitrary function $h \in H^1(\Omega)$ can be evaluated. This can be used to compute $\nabla\widetilde{J}(b)$ by solving the following Laplace equation in weak formulation

$$\int_\Omega \frac{\partial \nabla\widetilde{J}(b)}{\partial x}\frac{\partial h}{\partial x} + \nabla\widetilde{J}(b)\, h\,\mathrm{d}x = \lambda\,(b,h)_{H^1(\Omega)} - \int_Q h\, f \frac{\partial p}{\partial x}\,\mathrm{d}x\,\mathrm{d}t \qquad \text{for all } h \in H^1(\Omega).$$

Therefore, gradient-based optimisation algorithms can be applied in order to find the minimum. These two options follow the optimise–then–discretise approach, which is also applied in Chapter 3 and Section 4.1. For the stochastic function identification method, we decide to follow the discretise–then-optimise approach and describe in the next subsection the necessary considerations.

4.2.5 Discretisation of the Stochastic Function Identification Problem

In this subsection, we discuss the discretisation of the minimisation problem (4.37). In contrast to Section 3.4 we use here the discretise–before–optimise approach. Therefore, we first present the discretisation of the infinite dimensional minimisation problem and cast it to a finite dimensional one.

For the discretisation of a Fokker-Planck equation, the scheme of Chang and Copper, see [CC70], appears to be a very good choice. This numerical method has the property that it conserves the positivity of the solution for positive initial conditions. Moreover, the probability mass is also conserved. See [MB15, GAB] for the numerical analysis of this scheme. We briefly present the formulas for the implementation.

Using the method of lines, we first discretise the partial differential equation (4.34) in space for $\Omega = [x_{\min}, x_{\max}]$. The probability density f is approximated on an equidistant grid in the space variable at the points $x_i = x_{\min} + i\,h$ $(i = 0, \dots, N)$, where $h = \frac{x_{\max} - x_{\min}}{N}$ and N is a natural number. By defining $B = \frac{1}{2}\frac{\partial \sigma^2}{\partial x} - b$ and $C = \frac{1}{2}\sigma^2$ the flux can be written as $F = B\,f + C\,\frac{\partial f}{\partial x}$ and the Fokker-Planck equation is given in flux form as follows

$$\frac{\partial f}{\partial t} = \frac{\partial F}{\partial x}.$$

The derivative of the flux F is discretised by a central difference, where F is evaluated at intermediate grid points as follows

$$\frac{\mathrm{d}}{\mathrm{d}t} f_i = \frac{1}{h}\left(F_{i+\frac{1}{2}} - F_{i-\frac{1}{2}}\right).$$

While the derivative of f in the definition of the flux F is also discretised by a central difference, the intermediate value $f_{i+\frac{1}{2}}$ has to be interpolated by a convex combination. We have

$$F_{i+\frac{1}{2}} = B_{i+\frac{1}{2}}\left(\delta_{i+\frac{1}{2}} f_i + (1 - \delta_{i+\frac{1}{2}}) f_{i+1}\right) + C_{i+\frac{1}{2}} \frac{f_{i+1} - f_i}{h}.$$

Chang and Cooper observed that with the choice $\delta := \frac{1}{w} - \frac{1}{\mathrm{e}^w - 1}$, where $w := h\frac{B}{C}$, stationary solutions of a Fokker-Planck equation are conserved. Moreover, we have $1 - \delta = \frac{e^w}{\mathrm{e}^w - 1} - \frac{1}{w}$. For the space dependent function B and C we define $B_{i+\frac{1}{2}} = B(x_i + \frac{1}{2}h)$ and $C_{i+\frac{1}{2}} = C(x_i + \frac{1}{2}h)$. The same convention is used for variables defined by B and C such as δ, w, V, and W. Therefore, we arrive at

$$\begin{aligned}
\frac{\mathrm{d}}{\mathrm{d}t} f_j =& \frac{1}{h}\left[\left(B\left(\frac{e^w}{\mathrm{e}^w - 1} - \frac{1}{w}\right) + \frac{1}{h}C\right)_{i+\frac{1}{2}} f_{i+1} - \left(B\left(\frac{1}{w} - \frac{1}{\mathrm{e}^w - 1}\right) - \frac{1}{h}C\right)_{i+\frac{1}{2}} f_i\right] \\
& - \frac{1}{h}\left[\left(B\left(\frac{e^w}{\mathrm{e}^w - 1} - \frac{1}{w}\right) + \frac{1}{h}C\right)_{i-\frac{1}{2}} f_i - \left(B\left(\frac{1}{w} - \frac{1}{\mathrm{e}^w - 1}\right) - \frac{1}{h}C\right)_{i-\frac{1}{2}} f_{i-1}\right] \\
=& \frac{1}{h^2}\left(W_{i+\frac{1}{2}} f_{i+1} - \left(V_{i+\frac{1}{2}} + W_{i-\frac{1}{2}}\right) f_i + V_{i-\frac{1}{2}} f_{i-1}\right),
\end{aligned}$$

where we use the identity $\frac{B}{w} - \frac{C}{h} = 0$ and the definitions $V \coloneqq C\frac{w}{\mathrm{e}^{w}-1}$ and $W \coloneqq C\frac{-w}{\mathrm{e}^{-w}-1}$. We arrive at the following $N+1$ dimensional system of ordinary differential equations

$$\frac{\mathrm{d}}{\mathrm{d}t}\boldsymbol{f} = M\,\boldsymbol{f},$$

with the state vector $\boldsymbol{f} = (f_0, \dots, f_N)^\top$ and the $N+1$ dimensional system matrix M given by

$$\begin{aligned} M_{i,i-1} &= V_{i-\frac{1}{2}} && \text{for } i = 2, \dots, N, \\ M_{i,i} &= -W_{i-\frac{1}{2}} - V_{i+\frac{1}{2}} && \text{for } i = 2, \dots, N-1, \\ M_{i,i+1} &= W_{i+\frac{1}{2}} && \text{for } i = 1, \dots, N-1, \end{aligned}$$

and zero elsewhere. We incorporate the zero flux boundary condition by defining $F_{-\frac{1}{2}} = F_{N+\frac{1}{2}} = 0$, which results in $M_{0,0} = -V_{\frac{1}{2}}$ and $M_{N,N} = -W_{N-\frac{1}{2}}$.

Introducing a temporal grid $t_m = m\,\delta t$, where $\delta t = \frac{t_f}{Q+1}$, and approximating the values of $\boldsymbol{f}(t_m)$ by $\boldsymbol{f}^m$, we solve the system of ordinary differential equations by the implicit Euler scheme, which is defined by

$$\frac{\boldsymbol{f}^m - \boldsymbol{f}^{m-1}}{\delta t} = M^m\,\boldsymbol{f}^m \qquad \text{for } m = 1, \dots, Q.$$

Note that for a time-dependent drift b and diffusion σ the functions B and C are time-dependent and, therefore, the matrix M is also dependent on the time variable t. In this case we have $M^m \coloneqq M(t_m)$. The initial value $\boldsymbol{f}^0$ is obtained by evaluating the initial condition $f_i^0 \coloneqq f_0(x_i)$; see (4.34c).

Next, we discretise the objective functional. We use the trapezoidal rule for numerical integration for computing the expected value used in the definition of J; see (4.37a). Similarly as in Subsection 4.1.5, we discretise the infinite dimensional space $H^1(\Omega)$ by radial basis functions as follows

$$b(x) = \sum_{1}^{K} u_k \Phi_k(x).$$

Hence, a discrete analogue to the objective functional J is given by

$$J_d(\boldsymbol{u}, \boldsymbol{f}) \coloneqq \sum_{l=1}^{L} \frac{1}{2}\left(\boldsymbol{x}^\top T\,\boldsymbol{f}^{m_l} - \xi_l\right)^2 + \frac{\lambda}{2}\boldsymbol{u}^\top S\boldsymbol{u},$$

where the index m_l is defined such that $\tau_l = t_{m_l}$ holds and the vector $\boldsymbol{f}^{m_l}$ is an approximation of $f(\cdot, \tau_l)$. Moreover, we have $\boldsymbol{x}^\top = (x_0, \dots, x_N)$. The matrix T defines the discrete analogue of the L^2 inner product and is given by

$$T = \operatorname{diag}\left(\frac{h}{2}, h, \dots, h, \frac{h}{2}\right).$$

Hence, the term $\boldsymbol{x}^\top T\,\boldsymbol{f}^l$ is an approximation of the expected value at time τ_l. The symmetric positive-definite matrix S defined by $S_{i,j} = (\Phi_i, \Phi_j)_{H^1(\mathbb{R})}$ maps the H^1 inner product to the finite dimensional vector space $\mathbb{R}^K$. The coefficients of the radial basis functions are collected in the vector $\boldsymbol{u}^\top = (u_1, \dots, u_K)$.

Finally, we use the following finite-dimensional minimisation problem as an approximation to (4.37). It is given by

$$\min_{\boldsymbol{u}\in\mathbb{R}^K} J_d(\boldsymbol{u},\boldsymbol{f}) = \sum_{l=1}^{L} \frac{1}{2}\left(\boldsymbol{x}^\top T\,\boldsymbol{f}^{m_l} - \xi_l\right)^2 + \frac{\lambda}{2}\boldsymbol{u}^\top S\boldsymbol{u} \tag{4.43a}$$

$$\text{subject to } \frac{\boldsymbol{f}^m - \boldsymbol{f}^{m-1}}{\delta t} = M^m(\boldsymbol{u})\,\boldsymbol{f}^m \qquad \text{for } m = 1,\dots,Q. \tag{4.43b}$$

Note that we explicitly denote the dependence of the transition matrix M on the coefficients $\boldsymbol{u}$ of the radial basis functions discretisation of the drift b.

As $\boldsymbol{f}$ is uniquely determined by $\boldsymbol{u}$, we introduce the reduced functional $\widetilde{J}_d(\boldsymbol{u}) = J_d(\boldsymbol{u},\boldsymbol{f}(\boldsymbol{u}))$. We apply the Lagrange approach to find the gradient $\nabla\widetilde{J}_d(\boldsymbol{u})$ and define

$$L(\boldsymbol{u},\boldsymbol{f},\boldsymbol{p}) \coloneqq J_d(\boldsymbol{u},\boldsymbol{f}) - \sum_{m=1}^{Q}\left((I-\delta t\,M^m(\boldsymbol{u}))\,\boldsymbol{f}^m - \boldsymbol{f}^{m-1}\right)^\top T\,\boldsymbol{p}^{m-1},$$

where I is the $N+1$ dimensional identity matrix. Note that we use the discrete L^2 inner product for the constraint and the Lagrange multiplier $\boldsymbol{p}^m$, as the resulting equations for the Lagrange multiplier form in this case a special disretisation of the adjoint equation (4.40). It is well-known that

$$\nabla\widetilde{J}_d(\boldsymbol{u}) = \nabla_{\boldsymbol{u}} L(\boldsymbol{u},\boldsymbol{f},\boldsymbol{p})$$

holds, where $\boldsymbol{f}$ and $\boldsymbol{p}$ are given by

$$\nabla_{\boldsymbol{f}} L(\boldsymbol{u},\boldsymbol{f},\boldsymbol{p}) = 0, \tag{4.44a}$$

$$\nabla_{\boldsymbol{p}} L(\boldsymbol{u},\boldsymbol{f},\boldsymbol{p}) = 0. \tag{4.44b}$$

Notice that (4.44b) is equivalent to the Chang-Cooper discretisation (4.43b) of the governing Fokker-Planck equation. Moreover, we compute, for $m = 1,\dots,Q$,

$$\nabla_{\boldsymbol{f}^m} L(\boldsymbol{u},\boldsymbol{f},\boldsymbol{p}) = \delta_m\left(\boldsymbol{x}^\top T\,\boldsymbol{f}^m - \xi_l\right)T\,\boldsymbol{x} - (I-\delta t\,M^m(\boldsymbol{u}))^\top T\,\boldsymbol{p}^{m-1} + T\,\boldsymbol{p}^m, \tag{4.45}$$

where $\boldsymbol{p}^Q$ is defined to be zero. To account for the observations ξ_l defining the objective functional, we define $\delta_m = 1$ if there exists an index $l \in \{1,\dots,L\}$ such that the equality $\tau_l = t_m$ holds. Otherwise, we set $\delta_m = 0$ and the first term on the right-hand side in (4.45) vanishes. Hence, (4.44a) is equivalent to

$$-\frac{\widetilde{\boldsymbol{p}}^m - \boldsymbol{p}^{m-1}}{\delta t} = M^m(\boldsymbol{u})^\top\,\boldsymbol{p}^{m-1}, \tag{4.46a}$$

$$\widetilde{\boldsymbol{p}}^m = \boldsymbol{p}^m + \delta_m\left(\boldsymbol{x}^\top T\,\boldsymbol{f}^m - \xi_l\right)\boldsymbol{x}, \tag{4.46b}$$

for $m = 1,\dots,Q$. Compare (4.46) to the adjoint equation (4.40) of the continuous problem. As one expects that the optimality system of a discretised minimisation problem converges to the continuous optimality system, the transition matrix $M^m(u)^\top$ can be seen as a special discretisation of the adjoint second-order differential operator $-\frac{1}{2}\sigma^2\frac{\partial^2}{\partial x^2} - b\frac{\partial}{\partial x}$ together with homogeneous Neumann boundary conditions.

Further, the derivative of the Lagrange function L with respect to the minimisation variable $\boldsymbol{u}$ is given by

$$\nabla_{\boldsymbol{u}} L(\boldsymbol{u},\boldsymbol{f},\boldsymbol{p}) = \lambda\,S\,\boldsymbol{u} + \delta t\sum_{m=1}^{Q}\left(\nabla_{\boldsymbol{u}} M^m(\boldsymbol{u})\boldsymbol{f}^m\right)^\top T\,\boldsymbol{p}^{m-1},$$

where the derivative of the transition matrix $M^m(\boldsymbol{u})$ with respect to $\boldsymbol{u}$ is computed by considering the definitions of the Chang-Cooper scheme and the following formulas

$$\frac{\mathrm{d}V}{\mathrm{d}u_k} = C\frac{\mathrm{e}^w - 1 - w\,\mathrm{e}^w}{(\mathrm{e}^w-1)^2}\frac{\mathrm{d}w}{\mathrm{d}u_k} = \frac{\mathrm{e}^w - 1 - w\,\mathrm{e}^w}{(\mathrm{e}^w-1)^2}h\frac{\mathrm{d}B}{\mathrm{d}u_k},$$
$$\frac{\mathrm{d}W}{\mathrm{d}u_k} = C\frac{1 - \mathrm{e}^{-w} - w\,\mathrm{e}^{-w}}{(\mathrm{e}^{-w}-1)^2}\frac{\mathrm{d}w}{\mathrm{d}u_k} = \frac{1 - \mathrm{e}^{-w} - w\,\mathrm{e}^{-w}}{(\mathrm{e}^{-w}-1)^2}h\frac{\mathrm{d}B}{\mathrm{d}u_k}.$$

Moreover, as $B = \frac{1}{2}\frac{\partial}{\partial x}\sigma^2 - \sum_{k=1}^{K} u_k\Phi_k$ holds, we have $\frac{\mathrm{d}B}{\mathrm{d}u_k} = -\Phi_k$.

Finally, we present the following algorithm the evaluate the gradient of the reduced discrete objective functional $\widetilde{J}_d$

1: Given $\boldsymbol{u} \in \mathbb{R}^K$.
2: **for** $m = 1, \dots, Q$ **do**
3:
$$\frac{\boldsymbol{f}^m - \boldsymbol{f}^{m-1}}{\delta t} = M^m(\boldsymbol{u})\,\boldsymbol{f}^m$$
4: **end for**
5: **for** $m = Q, \dots, 1$ **do**
6:
$$-\frac{\widetilde{\boldsymbol{p}}^m - \boldsymbol{p}^{m-1}}{\delta t} = M^m(\boldsymbol{u})^\top\,\boldsymbol{p}^{m-1},$$
$$\widetilde{\boldsymbol{p}}^m = \boldsymbol{p}^m + \delta_m\left(\boldsymbol{x}^\top T\,\boldsymbol{f}^m - \xi_l\right)\boldsymbol{x}$$
7: **end for**
8: Evaluate
$$\nabla\widetilde{J}_d(\boldsymbol{u}) = \lambda\,S\,\boldsymbol{u} + \delta t\sum_{m=1}^{Q}\left(\nabla_{\boldsymbol{u}}M^m(\boldsymbol{u})\boldsymbol{f}^m\right)^\top T\,\boldsymbol{p}^{m-1}$$

Therefore, any gradient-based optimisation algorithm can be used to solve the discretised minimisation problem and identify the drift of a Fokker-Planck equation, which corresponds to the dynamics function of a stochastic differential equation.

4.2.6 Numerical Results for the Identification of the Toxicity Function

In this subsection, we apply the discussed theoretical and computational framework to the identification of a toxicity function. We use the same measurements of yeast biomass, sugar, and ethanol concentrations as in the case of the deterministic model; see Subsection 4.1.6. In order to reduce the computational effort, we do not extend the full fermentation model (2.8) to a system of stochastic differential equations, as this would lead to a five-dimensional Fokker-Planck equation. Therefore, we consider only the equations for the yeast and ethanol concentration. Moreover, in order to isolate the process of yeast death we start the simulation of the fermentation process after the growth of the yeast has ended and the extinction of yeast cells starts. The following system of stochastic differential equations models this late stage of the wine fermentation, where the growth term for the yeast equation is neglected. We consider

$$dX_t = -\Psi(E_t)X_t\,\mathrm{d}t + \sigma_1\,\mathrm{d}W_t^{(1)}, \tag{4.47a}$$
$$dE_t = a_1\frac{S(t)}{a_2 + S(t)}\frac{a_3}{a_3 + E_t}X_t\,\mathrm{d}t + \sigma_2\,\mathrm{d}W_t^{(2)}, \tag{4.47b}$$

in order to identify the toxicity function Ψ. The Wiener processes $W_t^{(1)}$ and $W_t^{(2)}$ are assumed to be stochastically independent and the diffusion is chosen to be constant with values σ_1 and σ_2, respectively. Moreover, the time dependent sugar concentration S in (4.47b) is given by a liner interpolation of the measurement values and is therefore known. Note that we apply our results to a multi-dimensional model and the formulas for the Fokker-Planck equation and the corresponding minimisation problem have to be extended correspondingly.

Let $\xi_{X,l}$ denote the measurement of the yeast concentration at time $\tau_{X,l}$ for $l = 1, \dots, L_X$ and correspondingly let $\xi_{E,l}$ be the measurement of the ethanol concentration at time $\tau_{E,l}$ for $l = 1, \dots, L_E$. We formulate the following minimisation problem

$$\begin{aligned} \min_{\Psi \in H^1(\mathbb{R}), a \in \mathbb{R}^3} J(f, \Psi, a) = &\sum_{l=1}^{L_X} \frac{\lambda_X}{2} \left(\int_\Omega x_1 \, f(x, \tau_{X,l}) \, \mathrm{d}x - \xi_{X,l} \right)^2 \\ &+ \sum_{l=1}^{L_E} \frac{\lambda_E}{2} \left(\int_\Omega x_2 \, f(x, \tau_{E,l}) \, \mathrm{d}x - \xi_{E,l} \right)^2 \\ &+ \frac{\lambda_\Psi}{2} \|\Psi\|^2_{H^1(\mathbb{R})} + \frac{\lambda_a}{2} \|a - a_p\|^2_{\mathbb{R}^3}, \end{aligned} \tag{4.48a}$$

subject to

$$\begin{aligned} &\frac{\partial f}{\partial t} - \frac{1}{2}\sigma_1^2 \frac{\partial^2 f}{\partial x_1^2} + \frac{\partial}{\partial x_1}\left(-\Psi(x_2) x_1 \, f\right) \\ &\quad - \frac{1}{2}\sigma_2^2 \frac{\partial^2 f}{\partial x_2^2} + \frac{\partial}{\partial x_2}\left(a_1 \frac{S(t)}{a_2 + S(t)} \frac{a_3}{a_3 + x_2} x_1 \, f \right) = 0. \end{aligned} \tag{4.48b}$$

Similarly as in Subsection 4.1.6, we have to identify the model parameters $a = (a_1, a_2, a_3)^\top$ simultaneously and therefore we include the vector a in the minimisation problem with a regularisation term, where a_p is an a priori guess of the optimal parameters. Now, the Fokker-Planck equation (4.48b) governs the probability density function f of the stochastic process (X_t, E_t), which is the solution of the stochastic differential equation (4.47).

For the numerical solution of (4.48) we apply the results of Subsection 4.2.5 and discretise the Fokker-Planck equation by the Chang-Cooper scheme. Therefore, we use $\Omega = [-30, 70] \times [0, 200]$ as the computational domain and 51 equally spaced grid points in each space dimension. We simulate the fermentation process between day 8 and day 29 of the wine fermentation experiment and discretise the interval $[8, 29]$ with 211 time points. For the initial condition, we assume that (X_0, E_0) is distributed with a Gaussian probability density function as follows

$$f_0(x_1, x_2) = \frac{1}{2\pi\sigma_X\sigma_E} \exp\left(-\frac{(x_1 - \mu_X)^2}{2\sigma_X^2} - \frac{(x_2 - \mu_E)^2}{2\sigma_E^2} \right),$$

where μ_X and μ_E are the measured values of yeast and ethanol at day 8, respectively. We choose the variances as $\sigma_X = \sigma_E = 3$. Moreover, the diffusion parameters are chosen constant as $\sigma_1 = \sigma_2 = 1$, and we use the following regularisation parameters

$$\lambda_X = 1, \qquad \lambda_E = 1, \qquad \lambda_\Psi = 500, \qquad \lambda_a = 10.$$

For the discretisation of the toxicity function, we use, similarly as in Subsection 4.1.6, 30 shifted versions of Wendland's piecewise polynomial, positive definite, and compactly

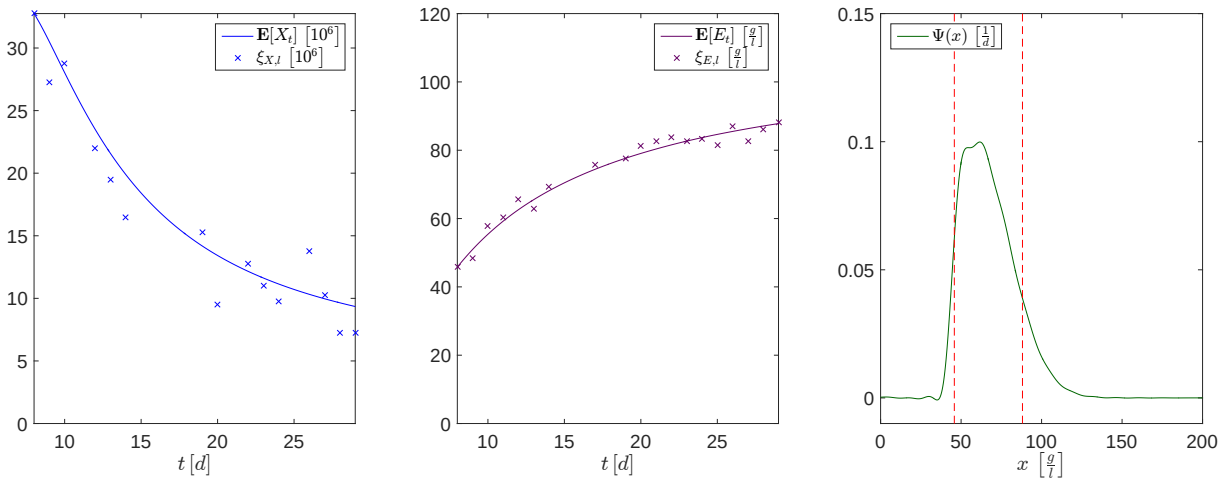

Figure 4.3: Expected values of the stochastic process (X_t, E_t) with respect to the optimal toxicity function Ψ (right) in comparison with measured values for the yeast cell numbers $\xi_{X,l}$ (left) and for the ethanol concentration $\xi_{E,l}$ (middle).

supported radial basis functions of minimal degree with nodal points that are equally distributed between 0 and 200.

The results of the toxicity function identification are obtained by a BFGS optimisation algorithm and can be seen in Figure 4.3 and Figure 4.4. The probability density function is used to calculate the expected values of the stochastic process as follows

$$\mathbf{E}[X_t] = \int_\Omega x_1 f(x,t)\,\mathrm{d}x, \qquad \mathbf{E}[E_t] = \int_\Omega x_2 f(x,t)\,\mathrm{d}x.$$

The expected values for the yeast cell number and ethanol concentration can be seen in the left and middle plot of Figure 4.3, respectively. In comparison, the experimentally measured values $\xi_{X,l}$ and $\xi_{E,l}$ that are used for the identification procedure are visualised by blue and purple crosses in the same plots, respectively. We observe that the expected values of the simulation evolve such that its distance to the measured values is as small as possible. Moreover, the right plot of Figure 4.3 shows the identified toxicity function. The measured values of ethanol concentration are contained in an interval that is indicated by red vertical lines. In this regime, we have information about how the system evolves and we can expect to identify the toxicity function only in this interval. Note that we have now a smaller interval compared to the identification in Subsection 4.1.6 due to the smaller set of measured values. Hence, we cannot identify the toxicity for lower ethanol concentrations than approximately $45\,\frac{g}{l}$, which is supposed to be around zero by the results of the deterministic function identification. For the interval of interest between approximately $45\,\frac{g}{l}$ and $90\,\frac{g}{l}$, we observe a plateau at a value of about $0.1\,\frac{1}{d}$. This peak is higher than the one in the corresponding identification process for the deterministic case, see Figure 4.2, and this discrepancy can have many reasons. On one hand, we have here a stochastic differential equation and many different realisations for the wine fermentation process are taken into account, where only the mean value is used for the identification process. On the other hand, we have a smaller system of equations and simulate only the second part of the fermentation process. A further aspect that attracts attention is that the toxicity declines for higher ethanol concentrations, which seems unrealistic at a first glance. Nevertheless, we have assumed a time independent toxicity function that is valid for the whole process of the wine fermentation. This assumption is arguable, as the yeast

cell can also adapt to the new environment with a higher ethanol concentration. Hence, this decline can be a hint on the fact that yeast cell are exposed to such high ethanol concentrations only at the end of the fermentation process and have possibly already adopted to the change in the environmental conditions.

Finally, we can track the evolution of the probability density function f that is calculated with respect to the optimal toxicity function and optimal parameters in Figure 4.4. The probability mass that is centred around the point $(\mu_X, \mu_E) \approx (32.8, 45.8)$ at the beginning of the simulation. In the course of the simulation, this mass is transported in the direction of lower yeast cell numbers and higher ethanol concentration. Hereby, the initially symmetric distribution is smeared especially in the direction of the ethanol axis.

Conclusion

In this subsection, we presented one possible extension of the function identification method for ordinary differential equation presented in Section 4.1. Therefore, we introduced stochastic differential equations and their corresponding Fokker-Planck equations. We formulated and analysed a minimisation problem that aims to fit the average values of the stochastic process by choosing the correct representative of the unknown function from a function space. This enabled us to apply this method to the identification of the toxicity function for the wine fermentation process. The results of this identification are comparable to those in the deterministic case with ordinary differential equations. Nevertheless, it is desirable to have more experimental data in order to investigate the toxic influence of high ethanol concentrations on yeast cells further. Moreover, in this case it could be possible to evaluate whether a deterministic approach is sufficient for a good identification procedure or a stochastic model provides better results.

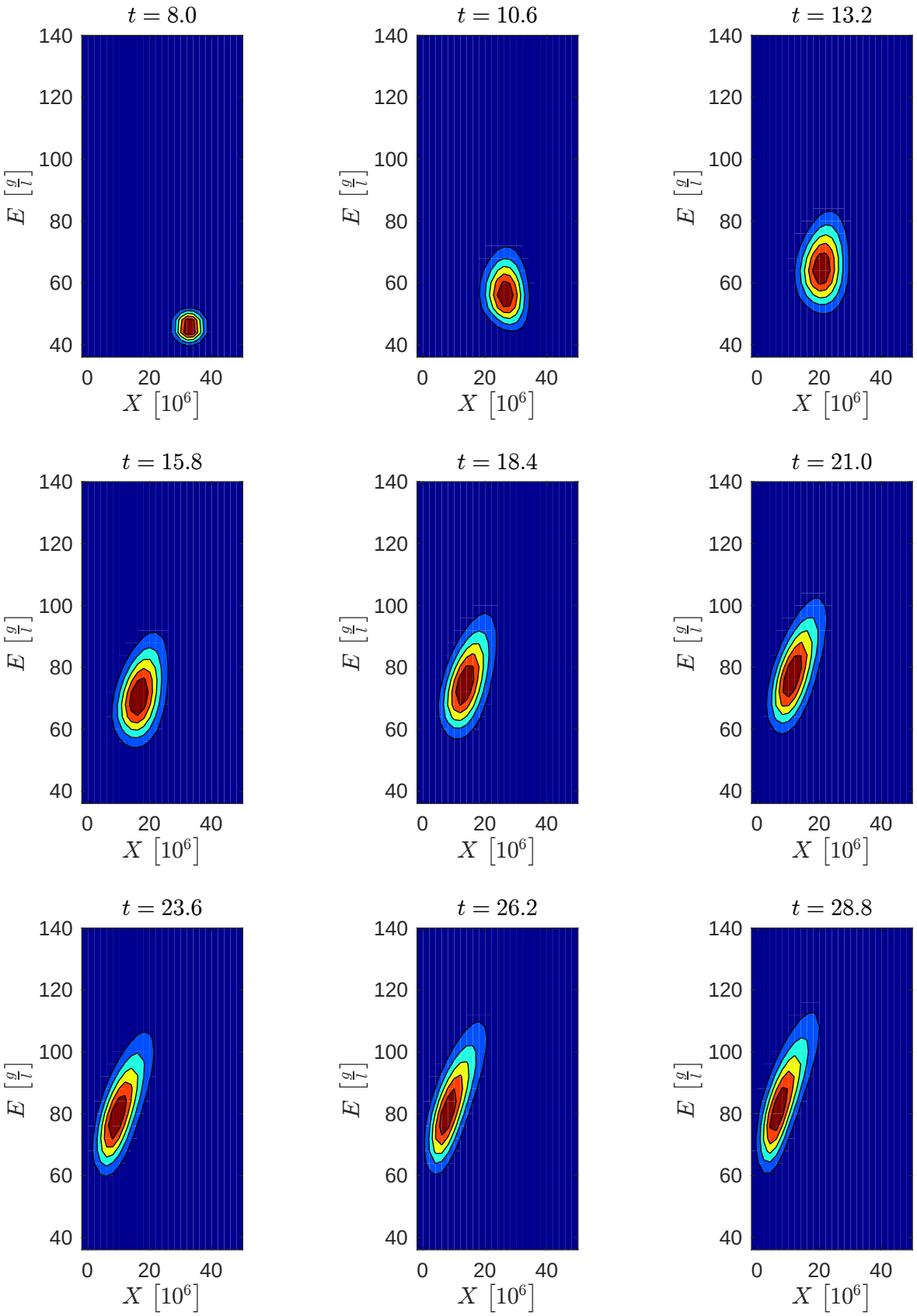

Figure 4.4: Evolution of the probability density function f computed with respect to the optimal toxicity function and optimal parameters. Blue colour corresponds to a value of zero, while red colour indicates high values.

Chapter 5

Summary

In the context of mathematical modelling, simulation, and optimisation, this thesis presented various results for the wine fermentation process as a representative biological model.

First, a refined model for the wine fermentation was described, which takes further aspects into account compared to the state-of-the-art models in the literature. In particular, the dependence of yeast growth on oxygen availability, a sophisticated modelling of the toxic influence of ethanol, and the spatial inhomogeneity by a system of reaction-diffusion equations were regarded.

Further, the optimal control of the fermentation process was considered. Therefore, the minimisation of a suitably defined objective functional subject to the reaction-diffusion equations modelling the wine fermentation was used to find control temperature profiles. On one hand, they minimised the remaining sugar at the end of this process and, on the other hand, a moderate temperature within the fermentation vessel was maintained. In order to justify the computational approach carried out for this optimal control problem a rigorous mathematical analysis of the fermentation model and the corresponding infinite dimensional optimisation problem was presented.

Another aspect discussed here was the identification of an unknown function participating in a dynamical model. In the deterministic case, a minimisation problem was treated subject to an ordinary differential equation, whereas a stochastic differential equation or rather the corresponding Fokker-Planck equation was regarded in the stochastic case. In both cases, the differentiability properties of the reduced objective functional were proven and the existence of minimisers was shown. The unknown function was discretised by radial basis functions, as this choice offers a simple generalisation for the treatment of multivariate functions. The proposed function identification method was applied to the unknown toxicity function of the wine fermentation model and numerical results were reported both in the deterministic as well as in the stochastic case.

Having gained experience with a biological model with moderate complexity the results presented in this thesis can be applied to more complex models. One example, which is worth for consideration, is the optimisation of the fermentation of biogas, as this additional environmentally friendly source of energy is gaining more and more attention in recent years.

Bibliography

[AB13a] M. Annunziato and A. Borzì. Fokker-Planck-based control of a two-level open quantum system. *Mathematical Models and Methods in Applied Sciences*, 23(11):2039–2064, 2013.

[AB13b] M. Annunziato and A. Borzì. A Fokker-Planck control framework for multidimensional stochastic processes. *Journal of Computational and Applied Mathematics*, 237(1):487–507, 2013.

[ABMW15] M. Annunziato, A. Borzì, M. Magdziarz, and A. Weron. A fractional fokker–planck control framework for subdiffusion processes. *press to Optimal Control, Applications and Methods. doi*, 10:1002, 2015.

[AF03] R. A. Adams and J. J. F. Fournier. *Sobolev Spaces*, volume 140 of *Pure and Applied Mathematics (Amsterdam)*. Elsevier/Academic Press, Amsterdam, second edition, 2003.

[Arn74] L. Arnold. *Stochastic differential equations: theory and applications*. Wiley-Interscience [John Wiley & Sons], New York-London-Sydney, 1974. Translated from the German.

[ARS97] U. M. Ascher, S. J. Ruuth, and R. J. Spiteri. Implicit-explicit Runge-Kutta methods for time-dependent partial differential equations. *Applied Numerical Mathematics. An IMACS Journal*, 25(2-3):151–167, 1997. Special issue on time integration (Amsterdam, 1996).

[ATGSFB+04] B. Andres-Toro, J. M. Giron-Sierra, P. Fernandez-Blanco, J. A. Lopez-Orozco, and E. Besada-Portas. Multiobjective optimization and multivariable control of the beer fermentation process with the use of evolutionary algorithms. *Journal of Zhejiang University SCIENCE*, 5(4):378–389, 2004.

[Aub63] J.-P. Aubin. Un théorème de compacité. *Comptes Rendus de l'Acadèmie des Sciences, Paris*, 256:5042–5044, 1963.

[Bar74] Y. Bard. *Nonlinear parameter estimation*. Academic Press [A subsidiary of Harcourt Brace Jovanovich, Publishers], New York-London, 1974.

[BDB86] L. T. Biegler, J. J. Damiano, and G. E. Blau. Nonlinear parameter estimation: a case study comparison. *AIChE Journal*, 32(1):29–45, 1986.

[BG06] A. Borzì and R. Griesse. Distributed optimal control of lambda-omega systems. *Journal of Numerical Mathematics*, 14(1):17–40, 2006.

[BJT10] W. Barthel, C. John, and F. Tröltzsch. Optimal boundary control of a system of reaction diffusion equations. *ZAMM. Zeitschrift für Angewandte Mathematik und Mechanik. Journal of Applied Mathematics and Mechanics*, 90(12):966–982, 2010.

[BMM+14] A. Borzì, J. Merger, J. Müller, A. Rosch, C. Schenk, D. Schmidt, S. Schmidt, V. Schulz, K. Velten, C. von Wallbrunn, and M. Zänglein. Novel model for wine fermentation including the yeast dying phase. *arXiv preprint arXiv:1412.6068*, 2014.

[Boc87] H. G. Bock. *Randwertproblemmethoden zur Parameteridentifizierung in Systemen nichtlinearer Differentialgleichungen.* Bonner Mathematische Schriften [Bonn Mathematical Publications], 183. Universität Bonn, Mathematisches Institut, Bonn, 1987. Dissertation, Rheinische Friedrich-Wilhelms-Universität, Bonn, 1985.

[Bou03] J. Boussinesq. *Théorie analytique de la chaleur: mise en harmonie avec la thermodynamique et avec la théorie mécanique de la lumière*, volume 2. Gauthier-Villars, 1903.

[BPW13] M. Burger, J.-F. Pietschmann, and M.-T. Wolfram. Identification of nonlinearities in transport-diffusion models of crowded motion. *Inverse Problems and Imaging*, 7(4):1157–1182, 2013.

[BS12] A. Borzì and V. Schulz. *Computational Optimization of Systems Governed by Partial Differential Equations*, volume 8 of *Computational Science & Engineering.* Society for Industrial and Applied Mathematics (SIAM), Philadelphia, PA, 2012.

[Buh03] M. D. Buhmann. *Radial basis functions: theory and implementations*, volume 12 of *Cambridge Monographs on Applied and Computational Mathematics.* Cambridge University Press, Cambridge, 2003.

[Cas97] E. Casas. Pontryagin's principle for state-constrained boundary control problems of semilinear parabolic equations. *SIAM Journal on Control and Optimization*, 35(4):1297–1327, 1997.

[CC70] J. S. Chang and G. Cooper. A practical difference scheme for fokker-planck equations. *Journal of Computational Physics*, 6(1):1–16, 1970.

[CDD+10] B. Charnomordic, R. David, D. Dochain, N. Hilgert, J.-R. Mouret, J.-M. Sablayrolles, and A. Vande Wouwer. Two modelling approaches of winemaking: first principle and metabolic engineering. *Mathematical and Computer Modelling of Dynamical Systems. Methods, Tools and Applications in Engineering and Related Sciences*, 16(6):535–553, 2010.

[Cho] K. Chojnacka. Fermentation products. *Chemical Engineering and Chemical Process Technology*, V:12. `http://www.eolss.net/outlinecomponents/Chemical-Engineering-Chemical-Process-Technology.aspx`.

[Cia13] P. G. Ciarlet. *Linear and Nonlinear Functional Analysis with Applications.* Society for Industrial and Applied Mathematics, Philadelphia, PA, 2013.

[CMS07] S. Colombié, S. Malherbe, and J.-M. Sablayrolles. Modeling of heat transfer in tanks during wine-making fermentation. *Food Control*, 18(8):953–960, 2007.

[DDM+10] R. David, D. Dochain, J.-R. Mouret, A. Vande Wouwer, and J.-M. Sablayrolles. Dynamical modeling of alcoholic fermentation and its link with nitrogen consumption. In *Proceedings of the 11th International Symposium on Computer Applications in Biotechnology (CAB 2010). Leuven, Belgium*, pages 496–501, 2010.

[DDM+11] R. David, D. Dochain, J.-R. Mouret, A. Vande Wouwer, and J.-M. Sablayrolles. Modeling of the aromatic profile in wine-making fermentation: the backbone equations. In *Proceedings of the 18th IFAC World Congress, Milano*, pages 10597–10602, 2011.

[DL88] R. Dautray and J.-L. Lions. *Mathematical analysis and numerical methods for science and technology. Vol. 2.* Springer-Verlag, Berlin, 1988. Functional and variational methods, With the collaboration of Michel Artola, Marc Authier, Philippe Bénilan, Michel Cessenat, Jean Michel Combes, Hélène Lanchon, Bertrand Mercier, Claude Wild and Claude Zuily, Translated from the French by Ian N. Sneddon.

[DL92] R. Dautray and J.-L. Lions. *Mathematical Analysis and Numerical Methods for Science and Technology. Vol. 5.* Springer-Verlag, Berlin, 1992. Evolution Problems. I, With the collaboration of Michel Artola, Michel Cessenat and Hélène Lanchon, Translated from the French by Alan Craig.

[DR04] P. G. Drazin and W. H. Reid. *Hydrodynamic Stability.* Cambridge Mathematical Library. Cambridge University Press, 2004.

[EFP05] H. W. Engl, P. Fusek, and S. V. Pereverzev. Natural linearization for the identification of nonlinear heat transfer laws. *Journal of Inverse and Ill-Posed Problems*, 13(3-6):567–582, 2005. Inverse problems: modeling and simulation.

[Ein05] A. Einstein. The theory of the brownian movement. *Ann. der Physik*, 17:549, 1905.

[EPS14a] H. Egger, J.-F. Pietschmann, and M. Schlottbom. Numerical identification of a nonlinear diffusion law via regularization in Hilbert scales. *Inverse Problems. An International Journal on the Theory and Practice of Inverse Problems, Inverse Methods and Computerized Inversion of Data*, 30(2):025004, 2014.

[EPS14b] H. Egger, J.-F. Pietschmann, and M. Schlottbom. Simultaneous identification of diffusion and absorption coefficients in a quasilinear elliptic problem. *Inverse Problems. An International Journal on the Theory and Practice of Inverse Problems, Inverse Methods and Computerized Inversion of Data*, 30(3):035009, 2014.

[EPS15a] H. Egger, J.-F. Pietschmann, and M. Schlottbom. Identification of chemotaxis models with volume-filling. *SIAM Journal on Applied Mathematics*, 75(2):275–288, 2015.

[EPS15b] H. Egger, J.-F. Pietschmann, and M. Schlottbom. Identification of nonlinear heat conduction laws. *Journal of Inverse and Ill-posed Problems*, 23(5):429–437, 2015.

[Eva10] L. C. Evans. *Partial Differential Equations*, volume 19 of *Graduate Studies in Mathematics*. American Mathematical Society, Providence, RI, second edition, 2010.

[Fog10] H. S. Fogler. *Essentials of Chemical Reaction Engineering*. Pearson Education, 2010.

[GAB] B. Gaviraghi, B. Annunziato, and A. Borzì. Analysis of splitting methods for solving a partial integro-differential Fokker-Planck equation (in review). *Applied Mathematics and Computation*.

[Gar83] C. W. Gardiner. *Handbook of stochastic methods*, volume 13 of *Springer Series in Synergetics*. Springer-Verlag, Berlin, 1983. For physics, chemistry and the natural sciences.

[GR88] D. A. Gee and W. F. Ramirez. Optimal temperature control for batch beer fermentation. *Biotechnology and Bioengineering*, 31(3):224–234, 1988.

[GSAB] B. Gaviraghi, A. Schindele, B. Annunziato, and A. Borzì. Investigation of optimal control problems of jump-diffusion processes with sparsity objectives (forthcoming).

[GV03] R. Griesse and S. Volkwein. *Analysis for optimal boundary control for a three-dimensional reaction-diffusion system*. Universität Graz/Technische Universität Graz. SFB F003-Optimierung und Kontrolle, 2003.

[Hal09] J. K. Hale. *Ordinary Differential Equations*. Dover Books on Mathematics Series. Dover Publications, 2009.

[HHTL15] D. N. Hào, B. V. Huong, P. X. Thanh, and D. Lesnic. Identification of nonlinear heat transfer laws from boundary observations. *Applicable Analysis. An International Journal*, 94(9):1784–1799, 2015.

[HLSY14] D. Hömberg, S. Lu, K. Sakamoto, and M. Yamamoto. Parameter identification in non-isothermal nucleation and growth processes. *Inverse Problems. An International Journal on the Theory and Practice of Inverse Problems, Inverse Methods and Computerized Inversion of Data*, 30(3):035003, 2014.

[HLT12] D. Hömberg, J. Liu, and N. Togobytska. Identification of the thermal growth characteristics of coagulated tumor tissue in laser-induced thermotherapy. *Mathematical Methods in the Applied Sciences*, 35(5):497–509, 2012.

[HP57] E. Hille and R. S. Phillips. *Functional analysis and semi-groups*. American Mathematical Society Colloquium Publications, vol. 31. American Mathematical Society, Providence, R. I., 1957. rev. ed.

[HV03] W. Hundsdorfer and J. Verwer. *Numerical Solution of Time-Dependent Advection-Diffusion-Reaction Equations*, volume 33 of *Springer Series in Computational Mathematics*. Springer-Verlag, Berlin, 2003.

[JA16] Merger J. and Borzì A. Dynamics identification in evolution models using radial basis functions. *Journal of Dynamical and Control Systems*, 2016.

[JG11] K. A. Johnson and R. S. Goody. The original michaelis constant: translation of the 1913 michaelis–menten paper. *Biochemistry*, 50(39):8264–8269, 2011.

[JS14] B. S. Jovanović and E. Süli. *Analysis of finite difference schemes: for linear partial differential equations with generalized solutions*, volume 46. Springer Science & Business Media, 2014.

[KE02] P. Kügler and H. W. Engl. Identification of a temperature dependent heat conductivity by Tikhonov regularization. *Journal of Inverse and Ill-Posed Problems*, 10(1):67–90, 2002.

[Kos10] P. Kosmol. *Optimierung und Approximation*. Walter de Gruyter & Co., Berlin, expanded edition, 2010.

[Kot08] T. Koto. IMEX Runge-Kutta schemes for reaction-diffusion equations. *Journal of Computational and Applied Mathematics*, 215(1):182–195, 2008.

[KS91] I. Karatzas and S. E. Shreve. *Brownian motion and stochastic calculus*, volume 113 of *Graduate Texts in Mathematics*. Springer-Verlag, New York, second edition, 1991.

[Küg03] P. Kügler. Identification of a temperature dependent heat conductivity from single boundary measurements. *SIAM Journal on Numerical Analysis*, 41(4):1543–1563, 2003.

[Lio69] J.-L. Lions. *Quelques méthodes de résolution des problèmes aux limites non linéaires*. Dunod; Gauthier-Villars, Paris, 1969.

[Lio71] J.-L. Lions. *Optimal Control of Systems Governed by Partial Differential Equations*. Translated from the French by S. K. Mitter. Die Grundlehren der mathematischen Wissenschaften, Band 170. Springer-Verlag, New York-Berlin, 1971.

[LO13] E. Laurien and H. Oertel. *Numerische Strömungsmechanik: Grundgleichungen und Modelle - Lösungsmethoden - Qualität und Genauigkeit*. SpringerLink : Bücher. Springer Fachmedien Wiesbaden, 2013.

[LOP05] Z. Li, M. R. Osborne, and T. Prvan. Parameter estimation of ordinary differential equations. *IMA Journal of Numerical Analysis*, 25(2):264–285, 2005.

[Lor82] A. Lorenzi. An inverse problem for a semilinear parabolic equation. *Annali di Matematica Pura ed Applicata. Serie Quarta*, 131:145–166, 1982.

[LTPM02] G. Lian, A. Thiru, A. Parry, and S. Moore. Cfd simulation of heat transfer and polyphenol oxidation during tea fermentation. *Computers and Electronics in Agriculture*, 34(1):145–158, 2002.

[Mas83] K. Masuda. On the global existence and asymptotic behavior of solutions of reaction-diffusion equations. *Hokkaido Mathematical Journal*, 12(3):360–370, 1983.

[MB15] M. Mohammadi and A. Borzì. Analysis of the chang–cooper discretization scheme for a class of fokker–planck equations. *Journal of Numerical Mathematics*, 23(3):271–288, 2015.

[MBH16] J. Merger, A. Borzì, and R. Herzog. Optimal control of a system of reaction-diffusion equations modeling the wine fermentation process. *Optimal Control Applications and Methods*, 2016.

[MFHS04] S. Malherbe, V. Fromion, N. Hilgert, and J.-M. Sablayrolles. Modeling the effects of assimilable nitrogen and temperature on fermentation kinetics in enological conditions. *Biotechnology and Bioengineering*, 86(3):261–272, 2004.

[MM13] L. Michaelis and M. L. Menten. Die Kinetik der Invertinwirkung. *Biochemische Zeitschrift*, 49(333-369):352, 1913.

[Mur93] J. D. Murray. *Mathematical biology*, volume 19 of *Biomathematics*. Springer-Verlag, Berlin, second edition, 1993.

[NHG10] Z. Neufeld and E. Hernández-García. *Chemical and Biological Processes in Fluid Flows: A Dynamical Systems Approach*. Imperial College Press, 2010.

[NW06] J. Nocedal and S. J. Wright. *Numerical Optimization*. Springer Series in Operations Research and Financial Engineering. Springer, New York, second edition, 2006.

[OIL08] T. T. M. Onyango, D. B. Ingham, and D. Lesnic. Reconstruction of heat transfer coefficients using the boundary element method. *Computers & Mathematics with Applications. An International Journal*, 56(1):114–126, 2008.

[Pao92] C. V. Pao. *Nonlinear Parabolic and Elliptic Equations*. Plenum Press, New York, 1992.

[RAB16] S. Roy, M. Annunziato, and A. Borzì. A fokker–planck feedback control-constrained approach for modelling crowd motion. *Journal of Computational and Theoretical Transport*, 2016.

[Ris89] H. Risken. *The Fokker-Planck equation*, volume 18 of *Springer Series in Synergetics*. Springer-Verlag, Berlin, second edition, 1989. Methods of solution and applications.

[RM07] W. F. Ramirez and J. Maciejowski. Optimal beer fermentation. *Journal of the Institute of Brewing*, 113(3):325–333, 2007.

[Rös94] A. Rösch. Identification of nonlinear heat transfer laws by optimal control. *Numerical Functional Analysis and Optimization. An International Journal*, 15(3-4):417–434, 1994.

[Rös96a] A. Rösch. Fréchet differentiability of the solution of the heat equation with respect to a nonlinear boundary condition. *Zeitschrift für Analysis und ihre Anwendungen. Journal for Analysis and its Applications*, 15(3):603–618, 1996.

[Rös96b] A. Rösch. Stability estimates for the identification of nonlinear heat transfer laws. *Inverse Problems. An International Journal on the Theory and Practice of Inverse Problems, Inverse Methods and Computerized Inversion of Data*, 12(5):743–756, 1996.

[Rös98] A. Rösch. Second order optimality conditions and stability estimates for the identification of nonlinear heat transfer laws. In *Control and estimation of distributed parameter systems (Vorau, 1996)*, volume 126 of *Internat. Ser. Numer. Math.*, pages 237–246. Birkhäuser, Basel, 1998.

[Rös02] A. Rösch. A Gauss-Newton method for the identification of nonlinear heat transfer laws. In *Optimal control of complex structures (Oberwolfach, 2000)*, volume 139 of *Internat. Ser. Numer. Math.*, pages 217–230. Birkhäuser, Basel, 2002.

[RT92] A. Rösch and F. Tröltzsch. An optimal control problem arising from the identification of nonlinear heat transfer laws. *Polish Academy of Sciences. Committee of Automatic Control and Robotics. Archives of Control Sciences*, 1(3-4):183–195, 1992.

[Sab09] J.-M. Sablayrolles. Control of alcoholic fermentation in winemaking: Current situation and prospect. *Food Research International*, 42(4):418–424, 2009.

[Sho97] R. E. Showalter. *Monotone operators in Banach space and nonlinear partial differential equations*, volume 49 of *Mathematical Surveys and Monographs*. American Mathematical Society, Providence, RI, 1997.

[Smo94] J. Smoller. *Shock Waves and Reaction-Diffusion Equations*, volume 258 of *Grundlehren der Mathematischen Wissenschaften [Fundamental Principles of Mathematical Sciences]*. Springer-Verlag, New York, second edition, 1994.

[Trö10] F. Tröltzsch. *Optimal Control of Partial Differential Equations*, volume 112 of *Graduate Studies in Mathematics*. American Mathematical Society, Providence, RI, 2010. Theory, methods and applications, Translated from the 2005 German original by Jürgen Sprekels.

[VDI02] VDI-Gesellschaft Verfahrenstechnik und Chemieingenieurwesen (GVC). Verein Deutscher Ingenieure. *VDI-Wärmeatlas: Berechnungsblätter für den Wärmeübergang*. 2002.

[Vel09] K. Velten. *Mathematical Modeling and Simulation*. Wiley-VCH Verlag GmbH & Co. KGaA, Weinheim, 2009. Introduction for scientists and engineers.

[Wen95] H. Wendland. Piecewise polynomial, positive definite and compactly supported radial functions of minimal degree. *Advances in Computational Mathematics*, 4(4):389–396, 1995.

[Wen98] H. Wendland. Error estimates for interpolation by compactly supported radial basis functions of minimal degree. *Journal of Approximation Theory*, 93(2):258–272, 1998.

[WS93] Z. M. Wu and R. Schaback. Local error estimates for radial basis function interpolation of scattered data. *IMA Journal of Numerical Analysis*, 13(1):13–27, 1993.

[Yos80] K. Yosida. *Functional analysis*, volume 123 of *Grundlehren der Mathematischen Wissenschaften [Fundamental Principles of Mathematical Sciences]*. Springer-Verlag, Berlin-New York, sixth edition, 1980.

[Zei95] E. Zeidler. *Applied Functional Analysis*, volume 109 of *Applied Mathematical Sciences*. Springer-Verlag, New York, 1995. Main principles and their applications.